# Investigating the interactions in concentrated suspensions of fine particle mixtures to enhance the sustainable complex ore beneficiation

Olga Chernoburova

Université de Lorraine, Laboratoire GeoRessources
UMR 7359, F-54505, Vandoeuvre-lès-Nancy, France
Ecole doctorale SIReNa – Sciences et Ingénierie des Resources Naturelles)
(précédemment RP2E – Ressources, Procédés, Produits et Environnement)

**Thèse**

Présentée pour l'obtention du grade de
Docteur de l'Université de Lorraine (Nancy)
en Géosciences

par

**Olga Chernoburova**

# ETUDE DES INTERACTIONS ENTRE LES PARTICULES FINES DANS LES SUSPENSIONS CONCENTREES POUR AMELIORER LA VALORISATION DE MINERAIS COMPLEXES DURABLE

---

# INVESTIGATING THE INTERACTIONS IN CONCENTRATED SUSPENSIONS OF FINE PARTICLE MIXTURES TO ENHANCE THE SUSTAINABLE COMPLEX ORE BENEFICIATION

*Soutenance publique le 5 Decembre 2018*

***Membres du jury***

| | |
|---|---|
| **Directeur de thèse**<br>Prof. Jean-Marc Montel | *Université de Lorraine*, ENSG, GeoRessources laboratory, OTELo, F-54500, Vandoeuvre-lès-Nancy, France |
| **Co-directeur de thèse**<br>Assoc. Prof. Akira Otsuki | *Université de Lorraine*, GeoRessources laboratory, UMR7359, BP10162, F-54500, Vandoeuvre-lés-Nancy, France |
| **Examinateurs**<br>Assoc. Prof. Matthieu Jenny | *Université de Lorraine*, LEMTA, UMR 7563, CNRS, F-54500 Vandoeuvre-lés-Nancy, France |
| Prof. Sandra Lerouge | *Université Paris-Diderot*, Department of Physics, Laboratory Matière et Systèmes Complexes, CNRS, F-75205 Paris Cedex 13, France |
| **Rapporteurs**<br>Prof. François Martin | *Université de Toulouse*, ERT 1074 Géomatériaux, GET UMR 5563 CNRS, F-31000, Toulouse, France |
| Dr. Laurent Michot | *Sorbonne Université*, UPMC, Laboratoire Phenix, CNRS, UMR 8234, F-75252, Paris Cedex 5, France. |

# Résumé

Les suspensions minérales de particules fines sont connues pour leur comportement non-Newtonien sous l'écoulement. Les interactions particule-particule dans de tels systèmes (c'est-à-dire, suspensions minérales) sont au-dessus du contact physique en raison de la collision et du frottement. Une capacité des minéraux de développer une charge dans l'environnement aqueux justifie des comportements différents des systèmes similaires de première vue. Étant caractérisées avec la même fraction volumétrique, même composition chimique et la même granulométrie des solides et la densité de dispersants, deux suspensions peuvent montrer un comportement rhéologique différent en raison de la chimie de la solution. Dans ce cas, la composition ionique du dispersant définit le chargement des particules, et donc le degré d'agglomération/dispersion dans la suspension.

Certains minéraux sont connus pour être particulièrement problématiques dans les processus d'enrichissement des minerais, comme, par exemple, les argiles phyllosilicates. L'origine de ces minéraux phyllosilicatés explique leur inhomogénéité chimique spatiale, c'est-à-dire que le bord et la face de la particule ont des propriétés chimiques différentes et présentent donc des propriétés physiques différentes. La présence de tels minéraux dans les dispositifs d'agitation (réservoirs d'agitation, cellules de flottation) est souvent caractérisée par la coexistence des volumes de suspension bouchés et agités (Bakker et al. 2009, 2010), qui a un impact négatif sur l'efficacité de l'agitation. Dans ce travail, les suspensions aqueuses diluées de Na-bentonite ont été examinées par vélocimétrie par l'imagerie résonance magnétique pour étudier l'influence du pH et du type d'électrolyte monovalent sur leur comportement rhéologique local. Les résultats ont indiqué que les suspensions contenant 0,1% de solide en volume peuvent présenter une bande de cisaillement, une localisation de cisaillement ou aucun phénomène local en fonction de la chimie du milieu de suspension. Les changements structurels induits par la modification de la chimie des suspensions ont été examinés par microscopie électronique à balayage (MEB). Le résultat a été discuté du point de vue de DLVO (Derjaguin-Landau-Verwey-Overbeek, Hunter 1986) et "card house" (maison de cartes) théories. Il a été suggéré que l'existence de «master curve» (ou courbe d'écoulement globale) pour les suspensions diluées dépendait de l'organisation des

particules de bentonite dans la suspension, cette organisation est influencée par la chimie de solution et l'historique des contraintes précédentes.

Au cours de l'étape suivante, la complexité du système a été augmentée par l'ajout de la deuxième phase minérale, l'hématite ou le quartz, dans la matrice de bentonite. L'intérêt d'étudier ces systèmes est lié au comportement en écoulement d'une matrice formée avec différents types de contacts entre particules. Par exemple, à pH 4, l'interaction électrostatique résultante entre le bord de la bentonite chargé positivement et le quartz chargé négativement est attrayante, alors qu'au même pH, elle est répulsive avec l'hématite car ce minéral est chargé positivement. D'autre part, la face de la particule de bentonite chargée négativement attirera la particule d'hématite à pH 4, mais repoussera le quartz. Ces interactions électrostatiques s'expriment par une organisation différente des particules de matrice autour d'autre phase minérale. Avec l'augmentation de la fraction volumique des particules d'hématite ou de silice ajoutées, la quantité de réarrangements dans la matrice augmente, ce que justifie une réponse rhéologique modifiée. Dans le système avec des interactions strictement répulsives entre tous les sites de toutes les phases minérales (par exemple quartz et bentonite, pH 10), la déviation du comportement newtonien est justifiée par les réarrangements des particules, la collision et le frottement induits par le cisaillement. La différence dans la position des agrégats de particules de bentonite autour des particules d'hématite ou de quartz a été observée avec le MEB.

Enfin, la complexité du système a été encore plus augmentée par l'ajout de la troisième phase minérale. Les types de contacts établis dans les suspensions avec une chimie différente du milieu ont été discutés, ainsi que leur influence sur la formation de la matrice et son manière d'écoulement.

# Abstract

Fine particle mineral slurries are known to exhibit non-Newtonian behavior under the load. The particle-particle interactions in such systems (meaning, mineral suspensions) go beyond physical contact due to the collision and friction. An ability of minerals to gain the charge in the aqueous environment justifies different behaviors of the similar from the first sight systems. Being characterized with the same volumetric fraction, chemistry and particle size distribution of solids, and specific gravity of dispersing media, two suspensions can possess different rheological behavior due to the chemistry of the solution. In this case, the ionic composition of the media defines particle charging, and thus the degree of agglomeration/dispersion in the suspension.

Certain minerals are known to be particularly problematic in the mineral beneficiation processes, such as, for example, phyllosilicate clays. The nature of these sheet phyllosilicate minerals leads their spatial chemical inhomogeneity, meaning that the particle edge and face possess different chemical properties, and, thus, exhibit different physical properties. The presence of such minerals in the stirring devices (stirring tanks, flotation cells) is often characterized with coexistence of stagnant and agitated volumes of slurry (Bakker et al. 2009, 2010), which negatively impacts the efficiency of stirring. In this work, the dilute aqueous Na-bentonite suspensions were examined via magnetic resonance imaging velocimetry to investigate the influence of pH and type of monovalent electrolyte on their local rheological behavior. The results indicated that suspensions with 0.1 vol.% solid can exhibit shear banding, shear localization or no local phenomenon as a function of chemistry of the suspending media. Structural changes induced by modification of suspensions chemistry were examined via scanning electron microscopy (SEM). The result was discussed from the point of view of DLVO (Derjaguin-Landau-Verwey-Overbeek, Hunter 1986) and “card house” (van Olphen 1964) theories. It was suggested that the existence of master curve (or global flow curve) for dilute suspensions was dependent on the bentonite particle organization in the suspension, which was influenced by the chemistry of the environment and the previous flow history.

As the next step, the complexity of the system was enhanced by addition of the second mineral phase, i.e., hematite or quartz, to the bentonite matrix. The interest in examination of such systems is related to the flow behavior of matrix formed with different

kinds of inter-particle contacts. For example, at pH 4 the resulting electrostatic interaction between positively charged bentonite edge and negatively charged quartz is attractive, whereas at the same pH it is repulsive with the positively charged hematite. On the other hand, the negatively charged face of the bentonite particle will attract the hematite particle at pH 4, but will repel the quartz. These electrostatic interactions result in different organization of matrix particles around another mineral phase. With increasing volume fraction of added hematite or silica particles, the amount of rearrangements in the matrix increases justifying modified rheological response. In the system with solely repulsive interactions between all sites of all mineral phases (e.g., quartz and bentonite, pH 10) the deviation from Newtonian behavior is justified by the shear-induced particle rearrangements, collision and friction. The difference in the arrangement of bentonite particle aggregates around the hematite or quartz particles was observed using SEM.

Finally, the complexity of the system was enhanced via addition of the third mineral phase. The types of contacts established in the suspensions with different chemistry of the media were discussed along with their influence on the matrix formation and its flow under the load.

## Bibliography

Bakker CW, Meyer CJ, Deglon DA (2010) The development of a cavern model for mechanical flotation cells. In: Minerals Engineering. pp 968–972

Bakker CW, Meyer CJ, Deglon DA (2009) Numerical modelling of non-Newtonian slurry in a mechanical flotation cell. Miner Eng 22:944–950 . doi: 10.1016/j.mineng.2009.03.016

Hunter RJ (1986) Foundations of colloid science. Vol. 1. Oxford University Press Inc., New York

van Olphen H (1964) Internal mutual flocculation in clay suspensions. J Colloid Sci 19:313–322 . doi: 10.1016/0095-8522(64)90033-9

# Contents

# List of figures

# List of tables

# Chapter I – A general overview

## Introduction

Nowadays, mineral industry has to face the challenges of treating finely disseminated ores more and more often due to the mineral resource depletion (Malhotra et al. 2009; Wills and Finch 2016). Some of these ores are characterized with a liberation size as small as few micrometers (e.g., REE, Ni laterite), or even smaller (e.g., refractory Au ore). Ore beneficiation industry of today is in a constant search for a better technical solution: lower energy consumption (Abouzeid and Fuerstenau 2009), environmentally friendly technologies (Pedain et al. 2014), automatized 'smart' systems (Geng et al. 2008), enhanced process performance (Liu et al. 2016). Choice of the processing route and the technologies to apply is determined by the nature of the mineral matter. Major challenges related to treatment of finely disseminated ores are related to energy-efficient size reduction, liberation and extraction of the valuable component in its purest form. Producers of highly efficient comminution devices (e.g., stirred mills) readily faced the challenge, making it possible to perform size reduction down to -12 μm in a simple, economically favorable manner (Pease et al. 2006; Celep and Yazici 2013). Today, the technologies allowing liberation of finely disseminated minerals are no longer a limiting stage. But what does treatment of fine particles mean for the mineral processing chain? Are the downstream operations sufficiently developed to allow concentration of target component from a finely ground mineral mixture?

Fig. 1 demonstrates different mineral processing techniques available depending on the properties and liberation size of the treated mineral. Despite of seeming variety of solutions, most of these techniques are predominantly applied for relatively coarse materials. According to the Fig. 1, below 10 μm one is left with hydrocyclonation, flowing film, wet high gradient magnetic separation, and flotation. One may fairly suggest to add here a Falcon gravity concentrator and, in some cases, a shaking table. In order to extract a mineral phase from the grinded mixture it is important to know at least one property of the desired mineral that significantly differs from the properties of the rest of minerals in the mixture. Density, magnetic susceptibility, shape, hydrophobicity – each of these

properties can justify the choice of the beneficiation technique and, thus, the equipment unit.

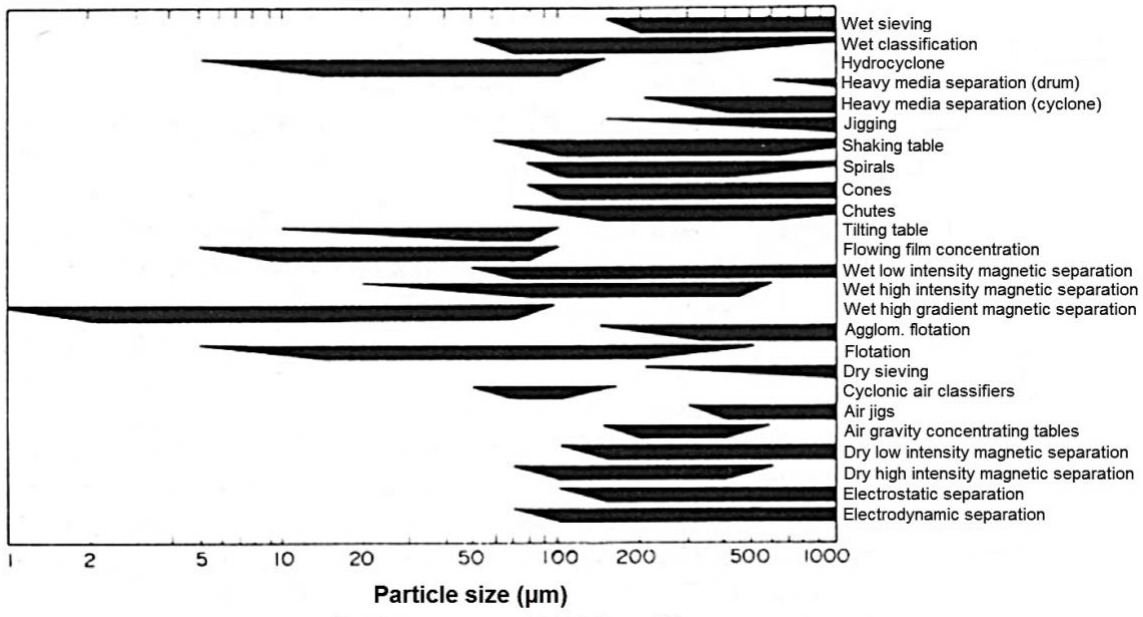


*Figure 1 - Diagram of mineral processing techniques vs mean size of the feed martial (adapted from Rosenkranz, 2015)*

High gradient magnetic separation is applied when the mineral of interest has significant difference in magnetic susceptibility comparing to other minerals in mixture. Tilting and shaking tables, flowing film and Falcon require noticeable difference in specific gravity of the minerals; note, that the methods are particle shape-sensitive, as are most of the wet treatment methods. In addition, beneficiation methods whose productivity is dependent on the available plane surface are known to have a low throughput. For techniques such as shaking table and Falcon, the preference is given to the precious minerals and metals, such as, for example, gold. Non-heavy media hydrocyclones may be used for the enrichment, and require concentration of valuable component in a certain size fraction upon size reduction. These properties are barely tunable and strongly depend on the nature of the mineral of interest. Flotation technique is based on the physicochemical surface properties of the minerals. And, in contrary to other methods listed above, these properties are often fairly easy to tune. This guaranteed a worldwide application of the flotation method, in the mineral processing industry and outside of it.

Closer look into the process shall be given in the following chapters (see chapter I, part I "Froth flotation").

In case of fine particle handling, it is more common to deal with the pulps and slurries, rather than with a dry material stream (all the techniques discussed above are "wet" techniques). Mineral pulps possess different properties depending on many factors (e.g., mineral chemistry, chemistry of suspending media, particle size and percent solids) that affect their handling. Controlling some of these properties can be achieved (e.g., percent solid), whereas for others it can be difficult (e.g., mineral composition) or economically unfeasible (e.g., requiring cost-intensive reagents).

Beneficiation processes suitable for fine particles are highly dependent on physico-chemical and mechanical properties of the pulp. In majority of cases the mechanics of relatively concentrated fine particle mineral suspension differs from the mechanics of Newtonian fluid and depends on the interactions between the suspended particles. In is important to study the mechanical properties on the mineral pulps for they influence the key processes in the mineral beneficiation chain, material transport, handling, dewatering and storage (Boger 2009; Farrokhpay 2012). Science that deals with mechanical properties of non-Newtonian flows is called "Rheology".

Rheology as a characterization tool that has found its application in diverse sciences and industries such as medicine (Viallat and Abkarian 2014; Connes et al. 2016), pharmaceuticals (Gallegos and Franco 1999), paints (McKay 1993), food production (Gallegos and Franco 1999; Shewan and Stokes 2013; McCann et al. 2016; West and Rousseau 2016), cosmetics (Gallegos and Franco 1999; Miller et al. 1999), metallurgy (Saby et al. 2014), drilling muds and petroleum industry (Guzek et al. 2015), concrete production (Tregger et al. 2010). Significant work has been done in mineral processing: grinding (Kawatra and Eisele 1988; Mangesana et al. 2008), slurry conditioning (Bakker et al. 2010) and transport (Boger 2009), thickening and tailing storage (Johnson et al. 2000; Boger 2009). However, limited amount of works link rheology and flotation in an intelligible manner. In the recent years several scientists highlighted the need of the rheological evaluation of the flotation foams and slurries, mentioning as well the fact that flotation-rheology linkage is yet not well established (Farrokhpay 2012; Farrokhpay et al. 2016; Li et al. 2016). Main concern of the previous works was the hydrodynamics of the process, where the basis of the theories assumed Newtonian fluid (Liu and Schwarz 2009; Schwarz et al. 2015) which is different from majority of mineral suspensions treated by

froth flotation these days. Huge efforts were made for the computational fluid dynamics modelling and succeeded in performing pretty realistic macro scale non-Newtonian simulations, relatively recently (Liu and Schwarz 2009; Bakker et al. 2010; Schwarz et al. 2015). The pulp “cracking”, or cavern development is a serious issue related to the non-Newtonianity of mineral suspensions. The phenomenon implies coexistence of yielded (flowing) and stagnant zones of slurry in the agitated volume and causes severe problems in mineral processing operations, including stirring, mixing, agitation, flotation in mechanical cells (Moore et al. 1995; Bakker et al. 2009, 2010; Shabalala et al. 2011; Taner and Onen 2016). This effect was found to occur in fine particle slurries, in particular, the ones containing phyllosilicates (clays). Phyllosilicates are known to be shape- and charge-anisotropic, to concentrate in fine particle size fractions and, thus, have an inconvenient hydrodynamics that justifies clay contamination of concentrate streams. Suspensions of phyllosilicates often suggest complex rheological behavior (Ndlovu et al. 2011, 2013, 2014), thixotropy (Abu-Jdayil 2011) and the yield stress (Tombácz and Szekeres 2004; Zhang and Peng 2015). Behavior of swelling clays is of a particular interest. In suspensions, these clays build various networks depending on the chemical environment of the solvent. The dimensions of these networks depend of the chemistry of a swelling clays.

In this chapter (chapter I), a general overview, definitions and necessary explanations of froth flotation process (I.I), particle-particle interactions (I.II), rheology (I.III), clays in mineral beneficiation chain and rheological behavior of clay suspensions (I.IV) and mix-mineral suspensions (I.V) were given. It was demonstrated that there is a wide field of research even in such extensively studied domains as froth flotation, mineral pulp handling or influence of clays on the mechanical properties of mineral pulps. It is particularly important to obtain knowledge about the ways of improvement for such processes as they are spread worldwide. Using the rheology to monitor, examine and predict behavior of mineral suspensions has a great perspective.

Chapter II is dedicated to the study of mechanical properties of suspensions of a smectite clay – bentonite, in different chemical conditions. In this chapter, the dilute aqueous suspensions of bentonite particles were studied using magnetic resonance imaging velocimetry. The influence of pH and type of monovalent electrolyte on the local rheological behavior of bentonite suspensions was evaluated and discussed. The results evidenced simultaneous coexistence of flowing and static regions in the complex fluid in

acidic environment, as a result of phenomena called “shear banding” and “shear localization”. It was suggested that existence of these phenomena in dilute suspensions (0.1 vol.% solid) is due to the formation of continuous three-dimensional particle network under acidic chemical environment. The result was discussed from the point of view of DLVO (Derjaguin-Landau-Verwey-Overbeek, Hunter 1986) and “cubic card house” (van Olphen 1964) theories. It was suggested that the existence of master curve (or global flow curve) for dilute suspensions was dependent on the bentonite particle organization in the suspension, which was influenced by the chemistry of the environment and the previous flow history.

In the chapter III more complex systems were investigated, namely, polymineral suspensions, with two and three mineral phases involved. Second (quartz) and third (hematite) mineral phases were suspended in the bentonite matrix. The interest in examination of such systems is related to the flow behavior of matrix formed with different kinds of inter-particle contacts. The electrostatic interactions between the minerals result in homo- and heterocoagulation of mineral particles and, thus, a modified rheological response of the entire system. With increasing volume fraction of added hematite or silica particles, the amount of rearrangements in the matrix (due to DLVO interactions between the particles) increases, also justifying a change in the rheological response. The shear-induced particle rearrangements, collision and friction are used to explain the deviation from Newtonian behavior in the systems with solely repulsive interactions between all sites of all mineral phases.

## Bibliography


Abouzeid AZM, Fuerstenau DW (2009) Grinding of mineral mixtures in high-pressure grinding rolls. Int J Miner Process 93:59–65 . doi: 10.1016/j.minpro.2009.05.008

Abu-Jdayil B (2011) Rheology of sodium and calcium bentonite-water dispersions: Effect of electrolytes and aging time. Int J Miner Process 98:208–213 . doi: 10.1016/j.minpro.2011.01.001

Bakker CW, Meyer CJ, Deglon DA (2010) The development of a cavern model for mechanical flotation cells. In: Minerals Engineering. pp 968–972

Bakker CW, Meyer CJ, Deglon DA (2009) Numerical modelling of non-Newtonian slurry in a mechanical flotation cell. Miner Eng 22:944–950 . doi: 10.1016/j.mineng.2009.03.016

Boger D V. (2009) Rheology and the resource industries. Chem Eng Sci 64:4525–4536 . doi: 10.1016/j.ces.2009.03.007

Celep O, Yazici EY (2013) Ultra fine grinding of silver plant tailings of refractory ore using vertical stirred media mill. Trans Nonferrous Met Soc China (English Ed 23:3412–3420 . doi: 10.1016/S1003-6326(13)62882-4

Connes P, Alexy T, Detterich J, et al (2016) The role of blood rheology in sickle cell disease. Blood Rev 30:111–118 . doi: 10.1016/j.blre.2015.08.005

Farrokhpay S (2012) The importance of rheology in mineral flotation: A review. Miner Eng 36–38:272–278 . doi: 10.1016/j.mineng.2012.05.009

Farrokhpay S, Ndlovu B, Bradshaw D (2016) Behaviour of swelling clays versus non-swelling clays in flotation. Miner Eng 96–97:59–66 . doi: 10.1016/j.mineng.2016.04.011

Gallegos C, Franco JM (1999) Rheology of food, cosmetics and pharmaceuticals. Curr. Opin. Colloid Interface Sci. 4:288–293

Geng Z, Chai T, Yue H, et al (2008) Intelligent Control for Flotation Process. doi: 10.3182/20080706-5-KR-1001.2649

Guzek A, Shufrin I, Pasternak E, Dyskin A V. (2015) Influence of drilling mud rheology on the reduction of vertical vibrations in deep rotary drilling. J Pet Sci Eng 135:375–383 . doi: 10.1016/j.petrol.2015.09.016

Hunter RJ (1986) Foundations of colloid science. Vol. 1. Oxford University Press Inc., New York

Johnson SB, Franks G V, Scales PJ, et al (2000) Surface chemistry-rheology relationships in concentrated mineral suspensions

Kawatra SK, Eisele TC (1988) Rheological effects in grinding circuits. Int J Miner Process 22:251–259 . doi: 10.1016/0301-7516(88)90067-1

Li C, Runge K, Shi F, Farrokhpay S (2016) Effect of flotation froth properties on froth rheology. doi: 10.1016/j.powtec.2016.02.018

Liu R, Qin W, Jiao F, et al (2016) Enhanced flotation of refractory gold ore by using sulfur-oil agglomeration with (NH4)2S2O3 as regulator in weak acidic pulp. Miner Eng 93:24–31 . doi: 10.1016/j.mineng.2016.04.008

Liu TY, Schwarz MP (2009) CFD-based multiscale modelling of bubble-particle collision efficiency in a turbulent flotation cell. Chem Eng Sci 64:5287–5301 . doi: 10.1016/j.ces.2009.09.014

Malhotra D, Taylor P, LeVier M, Spiller E (2009) Recent Advances in Mineral Processing Plant Design. In: Recent Advances in Mineral Processing Plant Design

Mangesana N, Mainza AA, Govender I, et al (2008) The effect of particle sizes and solids

concentration on the rheology of silica sand based suspensions. Journal- South African Inst Min Metall 108:

McCann TH, Le Gall M, Day L (2016) Extensional dough rheology – Impact of flour composition and extension speed. J Cereal Sci 69:228–237 . doi: 10.1016/j.jcs.2016.03.012

McKay RB (1993) Crystal morphology of organic pigments and rheology of dispersions in ink and paint media. Prog Org Coatings 22:211–229 . doi: 10.1016/0033-0655(93)80025-6

Miller D, Wiener EM, Turowski A, et al (1999) O/W emulsions for cosmetics products stabilized by alkyl phosphates - Rheology and storage tests. In: Colloids and Surfaces A: Physicochemical and Engineering Aspects. pp 155–160

Moore IPT, Cossor G, Baker MR (1995) VELOCITY DISTRIBUTIONS IN A STIRRED TANK CONTAINING A YIELD STRESS FLUID. Chem Enoineerin 0 Sci 50:2467–2481

Ndlovu B, Becker M, Forbes E, et al (2011) The influence of phyllosilicate mineralogy on the rheology of mineral slurries. Miner Eng 24:1314–1322 . doi: 10.1016/j.mineng.2011.05.008

Ndlovu B, Farrokhpay S, Bradshaw D (2013) The effect of phyllosilicate minerals on mineral processing industry. Int J Miner Process 125:149–156 . doi: 10.1016/j.minpro.2013.09.011

Ndlovu B, Forbes E, Farrokhpay S, et al (2014) A preliminary rheological classification of phyllosilicate group minerals. Miner Eng 55:190–200 . doi: 10.1016/j.mineng.2013.06.004

Pease JD, Curry DC, Young MF (2006) Designing flotation circuits for high fines recovery. In: Minerals Engineering. pp 831–840

Pedain KU, Bezuidenhout J, Lipowsky G (2014) Synergistic effects of environmentally friendly collectors in the preconcentration step of a double float process on sedimentary phosphate ore. In: Procedia Engineering. pp 139–147

Rosenkranz J (2015) Course presentation

Saby M, Massoni E, Bozzolo N (2014) A metallurgical approach to individually assess the rheology of alpha and beta phases of Ti-6Al-4V in the two-phase domain. Mater Charact 89:88–92 . doi: 10.1016/j.matchar.2014.01.001

Schwarz MP, Koh PTL, Verrelli DI, Feng Y (2015) Sequential multi-scale modelling of mineral processing operations, with application to flotation cells. Miner. Eng.

Shabalala NZP, Harris M, Filho LSL, Deglon DA (2011) Effect of slurry rheology on gas dispersion in a pilot-scale mechanical flotation cell. doi: 10.1016/j.mineng.2011.07.004

Shewan HM, Stokes JR (2013) Review of techniques to manufacture micro-hydrogel particles for the food industry and their applications. J. Food Eng. 119:781–792

Taner HA, Onen V (2016) Control of clay minerals effect in flotation . A review. 2:6–11 . doi: 10.1051/e3sconf/20160801062

Tombácz E, Szekeres M (2004) Colloidal behavior of aqueous montmorillonite suspensions: the specific role of pH in the presence of indifferent electrolytes. Appl Clay Sci. doi: 10.1016/j.clay.2004.01.001

Tregger NA, Pakula ME, Shah SP (2010) Influence of clays on the rheology of cement pastes. Cem Concr Res 40:384–391 . doi: 10.1016/j.cemconres.2009.11.001

van Olphen H (1964) Internal mutual flocculation in clay suspensions. J Colloid Sci 19:313–322 . doi: 10.1016/0095-8522(64)90033-9

Viallat A, Abkarian M (2014) Red blood cell: From its mechanics to its motion in shear flow. Int. J. Lab. Hematol. 36:237–243

West R, Rousseau D (2016) Crystallization and rheology of palm oil in the presence of sugar. Food Res Int 85:224–234 . doi: 10.1016/j.foodres.2016.05.010

Wills BA, Finch JA (2016) Wills' Mineral Processing Technology. Elsevier

Zhang M, Peng Y (2015) Effect of clay minerals on pulp rheology and the flotation of copper and gold minerals. Miner Eng 70:8–13 . doi: 10.1016/j.mineng.2014.08.014

## I.I. Froth flotation

Froth flotation is a mineral processing technique that exploits the difference in minerals' hydrophobicity (ability to repel water) for their selective concentration to separate products (Wills and Finch 2016). Basic procedure of the method consists of feeding the slurry (two phase stream composed of various minerals suspended in water or reagent solution) into the cell, where it is agitated with air that acts as a transporting phase solely for the mineral particles with high hydrophobicity. Those mineral particles attach to the air bubbles and report to the top of the cell where they form the froth. Minerals that are not sufficiently hydrophobic to attach to the bubbles sediment all way down to the bottom of the cell where they get discharged. As a result of such operation two products are obtained: a froth concentrate (usually composed of valuable component) and tailings (classically, the gangue). Froth flotation can be realized in different types of cells (e.g., column flotation cell, Jameson cell), but the most widespread type of flotation cells are mechanical flotation cells, see Fig. 2. In a mechanical flotation cell, the pulp is fed to a tank where it is intensively agitated and mixed with air using a rotating device – impeller (Fig. 2).

The major advantage of the flotation is an ability to adjust the hydrophobic properties of the mineral particles. The methods of hydrophobization using specific chemical additives are well established nowadays. There are four main groups of reagents: frothers, collectors, activators/depressants and modifiers. Each reagent has their specific role in the process: frothers are responsible for creation of small and stable bubbles; collectors – for selective hydrophobization of the target mineral surfaces; activators adsorb onto specific surfaces to enhance collector adsorption onto the mineral surface, while depressants adsorb onto mineral surfaces to prevent the collector adsorption or decrease mineral's natural hydrophobicity; modifiers are mainly aimed to adjust the pH of the slurry. Sometimes same reagent can play two different roles in flotation process, being a depressant and a modifier at the same time, for example. Because of the ability to adjust and modify the hydrophobicity attributed to different mineral phases, flotation process became very flexible and economically interesting, which let it gain popularity worldwide.

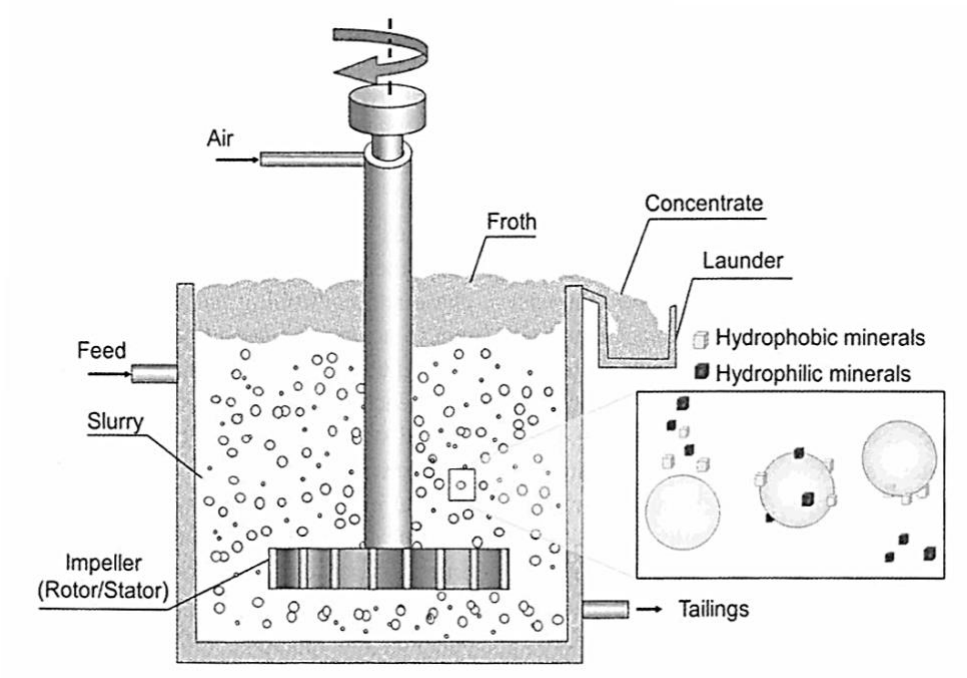


*Figure 2 - Schematic representation of a mechanical floatation cell (Wills and Finch 2016).*

The central process of flotation is the aggregate formation between a bubble and a hydrophobic particle. To create such an aggregate the bubble and the particle shall approach each other as close as the range of attractive surface forces. This event shall be followed by thinning the liquid film between the gas (air bubble) and the solid (particle) phase until the film ruptures and the three-phase contact line (gas-solid-liquid) is formed. Created three-phase contact line grows up to the moment when the stabile wetting perimeter is achieved. It results in formation of a stabile bubble-particle aggregate. However, if sufficient kinetic energy is provided, the particle may leave the bubble surface. Above described sequence of phenomenon are main flotation sub-processes: collision, attachment and detachment (Ralston & Dukhin, 1999; Ralston et al., 1999). In the simplest case efficiency of collection $(\mathrm{E})$ can be described as a product of three probabilities (see eq. 1):

$$\mathrm{E} = \mathrm{E_C E_A E_S}, \qquad [1]$$

where $\mathrm{E_C}$ is the collision efficiency, $\mathrm{E_A}$ is the attachment efficiency, $\mathrm{E_S}$ is the stability efficiency of the bubble-particle aggregate, which could be otherwise defined as 1-$\mathrm{E_D}$, with $\mathrm{E_D}$ being the probability of detachment.

The factors, or parameters, on which flotation process dependents can be roughly separated onto two groups: process-dependent and material-dependent. The first group includes throughput, type of the machine used, air rate, bubble size, percent solid in the slurry, reagent type and consumption, pH, etc. The second group includes particle size and shape, type of the mineral, oxidation degree of the surface, liberation degree, etc.

In the pulps, suspended mineral particles are of a wide size range and can be roughly split on two categories “inertial” and “non-inertial”. In the laminar flow, inertial particles are capable of deviating from the stream lines due to their mass and size. They are highly submitted to gravity (tend to sediment) and momentum in turbulent flows, which makes them very detachable from the air bubbles in turbulent eddies occurring in the flotation cells. Non-inertial particles tend to follow the stream lines in the laminal flows, they are light and small (e.g., overgrinded phyllosilicates, slimes); the inertial effects associated with such particles are minor. However, due to these properties, the non-inertial particles have low probability of collision with the bubbles in the flotation cells (Miettinen et al. 2010). Usually, particles treated by flotation are between 1 and 300 μm in size (Cruz et al. 2016).

Froth flotation has been recognized as one of the most widely employed ore beneficiation methods. It has been applied to a diverse range of materials and fairly well studied. Nevertheless, there is always place for the improvement; currently the main research and development paths are:

- innovations in the field of flotation reagents: new reagents and combinations, synergetic effects (e.g., Karlkvist et al., 2015; Filippova et al., 2014);
- capacity improvement without (significant) increase in occupied industrial area (Jameson 2010);
- development of new equipment units with improved hydrodynamics and energy consumption (Jameson, 2010; Zhang et al., 2013; Anderson et al., 2009; Valderrama & Rubio, 2008);
- process and sub-process predictive and descriptive modelling (Wang et al., 2015; Zhang et al., 2001; Vazirizadeh et al., 2015; Yoon, 2000);
- onsite process monitoring, control and automatization (Bonifazi et al., 2001; Geng et al., 2008);

- improvement of the efficiency of fine particle recovery (e.g., Jameson, 2010; Pease et al., 2006; Valderrama & Rubio, 2008);
- recognition of rheology as a tool for flotation process characterization and improvement (Farrokhpay, 2012; Otsuki et al., 2011; Shabalala et al., 2011).

Present research is mainly concentrated in the last domain of development, however, the research outcome is not necessarily enclosed in the frames of this domain.

Formation of caverns is a rheology-related problem, commonly faced in mechanical flotation cells and the agitation tanks. Occurrence of a "cavern" in the agitated volume of slurry implies establishment of two distinct, simultaneously existing, stagnant and agitated volumes of slurry. An agitated volume usually forms a ring or a cylinder around the impeller (or mixing vane), whereas the rest of the slurry in the tank is not affected by mixing (Bakker et al. 2009, 2010; Cruz et al. 2016). It was found (Bakker et al. 2009, 2010) that the size of the formed cavern is dependent on the rheological properties of the slurry, such as yield stress and viscosity (see chapter I, part III, "Rheology"). For a slurry characterized with a viscosity of 0.20 Pa s, density of 1400 kg/m$^3$ and local energy dissipation of 11 W/kg a reported average shear rate in a flotation cell is approximately 90 s$^{-1}$ (Ralston et al. 2006). This value of "approximate average shear rate of 100 s$^{-1}$" was reported in multiple studies as a reference average shear rate value. However, in conditions of cavern formation such estimation makes no sense. In fact, for a non-Newtonian slurry the variety of shear rates existing in the flotation cell, from highest in the proximity of the impeller to lowest in the quiescence zone, will correspond to a variety of viscosities (Bakker et al. 2010; Cruz et al. 2016). In flotation process, occurrence of caverns causes multiple severe problems, including reduced active volume of the flotation cell, non-optimal distribution of the gaseous phase across the cell perimeter and decreased bubble-particle collision efficiency (i.e., $\mathrm{E_C}$ in the eq. 1). Flotation is a key process in the mineral beneficiation chain that defines the final quality of the mineral concentrate. Malfunction of such important operation can yield significant loss of the mineral concentrate's economic value.

In industry, it is quite usual that flotation operators are tuning rheological properties (by water addition, for example) based on their working experience accumulated over the years. They know that for some slurry solid percent the process will not be efficient; or if the electricity shut down occurred for too long (if there was no

opportunity to keep the pulp suspended) the sediment in the cell will become so dense that the impeller start-up will cause the twist of the shaft. It is known, but there is little comprehensive approach developed.

## Bibliography


Anderson CJ, Harris MC, Deglon DA (2009) Flotation in a novel oscillatory baffled column. Miner Eng 22:1079–1087 . doi: 10.1016/j.mineng.2009.04.007

Bakker CW, Meyer CJ, Deglon DA (2010) The development of a cavern model for mechanical flotation cells. In: Minerals Engineering. pp 968–972

Bakker CW, Meyer CJ, Deglon DA (2009) Numerical modelling of non-Newtonian slurry in a mechanical flotation cell. Miner Eng 22:944–950 . doi: 10.1016/j.mineng.2009.03.016

Bonifazi G, Serranti S, Volpe F, Zuco R (2001) Characteristisation of flotation froth colour and structure by machine vision. Comput Geosci 27:1111–1117 . doi: 10.1016/S0098-3004(00)00152-7

Cruz N, Peng Y, Kruttschnitt J (2016) Rheology measurements for flotation slurries with high clay contents – A critical review. Miner Eng 98:137–150 . doi: 10.1016/j.mineng.2016.08.011

Farrokhpay S (2012) The importance of rheology in mineral flotation: A review. Miner Eng 36–38:272–278 . doi: 10.1016/j.mineng.2012.05.009

Filippova IV, Filippov LO, Duverger A, Severov VV (2014) Synergetic effect of a mixture of anionic and nonionic reagents: Ca mineral contrast separation by flotation at neutral pH. Miner Eng 66:135–144 . doi: 10.1016/j.mineng.2014.05.009

Geng Z, Chai T, Yue H, et al (2008) Intelligent Control for Flotation Process. doi: 10.3182/20080706-5-KR-1001.2649

Jameson GJ (2010) New directions in flotation machine design. In: Minerals Engineering. pp 835–841

Karlkvist T, Patra A, Rao KH, et al (2015) Flotation selectivity of novel alkyl dicarboxylate reagents for apatite-calcite separation. J Colloid Interface Sci 445:40–47 . doi: 10.1016/j.jcis.2014.11.072

Miettinen T, Ralston J, Fornasiero D (2010) The limits of fine particle flotation. Miner Eng 23:420–437 . doi: 10.1016/j.mineng.2009.12.006

Otsuki A, Barry S, Fornasiero D (2011) Rheological studies of nickel oxide and quartz/hematite mixture systems. Adv Powder Technol 22:471–475 . doi: 10.1016/j.apt.2011.04.004

Pease JD, Curry DC, Young MF (2006) Designing flotation circuits for high fines recovery. In: Minerals Engineering. pp 831–840

Ralston J, Dukhin SS (1999) The interaction between particles and bubbles. In: Colloids and Surfaces A: Physicochemical and Engineering Aspects. pp 3–14

Ralston J, Fornasiero D, Grano S, et al (2006) Reducing uncertainty in mineral flotation-flotation rate constant prediction for particles in an operating plant ore. doi: 10.1016/j.minpro.2006.08.010

Ralston J, Fornasiero D, Hayes R (1999) Bubble-particle attachment and detachment in flotation. Int J Miner Process 56:133–164 . doi: 10.1016/S0301-7516(98)00046-5

Shabalala NZP, Harris M, Filho LSL, Deglon DA (2011) Effect of slurry rheology on gas dispersion in a pilot-scale mechanical flotation cell. doi: 10.1016/j.mineng.2011.07.004

Valderrama L, Rubio J (2008) Unconventional column flotation of low-grade gold fine particles from tailings. Int J Miner Process 86:75–84 . doi: 10.1016/j.minpro.2007.11.003

Vazirizadeh A, Bouchard J, Del Villar R (2015) On the relationship between hydrodynamic characteristics and the kinetics of column flotation. Part I: Modeling the gas dispersion. Miner Eng

74:207–215 . doi: 10.1016/j.mineng.2014.09.026

Wang L, Peng Y, Runge K, Bradshaw D (2015) A review of entrainment: Mechanisms, contributing factors and modelling in flotation. Miner. Eng. 70:77–91

Wills BA, Finch JA (2016) Wills' Mineral Processing Technology. Elsevier

Yoon RH (2000) The role of hydrodynamic and surface forces in bubble-particle interaction. Int J Miner Process 58:129–143 . doi: 10.1016/S0301-7516(99)00071-X

Zhang H, Liu J, Wang Y, et al (2013) Cyclonic-static micro-bubble flotation column. Miner Eng 45:1–3 . doi: 10.1016/j.mineng.2013.01.006

Zhang Y, McLaughlin JB, Finch JA (2001) Bubble velocity profile and model of surfactant mass transfer to bubble surface. Chem Eng Sci 56:6605–6616 . doi: 10.1016/S0009-2509(01)00304-9

## I.II. Inter-particle forces

The behavior of fine particle mineral slurries is strongly dependent on the particle-particle interactions in the suspensions. These interactions result from the sum of various forces arising between the neighboring particles as they approach each other. Johnson (2000) provided a comprehensive overview summarizing the theory behind the various kinds of inter-particle forces influencing the rheology of mineral suspensions. A concise list of forces with their description and means of regulation is given in the Table 1.

*Table 1 - Main inter-particle forces*

| Name | Origin | Means of regulation |
|---|---|---|
| van der Waals force | Interaction between instantaneous dipoles of the atoms that form each particle | Particle size |
| Electrical double layer forces | Electrical charge obtained by the particles when they are immersed in water causes the re-distribution of ions in surrounding solution; as a consequence ionic layers are formed around the particle | pH, type and amount of electrolyte present in the suspension, charged surface-associating species, particle size |
| Structural (hydration) forces | Formation of strongly surface-associated layer of water molecules surrounding the particle | Type and concentration of electrolyte in the solution, pH, surfactant/polymeric species adsorbed onto the surface |
| Secondary hydration forces | Binding of hydrated ions onto the charged surfaces (surface-bound ions are forced to dehydrate as another surface approaches) | |

| | | |
|---|---|---|
| Hydrophobic forces | Reorientation of water molecules around non-polar substances; water structuring caused by this mechanism is highly entropically unfavorable | Introduction of the surfactants |
| Steric and electrosteric forces | Force results from *two different effects*, which could be explained on the example of two polymer-covered approaching particles: 1) *osmotic pressure increase* due to the local raise in the polymer concentration in the space between the particles, and 2) *elastic force* due to the compression of polymer molecules | Size, conformation and concentration of adsorbed polymer; in case of polyelectrolyte-coated particles – pH and ionic strength of suspension |
| Bridging forces | Polymer/polyelectrolyte binding several particles at a time keeping them together | Polymer/polyelectrolyte type, size and concentration |
| Depletion forces | Depletion force occurs when two particles approach each other in the concentrated solution of non-adsorbing polymer; once the particles are close, non-adsorbing polymeric species are pushed out from the gap between the particles, the resulting attraction between the particles is caused by compressive osmotic pressure | |

Some of these forces (i.e. hydrophobic forces) do not possess a single commonly agreed expression which could suggest a good correlation of models with the experimental results in a vast variety of cases. This leaves a place for improvement in development of mathematical models of some forces. The present work concentrated on the first two forces given in the Table 1, namely, the van der Waals and electrical double layer force. These forces lay in the core of the DLVO (Derjaguin-Landau-Verwey-Overbeek) theory - a widely known theory used to explain the colloidal stability. It implies existence of two opposing forces between the homogeneously charged particles of the same nature. One of these forces is causing them to attract (van der Waals) and another one – to repel (electrical double layer force). Above suggested net interaction is based on the assumption of similarity of interacting particles (i.e., chemistry of solid, shape). Van der Waals attraction between the mineral particles occurs due to the fluctuations of the electrons relative to protons in the atoms comprising each particle. At instant, these fluctuations result in dipole-like situation of positive and negative charges in the atom - phenomena, referred to as “instantaneous dipole”. Instantaneous dipoles of the neighboring atoms synchronize with each other, giving raise to mutual attraction.

Electrical double layer (EDL) force raises in proximity of a mineral surface when the mineral is immersed in the aqueous media with free ions available for adsorption. Upon the immersion in such solution, the mineral surface gains a charge due to the lattice imperfections (e.g., replacements in the crystal lattice, exposed chemical bonds). Charge on the mineral surface is balanced by the counter-ions attracted to the surface from the solution. First layer of counter-ions, densely adsorbed onto the mineral surface is called the “Stern layer” (see Fig. 3). The electric potential in this layer drops linearly; the potential on the border of Stern layer is caller “Stern potential”. Charge development from this point further into the solution is a function of concentration of co-ions and counter-ions, which decreases with the distance from the surface until it reaches the concentration in the bulk solution. This part of EDL is called “diffuse layer” (see Fig. 3). The electric potential decreases exponentially in this region (Hunter 1986; Israelachvili 2011).

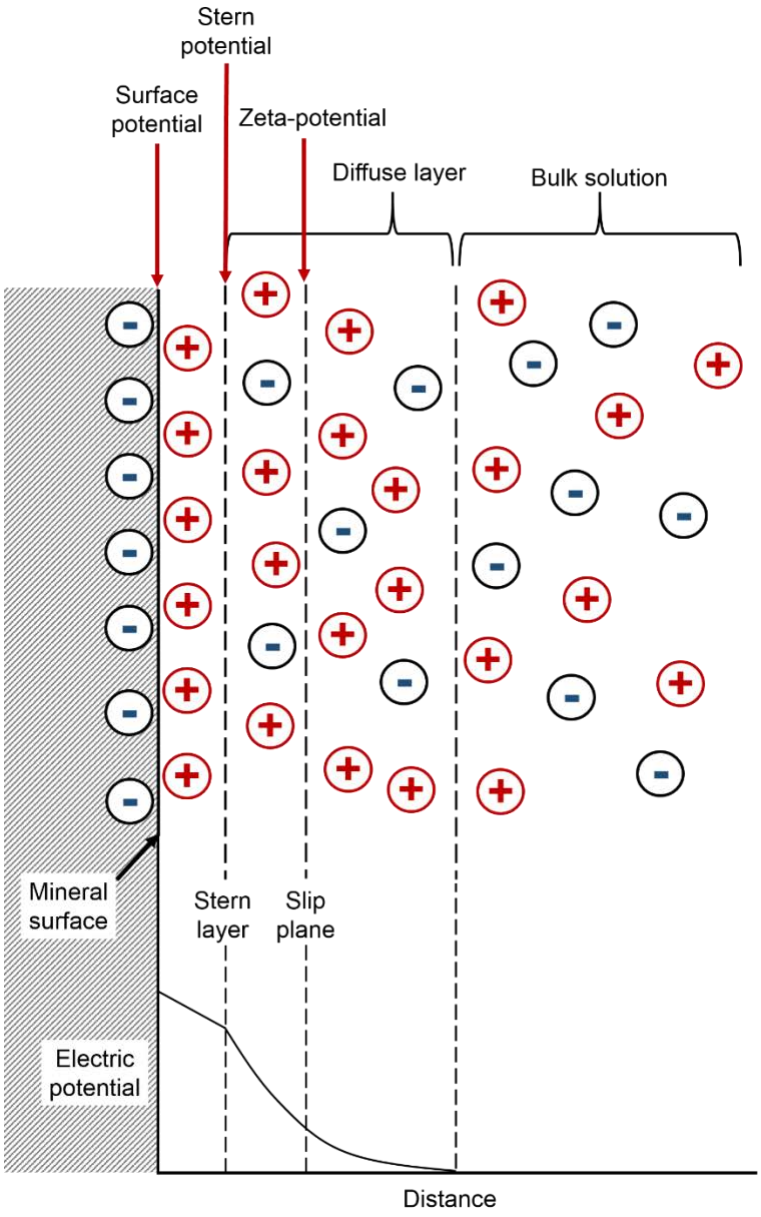


*Figure 3 - Schematic representation of EDL.*

It is suggested, that during the particle motion in the fluid, a part of its diffuse layer gets carried away with the enveloping flow. An imaginary border between the mobile and immobile parts of EDL is called the “slip plane” (Fig. 3). The electric potential on the slip plane is referred to as “zeta-potential” (or ζ-potential).

Mathematical expressions generally used to quantify DLVO forces are given below, in the eqs. 2, 3 and 4 for van Der Waals force ($F_{VDW}$) and eqs. 5 and 6 for electrical double layer force ($F_{EDL}$).

$$F_{VDW} = -\frac{aA_H}{12H^2}, \quad [2]$$

where – $a$ is radius of two identical spherical particles, $H$ is the distance between the particles, $A_H$ is the material property termed by the Hamaker constant.

General expression of the Hamaker constant for two bodies (indexed "1" and "2") interacting through the medium (indexed "3") is given in the eq. 3.

$$A_H = \frac{3kT}{4}\left(\frac{\varepsilon_1-\varepsilon_3}{\varepsilon_1+\varepsilon_3}\right)\left(\frac{\varepsilon_2-\varepsilon_3}{\varepsilon_2+\varepsilon_3}\right) + \frac{3h\nu_e}{8\sqrt{2}}\frac{(n_1^2-n_3^2)(n_2^2-n_3^2)}{\sqrt{n_1^2+n_3^2}\sqrt{n_2^2+n_3^2}\left[\sqrt{n_1^2+n_3^2}+\sqrt{n_2^2+n_3^2}\right]}, \quad [3]$$

where $n_i$ – is refractive index of 1st, 2nd or 3rd phase, $\varepsilon_i$ is the dielectric constant of media (1st, 2nd or 3rd), $\nu_e$ is the main absorption frequency in the ultraviolet region, $k$ is the Boltzmann constant, $h$ is the Planck constant, $T$ is the absolute temperature.

In the system where two interacting particles are identical (meaning, $\varepsilon_1 = \varepsilon_2$ and $n_1 = n_2$) the expression for Hamaker constant is simplified to eq. 4:

$$A_H = \frac{3kT}{4}\left(\frac{\varepsilon_1-\varepsilon_3}{\varepsilon_1+\varepsilon_3}\right)^2 + \frac{3h\nu_e}{8\sqrt{2}}\frac{(n_1^2-n_3^2)^2}{(n_1^2+n_3^2)2\sqrt{n_1^2+n_3^2}}. \quad [4]$$

Expression used to calculate the electrical double layer force is given in the eq. 5:

$$F_{EDL} = \frac{2\pi a\varepsilon_0\varepsilon\kappa\zeta^2 e^{-\kappa H}}{1+e^{-\kappa H}}, \quad [5]$$

where $\varepsilon_0$ is the permittivity of the free space, $\varepsilon$ is the dielectric constant of the bulk solution, $\kappa$ is Debye-Huckel parameter, $\zeta$ is the electrical potential generated by the charged surface (and ions attracted to it).

Expression for Debye-Huckel parameter calculation is given by the eq. 6:

$$\kappa = \sqrt{\frac{e^2 \sum p_i^0 z_i^2}{\varepsilon_0 \varepsilon k T}}, \qquad [6]$$

where $z_i$ ionic valence i-th species, $p_i$ is the number concentration of the i-th species, $e$ is the electronic charge.

As it can be seen in the eqs. 2 and 5, the magnitude of each force is a function of the separation distance ($H$) between the particle surfaces. Van der Waals attraction is dominant over the electrical double layer force at very small separation distances, due to its power law nature (i.e., $F_{VDW} \propto -\frac{1}{H^2}$, as it follows from the eq. 2). The double layer interaction energy is finite and rises much slower with decreasing $H$, as it follows from eq. 5. Schematic representation of the net interaction energy as a function of magnitude of each force at separation distance $H$ is depicted in the Fig. 4.

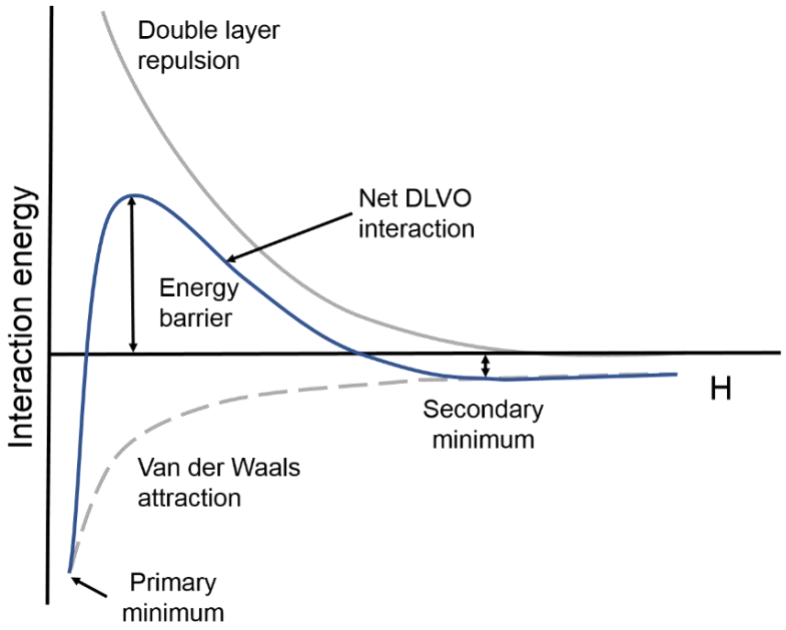


*Figure 4 - Schematic diagram of net DLVO interaction as a function of separation distance.*

It could be observed (Fig. 4) that the curve representing net DLVO interaction is characterized with two energy minima (responsible for particle-particle attraction) and the energy barrier (responsible for particle-particle repulsion, and, thus, colloidal stability).

Van der Waals attraction will always dominate at long and short distances (Hunter 1986), giving raise to long-range (secondary minimum) and short-range (primary minimum) attraction. The adhesion in the secondary minimum is much weaker and, thus, is easily reversible. Energy barrier originates from double layer repulsion occurring between the approaching particles with ionic structures of similar net charge. With increase in the electrolyte concentration, the double layer thickness decreases. At high electrolyte concentrations the EDL compression takes place, which lets particle aggregation. Note, that term “aggregation” in this work is used to describe the coagulation due to the DLVO forces, and term “flocculation” is reserved for the particle binding by polymer or polyelectrolyte molecules. In a stabile colloid the overall interaction between the particles is repulsive.

It has to be highlighted that the DLVO theory is based on some assumptions, most fundamental of which include:

- total interaction energy between two colloidal entities is composed of van der Waals and electrical double layer forces only;
- above mentioned interactions can be computed separately and are additive;
- solvent is treated as continuum;
- interactions are taking place between only two regarded bodies in an infinite medium (no many body effects or order-disorder transition considered);
- ions composing EDL are treated as point charges;
- all interacting surfaces are smooth and uniformly charged.

Zeta-potential is an important parameter for suspension stability. It is frequently used in the mineral processing as a measure of repulsive interaction between the particles. At pH where the positive and negative charges on the slip plane balance each other and zeta-potential is zero one is dealing with an “isoelectric point” (IEP) of the mineral. The energy barrier at the IEP is low and insufficient to prevent particle aggregation. Another important parameter used to characterize the stability of the colloid is the “point of zero charge” (PZC) which refers to a pH where the net electrical charge on the particle surface is zero. In an ideal system where a pure oxide in water adsorbs solely

potential-determining ions (no specific adsorption), mineral's IEP and PZC are situated at the same pH.

Above the case of similar homogeneously charged particles was considered. Homocoagulation (coagulation between alike particles) can also result from the electrostatic attraction between the differently charged sites of similar particles, the way it happens, for example, in case of phyllosilicates (see chapter I, part IV "Clays"). In this case, each particle site (edge and face, for sheet phyllosilicates) possesses its own EDL (Tombácz and Szekeres 2004). In case of opposite charging of these sites, both, van der Waals and EDL forces are attractive. Physico-chemical interactions discussed in this chapter were proven to have significant effect on the rheological properties of fine particle suspensions (Tadros 2010). The case of a system with dissimilar particles (different shape and chemistry) is analyzed in the chapter I, part V "Mix mineral systems" and chapter III.

## Bibliography

Hunter RJ (1986) Foundations of colloid science. Vol. 1. Oxford University Press Inc., New York

Israelachvili J (2011) Intermolecular and Surface Forces, Third eddi. Elsevier Inc.

Johnson SB, Franks G V., Scales PJ, et al (2000) Surface chemistry-rheology relationships in concentrated mineral suspensions. Int J Miner Process 58:267–304 . doi: 10.1016/S0301-7516(99)00041-1

Tadros TF (2010) Rheology of Dispersions: Principles and Applications

Tombácz E, Szekeres M (2004) Colloidal behavior of aqueous montmorillonite suspensions: the specific role of pH in the presence of indifferent electrolytes. Appl Clay Sci. doi: 10.1016/j.clay.2004.01.001

## I.III. Rheology

Rheology is a science that deals with the deformation of matter under applied stress. The 'matter' in this definition is a liquid or a 'soft solid' (alias 'soft matter'). According to Doi (2013), soft matters are defined as matters that consist of large molecules or molecular assembles which are moving collectively, giving a large and non-linear response to the applied force or a slow and non-equilibrium response; these include polymers, colloids, surfactants, liquid crystals, some biological materials, granular solids, glassy materials, gels, foams. Pulps, slurries and suspensions examined in the present work fall into the 'soft matter' category.

Rheological measurement can be conducted in different kinds of rheometers (e.g., rotational rheometer, pipe or capillary rheometer) with various geometries (e.g., cone and plate, parallel plate, bob and cup). For characterization of stirred mineral slurries often the rotational rheometer is used. There is a verity of advantages suggested by rotational rheometers, including: ability to be utilized in the laboratory and on the site (coupled with industrial settings), relative compactness, convenient sample volumes required for measurement and considerable simplicity of associated measurement procedures, easy data analysis (Fisher et al. 2007).

The "gap" of the geometry is a distance between two surfaces, filled with the sheared sample under the study. For example, in the parallel plate geometry, the gap is the distance between the fixed and the rotating plates; in the concentric cylinder geometry, the annular gap is the radial distance between the two cylinders. Since industrial suspensions often contain non-colloidal particles, it is impractical to use narrow-gap geometries (e.g., cone and plate, parallel plates) for their characterization. It is suggested that the gap size has to be ten times the biggest particle in the suspension under the measurement (Fisher et al. 2007). Thus, a Couette concentric cylinder (Fig. 5a) or the vane (Fig. 5b) geometries are used (Fisher et al. 2007; Boger 2009). Utilization of the vane allows to eliminate the slip on the rotating element of the geometry, reduce the sample disturbance upon the rotating element immersion and directly measure the yield stress (Dzuy and Boger 1985; Benna et al. 1999; Fisher et al. 2007; Boger 2009; Tadros 2010; Farrokhpay 2012); it is also less susceptible to the artifacts arising from the large particles (Fisher et al. 2007), which is why it is often preferred to the bob and cup geometry. It was shown (Keentok et al. 1985; Yan and James 1997) that an assumption of a uniform stress

distribution over a cylindrical yield surface around the rotating vane is valid for various kinds of yield stress fluids. The vane geometry may be used in both, infinite medium or in a cup (Barnes and Carnali 1990; Barnes and Dzuy Nguyen 2001; Fisher et al. 2007). In a latter case, the slippage may occur on the wall of the cup or external cylinder of the geometry that is in contact with the fluid. To prevent this kind of slippage, the inner surface of the cup may be roughened or grooved.

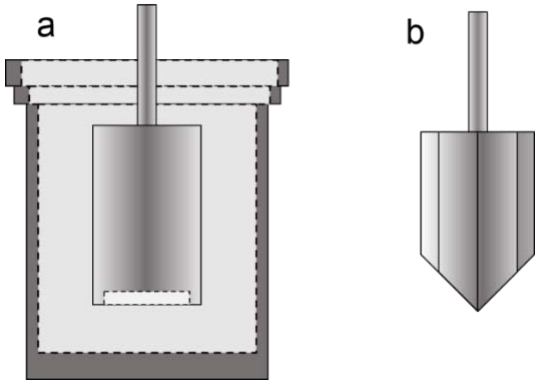


*Figure 5 – (a) concentric cylinder (Couette) and (b) vane geometries.*

Rheological measurement consists in stress application to the mater, usually aiming to simulate the real loadings experienced by the material during specific process, and collecting the rheological response. The response in this case is the measure of material's resistance against the applied stress. The forces applied to the matter and its response to the loading can be expressed with the following major parameters:

- torque ($T$), a flow resistance moment (otherwise, the shear force);
- rotational velocity ($\Omega$) – velocity of the inner rotating element (e.g., bob or vane);
- strain ($\epsilon$) - a measure of deformation describing the relative displacement of particles in the matter;
- shear stress ($\tau$) - a measure of internal forces occurring within the matter, it describes how the nearest particles interact with each other, $\tau \propto T$;
- shear rate ($\dot{\gamma}$) describes the rate of deformation of the matter in one single direction, it is a result of force acting per unit area, $\dot{\gamma} \propto \Omega$;
- viscosity ($\eta$) is a measure of material resistance to the applied loading.

Shear rate resulting from the rheological measurement is calculated via multiplication of the angular velocity by the shear rate factor; shear stress is extracted from multiplication of torque by a shear stress factor. Both factors are a function of the dimensions of utilized geometry. Shear stress is related to the shear rate via viscosity, see the eq 7,

$$\tau = \eta\dot{\gamma}. \qquad [7]$$

Depending on the response of the matter to the applied force, two main behavior patterns could be defined: Newtonian and non-Newtonian. Newtonian fluid is described with the linear shear stress-shear rate relation; its viscosity is constant for the same chemical composition, temperature and pressure. Non-Newtonian fluids are more complicated: apart from the parameters that influence the Newtonian fluid's viscosity, the viscosity of non-Newtonian fluid differs depending on the rate of the applied force, the history of the deformation and time period during which the matter was subjected to the loading. Non-Newtonian fluids have one more substantial parameter that is important to describe their behavior – the yield stress. The yield stress ($\tau_y$) is the minimum applied stress needed to initiate the flow (irreversible deformation) in the matter (Johnson et al. 2000). Mineral slurries can exhibit both, Newtonian and non-Newtonian behaviors and tend to exhibit the second one as the particle size decreases and the percent solid increases (Kawatra and Eisele 1988; Johnson et al. 2000; Boger 2009; Shabalala et al. 2011; Farrokhpay 2012; Xu et al. 2012). Figure 6 depicts the typical behaviors that various dispersions can exhibit under the load.

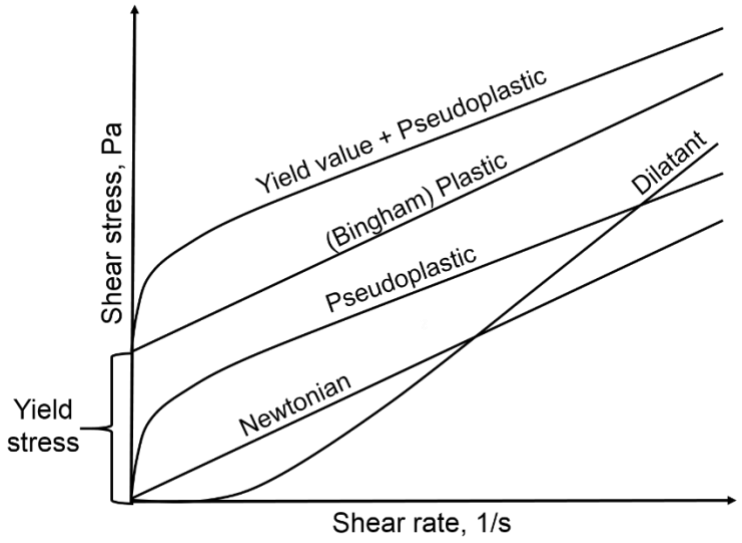


*Figure 6 - Schematic diagram of behavior of different fluids under the load (Tadros 2010).*

Newtonian fluid behavior can be found, for example, in stabile colloidal suspensions with low volumetric fraction of solids and repulsive electrostatic interactions or in simple liquids. Bingham plastic behavior (summarized in eq. 8) implies existence of a yield stress in the dispersion, such that below $\tau_y$ the $\eta \longrightarrow \infty$, and above $\tau_y$, $\eta$ is constant. This type of behavior can be found, for example, in mineral slurries (Farrokhpay 2012) and latex dispersions (Nashima and Furusawab 1991; Tadros 2010).

$$\tau = \tau_y + \eta_{pl}\dot{\gamma}, \qquad [8]$$

where $\eta_{pl}$ is a plastic viscosity (slope of the linear curve).

Pseudoplastic, also known as “shear thinning”, behavior was found in suspensions of polystyrene particles (Ishihara et al.). It is a usual behavior pattern for a variety of soft matters commonly utilized in everyday life, such as toothpaste, ball-point pen ink and molten chocolate (Tadros 2010). In this case the yield stress is absent and the fluid rather shows a limiting viscosity at low shear rates (η(0), named “residual” or “zero shear” viscosity). Ostwald de Waele model (see eq. 9) can be used to describe behavior of such fluids:

$$\tau = \kappa \dot{\gamma}^{n} \qquad [9]$$

where $\kappa$ is the consistency index and $n$ is the flow index; for the shear thinning matters $n<1$.

When a certain stress level (i.e., $\tau_y$) must be overcome in order to initiate the flow in the shear thinning fluid, one is dealing with a yield stress peudoplastic soft matter. Such matters are commonly described with eq. 10 (also known as Herschel–Bulkley model) and include mineral slurries (Boger 2009; Forbes et al. 2014), aqueous microgel dispersions (Kaneda 2016) and foams.

According to Tadros (2010), Herschel–Bulkley is the most widely utilized model for fitting the flow curves of dispersions.

$$\tau = \tau_y + \kappa \dot{\gamma}^{n}. \qquad [10]$$

Dilatant, or shear thickening, behavior is related to the presence of the close-packed structure in the soft matter; it, thus, can be found in the concentrated suspensions of solids (e.g., highly concentrated clay suspensions, wet sand). In dilatant fluids, the viscosity increases with the shear rate, which is often accompanied with the volume expansion of the fluid structure (Tanner 1985; Tadros 2010). Flow of a dilatant fluid can be described with the same power-law equation as the flow of pseudoplastic fluid (eq. 9), but with $n>1$.

Some complex fluids exhibit time-dependent rheological properties, meaning, that the viscosity of the fluid changes as a function of time of constant shearing. If the viscosity increases with the time under the constant load, the fluid is called “rheopectic”. On the other hand, if the viscosity decreases, the fluid is named “thixotropic”. In both cases structural rearrangements occurring in the complex fluid are responsible for the effect. In rheopectic fluid, the progressive *structure formation* is induced by shearing. In thixotropic fluid, the progressive *structure breakage* is induced by shearing. Both effects – establishing and breaking the structure under the constant load – are usually reversible. That is to say that when the load is removed the system returns to its initial state with the time of rest (Tanner 1985; Tadros 2010). Such behavior is often characterized with hysteresis in the flow curve, see example given in the Fig. 7. In the Fig. 7 the structured fluid is sheared with an increasing rate, which causes its internal structure to break until reaching complete destructuration at high shear rates. Immediately after the increasing

shear rate cycle, the decreasing shear rate cycle takes place. In the decreasing sequence of shear rates smaller shear stress is recorded. This is explained by lower amounts of energy required for the particle rearrangement in the unstructured system. Area within the loop depends on the degree of fluid structuring.

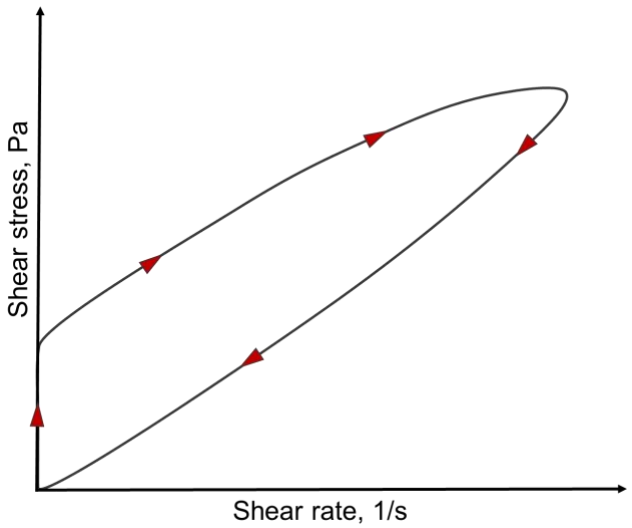


*Figure 7 - Schematic example of flow curve hysteresis in the thixotropic fluid (Tanner 1985); the arrows denote the direction of acquisition.*

An essential step towards a reliable rheological measurement lays in prevention of common errors. Most frequent sources of erroneous measurement of dispersion flow properties include:

- Sedimentation

Solid-liquid separation under the force of gravity has significant influence on the result of a rheological measurement. Due to the sedimentation, the volumetric fraction of suspended solids decreases which sometimes can lead to a dramatic change of the apparent rheological behavior of the suspension (e.g., from non-Newtonian to Newtonian). In a rotational rheometer, formation of a sediment around the moving inner piece of geometry (i.e., bob, cylinder or vane) can create a false impression of higher viscosity of the suspension under the measurement.

- Evaporation of the liquid phase

Liquid phase evaporation raises the effective solid volume fraction in the suspension. As a result, the flow properties of a system with different characteristics are measured. During the long-term experiments conducted in non-hermetic geometries, the suspension can thicken due to the loss of the liquid media. Such thickening over the course of the measurement can be easily confused with the thickening under the load.

- Particle migration (due to centrifugal force)

Particle migration towards periphery is a common problem when dealing with the suspensions of “inertial” particles. It is assumed that the measured matter (suspension) is homogeneous, implying that no stratification or concentration gradient is taking place. For example, in a Couette geometry, decreased solid volume fraction in layers of fluid near the inner rotating cylinder will result in a non-representative torque record. In cone and plate geometry, particle migration known to be one of the most important sources of experimental errors.

- Turbulence

When dealing with high shear rates, one may observe an apparent increase of viscosity with an increase in shear rate. The impression of dilatancy in this case is originating from the energy dissipation prompted by the turbulent eddies. There are empirical equations established to account for turbulence in the capillary and the pipe flows; however, the flow curves obtained in turbulent conditions in the concentric cylinder geometries are usually rejected (Tadros 2010).

- Chemical transformation of the matter during the experiment

Chemical reactions occurring within the suspension may change the nature of interactions of its constituents (e.g., via changing the chemistry of the EDL) and, thus, the rheological properties of the suspension. An intuitive example of a system affected by chemical transformation during the measurement is a suspension with dissolving solid constituents.

- Molecular rupture (long polymer chains)

When a molecule of a polymer is exposed to large amounts of stress, the polymer degradation via mechanical rupture takes place. In this case, the effective molecular

weight of a polymer is reduced and, hence, the viscosity of the soft matter decreases (Joshi and Denn 2003; Nødland et al. 2017; Al-Shakry et al. 2018).

- Wall slip

The wall slip effect is known to take place in the structured or weakly flocculated suspensions (Tadros 2010). In case of slippage in a Couette cell, the major flow assumptions are compromised, namely: 1) the fluid layer on the wall of external cylinder possesses zero velocity and/or 2) the fluid layer in contact with the internal cylinder has a velocity equal to the rotational velocity of the cylinder. Thereby, the slippage often results in erroneous estimation of the shear rate.

In theory, the rheological properties of slurries are determined by three major inputs (Zhou et al. 2000; Malhotra et al. 2009): hydrodynamic forces, Brownian motion, and colloidal forces. Hydrodynamic forces arise from shear-induced relative motion of particles in an uncompressible fluid. These forces are known to dominate at high shear rates. Brownian motion is a thermal randomizing force that determines the viscosity of soft matters at low shear rates (Zhou et al. 2000; Tadros 2010; Doi 2013). Brownian forces have noticeable effect in colloidal suspensions, where particles are smaller than 1 μm. In the suspensions with coarser particle sizes, the randomizing effect of Brownian motion is less or not at all pronounced. In a dispersion consisting of non-colloidal particles, the hydrodynamic forces are prevalent.

In a hard sphere suspension, where the rigid spheres are interacting with each other through a Newtonian fluid via hydrodynamic and Brownian forces, the suspension's viscosity shall only depend on the volumetric fraction of spheres, also known as "packing fraction", $\varphi$. In such system at low packing fractions (below approx. $\varphi$ = 0.15) the suspension behaves Newtonian and its viscosity can be readily calculated (Batchelor 1977; Zhou et al. 2000). Increasing the packing fraction results in establishment of two Newtonian plateaus at low and high shear rates, connected through a shear thinning region (see Fig. 8). First plateau situated in the Brownian region is attributed to the ability of the soft solid to maintain random equilibrium distribution under a mild shear. The low viscosity plateau in the hydrodynamic region is due to the particle alignment in the shear plane direction under intensive shearing. Particle displacement due to the Brownian motion or hydrodynamic forces has a characteristic time. Ratio of time, required for

Brownian ($t_B$) and hydrodynamic ($t_{\dot{\gamma}}$) rearrangements gives a dimensionless criteria, widely used in fluid mechanics - a Péclet number ($Pe$, 11, 12).

$$Pe = \frac{t_B}{t_{\dot{\gamma}}}, \qquad [11]$$

or, alternatively

$$Pe = \frac{2\dot{\gamma}\eta_f \pi a}{kT}, \qquad [12]$$

where $\eta_f$ is the viscosity of the suspending fluid (otherwise referred to as "solvent" or "suspending media"), $a$ is the radius of suspended particles, $k$ is the Boltzmann constant, $T$ is the temperature; $\dot{\gamma}\eta_f = \sigma$, meaning, the stress applied to the fluid, and $\frac{kT}{2\pi a}$ is the cohesive force within the fluid.

A conditional border between the Brownian and hydrodynamic regimes is where $Pe = 1$; it also corresponds to the critical shear rate, $\dot{\gamma}_c$.

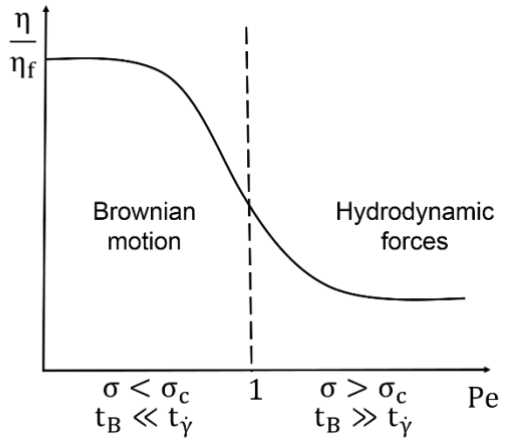


*Figure 8 - Schematic example of suspension flow curve, as a function of increasing $Pe$; φ is kept constant.*

Colloidal forces are elastic forces that are responsible for charging and agglomeration (or dispersion) of particles in the suspension. Origin, as well as the theory behind these forces, is explained in the chapter I, part II, "Inter-particle forces". Colloidal forces, like the Brownian forces, are the most influential in fine particle suspensions, at low and moderate shear rates. The importance of physico-chemical effects occurring in

mineral suspensions and their strong influence on the suspension rheology was highlighted by multiple scientists (e.g., Ohtsubo et al. 1991; De Kretser et al. 1998; Johnson et al. 2000; Zhou et al. 2000; Malhotra et al. 2009). The rheology of mineral pulps with high portion of fine (<10 μm) particles is often defined by the colloidal interactions occurring between those particles (Malhotra et al. 2009). Attractive interactions in the fine-particle mineral pulps result in aggregation and establishment of microstructures or networks. These networks often possess significant mechanical strength, and are responsible for such phenomena as yield stress, pseudoplasticity, dilatancy and thixotropy (Zhou et al. 2000; Malhotra et al. 2009).

Zhou et al. (2000) have shown the dependency of a yield stress of zirconia and titania suspensions from the pH and volumetric fraction of solids, by summarizing results from previously published reports (see Leong et al. 1993a, b; Liddell 1996; Leong 1999; Zhou 2000).The results evidenced that the yield stress of these suspensions increases as the pH of the suspension approaches the IEP of the particles of suspended metal oxide. The data obtained for different volume fractions of minerals ($\varphi$ = 0.12-0.24 for zirconia and 55-70 wt% for titania) was compared. The magnitude of the yield stress increased with the increasing volumetric fraction of mineral; in all cases, the highest $\tau_y$ was recorded at the IEP of the minerals under the study. Zhou (2000) and Zhou et al. (2000) has also investigated the influence of particle size on the yield stress of alumina suspensions ($\varphi$ = 0.3, average particle surface area diameters 0.19-0.58 μm), at different pH. Results evidenced an increased yield stresses in the proximity of IEP for all tested sizes; the magnitude of the yield stress and the viscosity of the suspension increased with decreasing particle size. Both, increased packing fraction and finer particle size result in higher density of inter-particle links, strengthening the suspension's microstructure.

It is rather uncommon to deal with the monodisperse systems when handling the mineral pulps and slurries. It is known, that in a hard sphere dispersion at a constant volume fraction of solid, a broad particle size distribution (PSD) can allow lower viscosity than a narrow distribution; however, in a flocculated (or aggregated) dispersion a broad PSD yields higher yield stress than a narrow PSD (Zhou et al. 1999, 2000). It was also found (Zhou et al. 1999) that the effect of the polydispersity on the yield stress can be well characterized by a surface area average diameter, and that the yield stress of a polydisperse flocculated suspension can be predicted using eq. 13:

$$\tau_{y\,poly} = \left( \sum_{i} x_{vi} \sqrt{\tau_{yi}} \right)^2, \qquad [13]$$

where $\tau_{y\,poly}$ is a yield stress of the polydisperse suspension, $x_{vi}$ is a volume fraction ration of the i-th suspension component and $\tau_{yi}$ is a yield stress of an i-th suspension component.

In otherwise even conditions ($\varphi$, PSD), a suspension of non-interacting hard spheres always gives the minimum viscosity; it also does not display a yield stress until the spheres are brought in contact (e.g., maximum packing fraction reached). On the other hand, addition of either attractive or repulsive interactions will yield an increased suspension viscosity and, possibly, cause occurrence of a yield stress (Zhou et al. 2000). In other words, nature and magnitude of particle-particle interactions can severely influence the bulk rheology of the suspension.

In an electrostatically stabile colloidal dispersion overall particle-particle interaction is repulsive. Such systems generally display Newtonian flow behavior. In order to simplify rheology of a flocculated (aggregated) mineral suspension one may attempt to influence its mechanical properties through the pH, moving it away from the IEP. In this case, the salt concentration shall be considered. Until a certain concentration (that depends on the type of salt and chemistry of the mineral phase), supplying salt to the mineral dispersion will result in an increasing particle-particle repulsion. This will yield reduced suspension viscosity. However, from a certain threshold, in the conditions of high ionic strength (high salt concentration and valency of ions-constituents), the particle EDL compresses, allowing for particle aggregation. Such aggregation results in an increase of suspension's viscosity (Zhou et al. 2000). Zhou (2000) and Zhou et al. (2000) reported rheology of the alumina suspensions with varying solid volume fraction ($\varphi$ = 0.4-0.6) at pH 5, 0.01 M $KNO_3$. The results evidenced that in conditions of constant ionic strength and pH (away form IEP), increasing the solid volume fraction results in a change of suspension behavior from almost Newtonian to shear thinning; a yield stress and shear thickening were found for their highest tested volume fraction. Shear thickening is usually found and attributed to the highly concentrated mineral suspensions. Nevertheless, Barnes (1989) suggested that the shear thickening shall take place in any suspension at sufficiently high shear rate, with respect to the condition that the particles do not mutually

attract. In the works of Zhou (2000) and Zhou et al. (2000) the occurrence of shear thickening in alumina suspensions ($\varphi$ = 0.56, 0.01 M $KNO_3$) was studied as a function of pH (4.3-6.8). As pH of the suspension was moved further away from the IEP of the mineral, shear thickening was manifested at increasingly higher shear stresses and shear rates. This was attributed to the decreased attraction between the particles. It was reported, that the increased salt concentration also yielded in occurrence of thickening at lower shear stresses and shear rates. In other words, the decrease in the repulsive interactions seems to facilitate thickening in such suspensions. In concentrated mineral suspensions, thickening is mostly reversible and can occur continuously, or abruptly (Zhou et al. 2000). Shear thickening in the suspension can be influenced through: volume fraction of particles, inter-particle interactions, particle PSD and their shape, and viscosity of suspending media. These findings are of importance to many industrial processes that involve material handling and transport (i.e., pipeline transport, agitation and stirring in tanks).

Coussot and Ancey (1998) have established a conceptual diagram (solid fraction vs shear rate) featuring the dominant interaction types, namely, Brownian, colloidal and hydrodynamic (see Fig. 9). In this diagram, it is assumed that all the other parameters, such as nature and viscosity of the suspending media, particle PSD and shape, ionic strength are constant and do not change with $\varphi$. Present work studied the "soft" suspensions (meaning, areas (A), (B), (C) and (D) in the Fig. 9). For the comments on the areas (E), (F), (G) and criteria $\mathrm{Le}$ and $\mathrm{Ba}$, situated between maximum packing fraction ($\varphi_m$) and critical fraction of solids ($\varphi_c$), the reader is reffered to the original work of Coussot and Ancey (1998). The parameters and criteria designated in the relevant areas of the Fig. 9 shall be specified below.

In the Fig. 9, area (A) corresponds to dominating Brownian effects, area (B) – to dominating of hydrodynamic effects; in the area (C), colloidal effects are prevalent; area (D) corresponds to domination of the turbulent effects.

The transition curve ( $N_r$ ) between the regime (A) and regime (C) is shear rate-independent and is determined by eq. 14. When $N_r$ <1, the Brownian interactions win over the colloidal interactions.

$$N_r = \frac{\Phi_0}{kT}, \qquad [14]$$

where $\Phi_0$ is an average energy barrier required to overcome when extracting a particle from its environment, after an infinite time of suspension rest.

The transition between the Brownian (A) and hydrodynamic (B) regimes was previously described in this chapter. It is characterized by the Péclet number (Pe, eq. 11, 12).

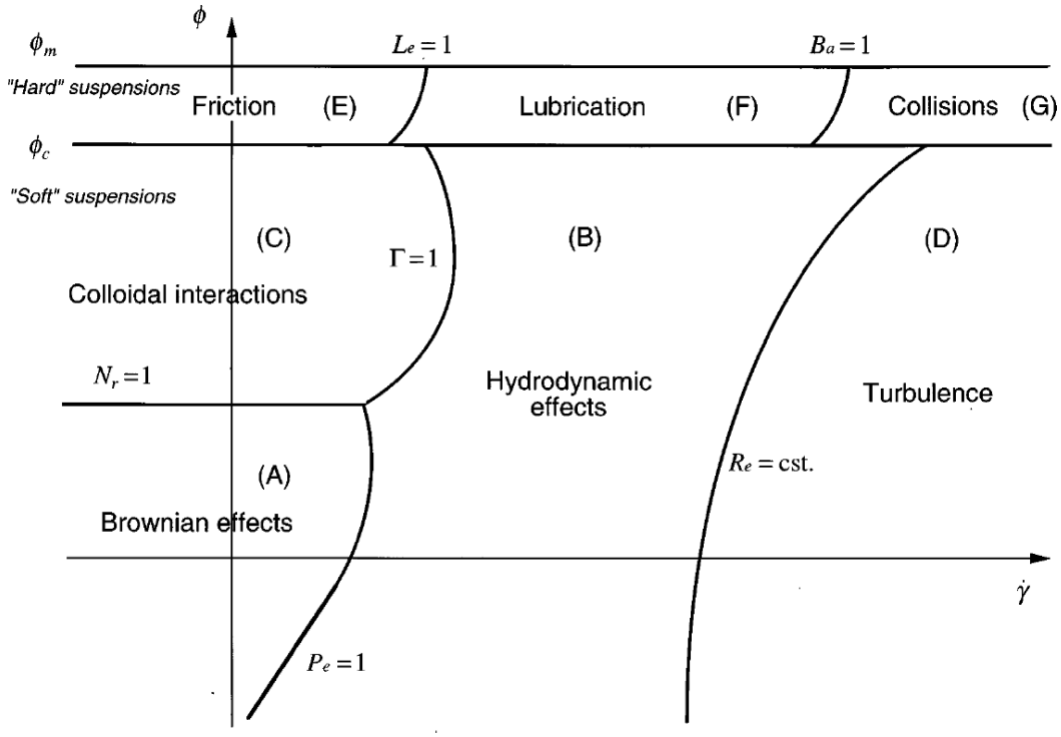


*Figure 9 - A diagram of predominant interactions within flowing concentrated suspensions under simple shear, logarithmic scale (Coussot and Ancey 1998).*

In case, when $N_r \gg 1$, it becomes possible to compare the importance of colloidal forces relative to hydrodynamic forces using eq. 15:

$$\Gamma = \frac{K\eta\dot{\gamma}b^2}{\Phi_0}, \qquad [15]$$

where $K$ is a size-, orientation- and shape-dependent coefficient (e.g., $K = 3\pi a$ for a sphere), $b$ is a characteristic mean distance between the two centers of neighboring particles.

At $\Gamma$ <1 the colloidal interactions (C) are winning over the hydrodynamic interactions (B). In the point, where $\Gamma$ =1, $Pe$ =1 and $Nr$ =1, colloidal, Brownian and hydrodynamic forces find themselves in a balance. $Re$ is the *macroscopic* Reynolds criteria given in the eq. 16,

$$Re = \frac{\rho\dot{\gamma}L^2}{\eta}, \qquad [16]$$

where $\rho$ is the viscosity of the suspension, $L$ is a characteristic dimension of the macroscopic flow characterized with a significant velocity variation. Reynolds number is the ratio of the viscous forces ($\rho\dot{\gamma}^2L^2$) and the hydrodynamic dissipation ($\eta\dot{\gamma}$).

It is often suggested that in the suspensions with non-colloidal particles, $\eta(\varphi) \to \infty$ as the $\varphi \to \varphi_m$, with overall Newtonian flow behavior. In these conditions, it is assumed that $\Phi_0$=0, meaning, that the colloidal interactions are negligible (regime (C) on the diagram in the Fig. 9 disappears), so are the Brownian effects, and the suspension behavior is fully controlled by the hydrodynamic component.

Coussot and Ancey (1998) proposed that the suspensions where the particle interactions determine the flow behavior shall be considered as “concentrated”, suggesting, that silica or clay suspensions with solid fractions of 0.1% fit this cretaria. From their diagram (Fig. 9) it follows that the dilute suspensions are characterized with Brownian plateau – shear thinning – turbulence, as the shear rate increases from low – to moderate – to high, respectively. In case of a concentrated colloidal suspension one deals with a yield stress, viscoelastic, thixotropic fluid, in which with increasing shear rate the hydrodynamic effects progressively become predominant, eventually giving place to the turbulence at the highest shear rates.

Main parameters influencing the rheology of aqueous suspensions include (but are not limited to): particle size, particle shape (most of the force models are considering spherical particles), chemistry of both: particles and suspending media (e.g., pH, type and concentration of electrolyte ions present), volumetric or mass fraction of the particles, presence of surfactants/polymers (Tanner 1985; Kawatra and Eisele 1988; Barnes et al. 1989; Johnson et al. 2000; Tadros 2010; Farrokhpay 2012; Doi 2013). These parameters are strongly overlapping with the ones that influence, for example, the flotation efficiency (see chapter I, part I, “Froth flotation”). In fact, it was highlighted by (Kawatra and Eisele 1988; He et al. 2004; Malhotra et al. 2009; Farrokhpay 2012) that rheological properties of pulps are an important factor to consider in variety of mineral processing operations, including: pumping and transport, grinding, classification and cyclonation, concentration under the force of gravity, flotation, mixing, agitation and leaching, thickening. In these operations non-Newtonian pulp flow characteristics directly affect the efficiency of the operation.

## Bibliography


Al-Shakry B, Skauge T, Shaker Shiran B, Skauge A (2018) Impact of Mechanical Degradation on Polymer Injectivity in Porous Media. Polymers (Basel) 10:742 . doi: 10.3390/polym10070742

Barnes HA (1989) Shear-Thickening ("Dilatancy") in Suspensions of Nonaggregating Solid Particles Dispersed in Newtonian Liquids. J Rheol (N Y N Y) 33:329–366 . doi: 10.1122/1.550017

Barnes HA, Carnali JO (1990) The vane-in-cup as a novel rheometer geometry for shear thinning and thixotropic materials. J Rheol (N Y N Y) 34:385 . doi: 10.1122/1.549926

Barnes HA, Dzuy Nguyen Q (2001) Rotating vane rheometry-a review

Barnes HA, Hutton JF, Walters K (1989) An Introduction to Rheology. Elsevier Science Publishers B.V.

Batchelor GK (1977) Effect of Brownian-Motion on Bulk Stress in a Suspension of Spherical-Particles. J Fluid Mech 83:97–117

Benna M, Kbir-Ariguib N, Magnin A, Bergaya F (1999) Effect of pH on Rheological Properties of Purified Sodium Bentonite Suspensions. J Colloid Interface Sci

Boger D V. (2009) Rheology and the resource industries. Chem Eng Sci 64:4525–4536 . doi: 10.1016/j.ces.2009.03.007

Coussot P, Ancey C (1998) Rheophysical classification of concentrated suspensions and granular pastes. Phys Rev E 59:4445–4457

De Kretser RG, Scales PJ, Boger D V (1998) Surface chemistry-rheology inter-relationships in clay suspensions. Physicochem Eng Asp 137:307–318

Doi M (2013) Soft Matter Physics, 1st edn. Oxford University Press., New York

Dzuy NQ, Boger D V. (1985) Direct Yield Stress Measurement with the Vane Method. J Rheol (N Y N Y) 29:335–347 . doi: 10.1122/1.549794

Farrokhpay S (2012) The importance of rheology in mineral flotation: A review. Miner Eng 36–38:272–278 . doi: 10.1016/j.mineng.2012.05.009

Fisher DT, Clayton SA, Boger D V, Scales PJ (2007) The bucket rheometer for shear stress-shear rate measurement of industrial suspensions. Cit J Rheol 51:821 . doi: 10.1122/1.2750657

Forbes E, Davey KJ, Smith L (2014) Decoupling rehology and slime coatings effect on the natural flotability of chalcopyrite in a clay-rich flotation pulp. Miner Eng 56:136–144 . doi: 10.1016/j.mineng.2013.11.012

He M, Wang Y, Forssberg E (2004) Slurry rheology in wet ultrafine grinding of industrial minerals: a review. doi: 10.1016/j.powtec.2004.09.032

Ishihara T, Takahashi F, Kuno H Pseudoplastic Flow of Suspensions of Large Spherical Polystyrene Particles

Johnson SB, Franks G V, Scales PJ, et al (2000) Surface chemistry–rheology relationships in concentrated mineral suspensions. Int J Miner Process 58:267–304

Joshi YM, Denn MM (2003) Rupture of entangled polymeric liquids in elongational flow. Cit J Rheol 47:135 . doi: 10.1122/1.1530622

Kaneda I (2016) Rheology of biological soft matter : fundamentals and applications. Springer

Kawatra SK, Eisele TC (1988) Rheological effects in grinding circuits. Int J Miner Process 22:251–259 . doi: 10.1016/0301-7516(88)90067-1

Keentok M, Milthorpe JF, O'donovan E (1985) On the shearing zone around rotating vanes in plastic liquids: theory and experiment. J Nonnewton Fluid Mech 17:23–35

Leong Y-K, Boger D V., Scales PJ, et al (1993a) Control of the Rheology of Concentrated Aqueous Colloidal Systems by Steric and Hydrophobic Forces. J Chem Soc Chem Commun 639–641 . doi: 10.1039/C39930000639

Leong YK (1999) Interparticle forces arising from an adsorbed strong polyelectrolyte in colloidal dispersions: charged patch attraction. Colloid Polym Sci 277:299–305 . doi: https://doi-org.bases-doc.univ-lorraine.fr/10.1007/s003960050385

Leong YK, Katiforis N, Harding DB, et al (1993b) Role of rheology in colloidal processing of ZrO2. J Mater Process Manuf Sci 445

Liddell P V. (1996) The rheology of titanium dioxide pigment suspensions. The University of Melbourne

Malhotra D, Taylor P, LeVier M, Spiller E (2009) Recent Advances in Mineral Processing Plant Design. In: Recent Advances in Mineral Processing Plant Design

Nashima T, Furusawab K (1991) The rheological behavior of a latex dispersion including a non-ionic polymer. Elsevier Sci Publ BV 55:149–161

Nødland O, Lohne A, Stavland A, Hiorth A (2017) A model for non-Newtonian flow in porous media at different flow regimes. Comput Geosci 21:1289–1312 . doi: 10.1007/s10596-017-9692-6

Ohtsubo M, Yoshimura A, Yong RN (1991) Particle interaction and rheology of illite-iron oxide complexes. Clays Clay Miner 39:347–354

Shabalala NZP, Harris M, Filho LSL, Deglon DA (2011) Effect of slurry rheology on gas dispersion in a pilot-scale mechanical flotation cell. doi: 10.1016/j.mineng.2011.07.004

Tadros TF (2010) Rheology of Dispersions: Principles and Applications

Tanner RI (1985) Engineering rheology. Oxford University Press, New York

Xu D, Ametov I, Grano SR (2012) Quantifying rheological and fine particle attachment contributions to coarse particle recovery in flotation. Miner Eng 39:89–98 . doi: 10.1016/j.mineng.2012.07.003

Yan J, James AE (1997) The yield surface of viscoelastic and plastic fluids in a vane viscometer

Zhou Z (2000) Rheology of metal oxide suspensions. The University of Melbourne

Zhou Z, Scales PJ, Boger D V (2000) Chemical and physical control of the rheology of concentrated metal oxide suspensions. Chem Eng Sci 56:2901–2920

Zhou Z, Solomon MJ, Scales PJ, et al (1999) The yield stress of concentrated flocculated suspensions of size distributed particles. J Rheol (N Y N Y) 43:651 . doi: 10.1122/1.551029

## I.IV. Clays

Beneficiation processes suitable for fine particles, such as flotation, are highly dependent on physico-chemical and mechanical properties of the pulp. In majority of cases the mechanics of the mineral pulp differs from the mechanics of Newtonian fluid and depends on the interactions between the suspended particles. Behavior of swelling clays is of a particular interest. In suspensions, these clays build various structures depending on the chemical environment of solvent. Apart from high aspect ratio and spatial chemical inhomogeneity of each particle, suspensions of swelling clays possess thixotropic properties (Abu-Jdayil 2011), often with the yield stress (Tombácz and Szekeres 2004; Zhang and Peng 2015). In flotation process, clays frequently appear to be problematic.

Indeed, beneficiation experts refer to clays as “flotation nightmare”, as this group of minerals possesses all the negative properties of the fine particles, including:

- Changing the froth stability (Farrokhpay et al. 2016; Leistner et al. 2017);
- Changing the bubble size (Shabalala et al. 2011);
- Increasing the pulp viscosity (and causing the turbulence damping) (Zhang and Peng 2015; Taner and Onen 2016);
- Cavern development in the flotation cell (Bakker et al. 2010; Shabalala et al. 2011; Taner and Onen 2016);
- Over-consumption of reagents (Leistner et al. 2017);
- Slime coating (Leistner et al. 2017);
- Mechanical entrainment (Taner and Onen 2016; Leistner et al. 2017).

Processing issues related to high clay contents are not exclusively encountered in the flotation process. Significant amount of problems up and down the material stream were also reported (Connelly 2013; Ndlovu et al. 2013; Gräfe et al. 2017). Efficiency of crushing and screening is often related to the presence of clays. Moist ores with high clay contents become sticky; that causes reduced efficiency of sieving due to the plugged grid apertures (phenomenon, also referred to as “blinding”). Bridging takes place in the cone crushers; dead zones of stagnant (non-flowing) material are formed in the tanks, hoppers and bins designed for storage and feeding. Presence of clay in the ore often justifies

installation of the conveyer washers. Functionality of mills and classification devices is highly affected by the increased pulp viscosity (caused by clays). Kinetics of the grinding media (e.g., balls in a ball mill) is reduced in the conditions of high slurry viscosity. Increased sedimentation time in the spiral classifier and accumulation of the material on the spiral provides less sharp separation. Decreased separation sharpness due to the high clay contents was also reported in the hydrocyclones. Affecting the settling rates of other minerals particles (through increased viscosities and establishment of heterocoagulated particle network), the clays complicate thickening, dewatering in ponds and tailing drainage. Compressibility of clay suspensions is known to negatively affect filtering. Lower water recoveries and clay-contaminated water overflows cause problems with water recirculation in the mineral processing plants. High clay contents in the ores put limitation on the choice of the pumping devices and often cause inadequate pumping capacities. Efficiency of piping is entirely dependent on the mechanical properties of slurries with the high clay content; knowing the slurry rheology for this transporting method is a must. Presence of clays is also known to cause low percolation in the heap leaching. Fine clay particle size yields an unwanted entrainment with the liquid phase in the separation processes, such as dense media, magnetic and high intensity magnetic separation, causing media contamination and decreased concentrate grades.

The effect of a clay on the mineral beneficiation process chain will depend on the quantity of the clay in the feed of each operation and on the type of the clay. Clay minerals are hydrous aluminum silicates classified in the following groups (Murray 2007): kaolin, smectite, palygorskite-sepiolite, illite, chlorite and mixed-layered clays. These groups unite different clay minerals basing on their structure and composition. In mineral processing, the term “clay” can also refer to the particle size (i.e., size fraction <0.002 mm). Some phyllosilicates, such as mica and talc, are not classified as “clays” from mineralogical point of view, but are often called so due to their tendency to concentrate in the fine particle size fractions.

Clay structure and composition define the physical and chemical properties of clays, and thus, their behavior in the processing operation. In this work, mechanical properties of clay suspensions were studied. For such suspensions, properties of major interest are swelling and the ion exchange capacity. Smectite clays (such as montmorillonite and bentonite) are highly swelling clays, with high cation exchange capacity. Kaolinite has low swelling and cation exchange capacities. Illite is a

non-expending clay with higher cation exchange capacity than the one of kaolinite, but lower than that of smectites. Different behavior of swelling and non-swelling clays in froth flotation was previously reported (Wang et al. 2015; Farrokhpay et al. 2016). Major influence on flotation performance was found to result from presence of swelling clays. Strongly reduced grade and recovery, high pulp viscosity and modified froth stability were reported for montmorillonite. Kaolinite was found to increase the froth stability, whereas Illite barely had any influence. Kaolinite and illite were found to contaminate the concentrate through particle entrainment. The negative effects caused by the presence of non-swelling clays were small comparing to that of the swelling clays. It was found (Burdukova et al. 2008; Ndlovu et al. 2014) that among phyllosilicates, commonly encountered in the mineral beneficiation industry, vermiculite, kaolinite and talc are unlikely to give complex viscosity patterns in the conditions of moderate shear, however, it is not the case for smectites, which have a dramatic effect on the viscosity of mineral pulps.

In this work, a bentonite clay was utilized. Bentonite is an aluminum phyllosilicate clay, composed mostly of montmorillonite with some other minerals present in low amounts (e.g. quartz, various oxides). It is well known and widely utilized due to its swelling and absorbing properties in multiple industries from medicine and cosmetics to waste disposal and drilling muds (Boger 2009; Abu-Jdayil 2011). There are several types of bentonite, Ca-bentonite and Na-bentonite, with the latter having higher swelling capacity. Fig. 10 illustrates the schematic structure of smectite clays (Murray 2007). Each particle of montmorillonite consists of sandwich-like sheets (or unit layers) held together via van der Waals force; a single sheet (unit layer) in this case is constructed with three layers: an octahedral alumina layer with two tetrahedral silica layers on both sides of it (Luckham and Rossi 1999). Distance between the $SiO_2$-$Al_2O_3$-$SiO_2$ sheets is of the order of 12 to 15 Å, with hydrated exchange cations (e.g., $Na^+$, $Ca^{2+}$, $Mg^{2+}$). It is known that the swelling capacity of bentonite (montmorillonite) is limited in certain media, such as ethanol (Chegbeleh et al. 2009; Tan et al. 2017).

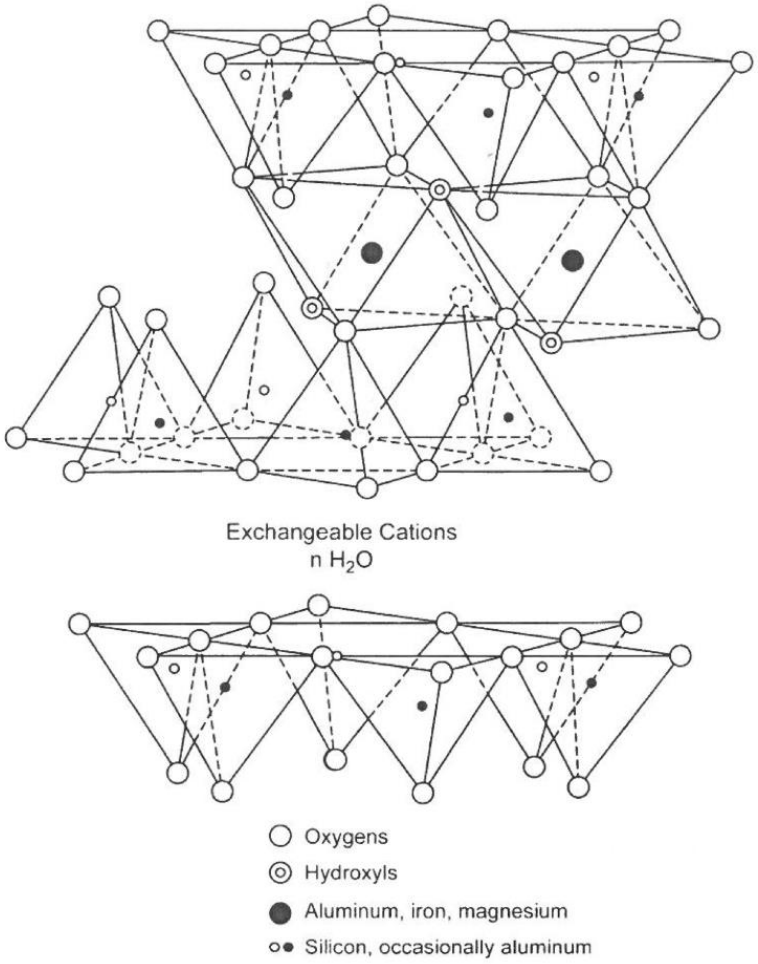


*Figure 10 - Schematic structure of smectites (Murray 2007).*

For the theoretical explanation and modelling, bentonite particles are often approximated as sheets or discs with high aspect ratio, i.e., 100-1000 times, between the face and the edge (Miyahara et al. 1998). Once the particle is immersed in aqueous salt solution, the difference in chemical composition of the face and the edge of the particle causes heterogeneity of electric charge distribution on its surface. Permanent negative charge on the face of the bentonite particles originates from the isomorphous substitutions. A pH-dependent charge is established on the edges of the particles. It originates from the ions attracted from the solution to the broken chemical bonds exposed on the edge. Acidic environment causes the edge of the particle to gain a positive charge, basic environment results in a negative charge on the edge; the charge of the face remains negative in all the pH range. In other words, the charge on the face and the edge of the

particles may differ not only in magnitude, but can be of an opposite sign, depending on the chemistry of the solution. It was reported that the edges of bentonite possess an IEP around pH 7-8 (Benna et al. 1999; Durán et al. 2000), meaning that at pH below the positive charge should dominate on the edge; at pH above the IEP– negative charge is dominant, and at pH 7-8 positive and negative sites on the edge balance each other. Some reports also suggest the IEP of bentonite edges at pH 4-5.3 (Pecini and Avena 2013). Due to little quantitative input of the edge in the overall particle charge, the bentonite particles are usually negatively charged in the whole pH range. An apparent negative particle charge is a common phenomenon for sheet silicates. Ndlovu et al. (2011) used the magnitude of difference between the IEP and PZC of the phyllosilicates (vermiculite and muscovite) to judge on the input of the face in the overall particle charge. More precisely, the authors suggested that in case of vermiculite (IEP at pH 3.3, PZC at pH 8.4) the faces carry strong negative charge, and in case of muscovite (IEP at pH 5.4, PZC at pH 4.6), on contrary, the faces carry a weak negative charge.

When multiple bentonite particles immersed in acidic solution are brought close enough to interact, they may organize in a way that the positive sites of one particle are oriented towards negative sites of another particle, resulting in a continuous network that is commonly referred to as “cubic card house” (van Olphen 1964). It is well-known that this kind of structuring results in high stresses (viscosities) at relatively low volume fractions of solid (Goh et al. 2011). At constant electrolyte concentration, several types of particle associations can occur in a bentonite suspension. Those types include: edge-to-face (E-F, dominant in “cubic card house”), edge-to-edge (E-E) or no dispersion whatsoever, as a function of pH (Benna et al. 1999; Luckham and Rossi 1999; Tombácz and Szekeres 2004), see Fig. 11. Association of E-F type is led by mutual attraction of oppositely charged sites, whereas E-E association is rather led by insufficient repulsion between the particle edges. That means that once the pH of the suspending media is close to the IEP of the edge, the energy barrier created due to electrostatic repulsion between the edges is too small to prevent edges from approaching due to van der Waals attraction, hence, the E-E association is established. Same mechanism works for the E-F association at the IEP of bentonite edge. In this case, dominating van der Waals attraction is accompanied by a slight attraction between the positive sites on the edges and the negatively charged particle faces. At pH above IEP, the edges and the faces of bentonite particles are negatively charged and mutually repel resulting in no association. Face-to-face (F-F) association is also possible, however this association type is most frequently

reported in the suspensions with high ionic strength of dispersing media (Luckham and Rossi 1999; Tombácz and Szekeres 2004). In this case, F-F association is justified by the compression of the double layers surrounding the bentonite particles.

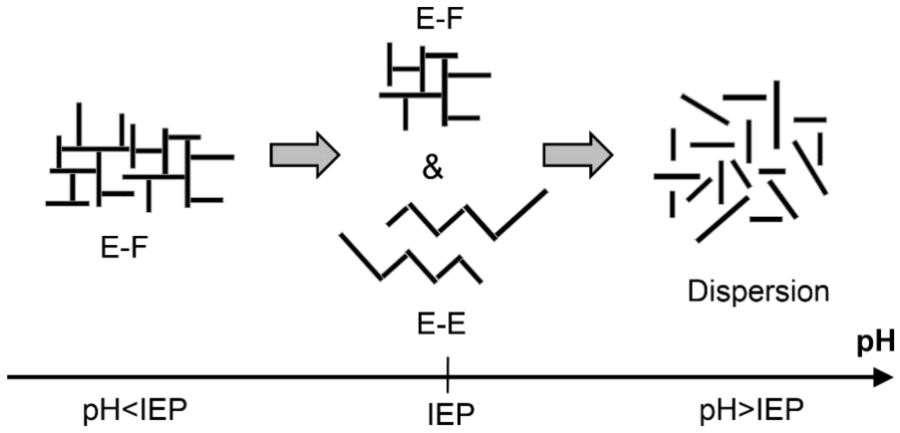


*Figure 11 - Schematic particle-particle associations in the solutions of different pH.*

In addition to the effect of the pH, the type and concentration of salt can also affect the bentonite particle association. Comprehensive study made by Tombácz and Szekeres (2004) suggested that below a certain salt concentration the double layer induced by the face "covers" the one of the edge – a "hidden double layer" is created. This situation prohibits bentonite lamellae from the structure formation. Above the threshold electrolyte concentration ($1 \times 10^{-2}$ M NaCl), the EDL of the edge "becomes visible" for other particles, and the structuring shall take place. To define the border between positively and negatively charged edges they used the concept of PZC, which was found to be at pH 6.5 for the bentonite edges. They also suggested that decrease in rheological properties in basic pH at $1 \times 10^{-2}$ - $1 \times 10^{-1}$ M of NaCl is governed by inter-particle electrostatic repulsion. Arrangement of F-F type takes place due to the EDL compression at high salt concentrations (≥$1 \times 10^{-1}$ M NaCl). This association type is characterized with large densely packed separate units that do not form a continuous structure (Luckham and Rossi 1999). Multiple studies showed the general trend of lower shear and yield stresses corresponding to increased ionic strength of solution (Kelessidis et al. 2007; Abu-Jdayil 2011).

Several works performed on the phyllosilicate minerals resulted in more or less general conclusions that can be applied within the group of similar minerals (e.g., platy, swelling). For example, Rand and Melton (1977) have established a qualitative diagram, featuring Bingham yields stress of kaolinite suspension as a function of pH, at low ionic strength (see Fig. 12). This diagram implies that the highest yield stresses correspond to the E-F association, lower ones – to the E-E and E-F associations combined, and no yield stresses when the particles are fully dispersed. Same qualitative response is expected for the bentonite suspensions.

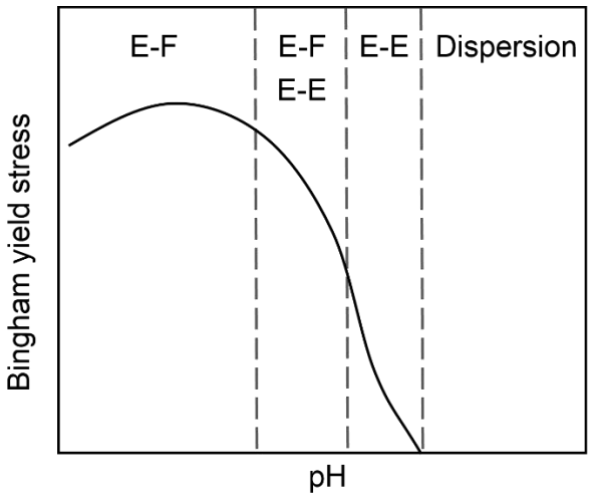


*Figure 12 - Bingham yields stress of kaolinite suspension as a function of pH, at low ionic strength (adapted from Rand and Melton, 1977).*

Ndlovu et al. (2011) have demonstrated the complexity of rheological behavior of phyllosilicate minerals (on the example of vermiculite and muscovite) in comparison to the isotropic minerals (in their case, quartz) and suggested a brief classification given in the Fig. 13. In this classification, smectites fall into the “spongy phyllosilicates” group. It was accented that the surface charging of tested sheet minerals is “central to the rheological behavior” of their suspensions. Smectites were suggested to have modest yield stresses, but more complex share rate-share stress relations.

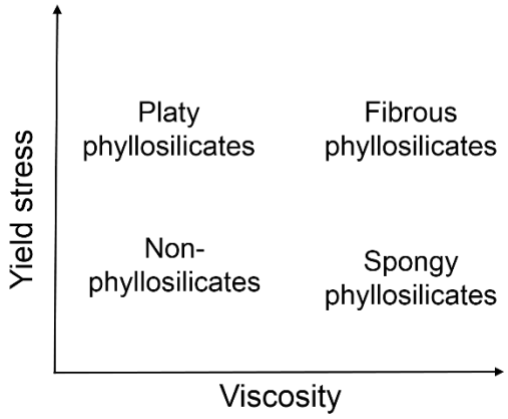


*Figure 13 - Classification of phyllosilicate minerals as a function of their shape and mechanical properties (adapted from Ndlovu et al., 2011).*

Thixotropy is a reversible time-dependent shear thinning property of soft matters (Tadros 2010), for more information about thixotropy see the chapter I, part III, “Rheology” and chapter II. Bentonite and montmorillonite dispersions are well-known to possess thixotropic properties. The area of thixotropic loop as a function of pH was measured by Tombacz and Szekeres (2004). It was found that the highest hysteresis area was obtained in the conditions of lowest tested pH (~ pH 5), meaning E-F association with the biggest difference in charge of the face and the edge. Thixotropic properties of clay dispersions are becoming more pronounced as the volumetric fraction of solid increases (Abu-Jdayil 2011). It was also demonstrated that the higher $Na^{+}/Ca^{2+}$ ratio in bentonites enhances the thixotropic behavior of bentonite suspensions (Abu-Jdayil 2011). From the above said it follows that the robust rheological measurement should take into account sensitivity of the suspension to the history of applied load.

Bentonite swelling does not happen instantaneously, this process is characterized with a certain kinetics that also affects the rheological response of the system. Aging time is a parameter that reflects the time period during which bentonite particles are exposed to the excess water available for the inter-sheet hydration and chemical transformations. As the aging time increases, thixotropy of the suspension becomes more pronounced, and the yield stress increases. It was reported (Abu-Jdayil 2011) that the major change was observed within first 24 h, and less significant changes took place in the following 24 h (48 h of saturation in total).

One more important parameter that influences the rheology of bentonite suspensions is the temperature. Temperature increase significantly affects the rheology of bentonite suspensions at "low" ($<200s^{-1}$) shear rates. Although, with the temperature increase higher stresses are obtained, the effect diminishes at "high" shear rates ($\gg 200s^{-1}$). The behavior of different bentonites may differ; but in the study on the temperature influence on the rheology of Wyoming sodium bentonite suspensions, the yield stress value increased linearly with the temperature (Vryzas et al. 2017).

All the conditions and parameters introduced above (i.e., pH, salt type and concentration, type of bentonite, temperature, ageing time) had to be fixed and respected when dealing with a system composed of pure bentonite clay suspended in the aqueous salt solution or its mixture with other minerals, suspended in the solution of the same nature.

In general, colloidal suspensions, depending on solid volume fraction and particle-particle interaction can flow – state is referred to as "sol" (e.g., low solid concentration, no inter-particle attraction), or cease to flow – state referred to as "gel" (e.g., high solid concentration, strong particle network). A transition from sol to gel may be promoted by manipulating the particle-particle interaction within the colloid (Doi 2013), as in case of bentonite suspensions at different pH. However, for bentonite suspensions under the shear coexistence of flowing and static zones of material simultaneously in one volume is possible (Coussot et al. 2002; Raynaud et al. 2002; Ovarlez et al. 2009). Phenomena characterized with such solid-liquid coexistence are referred to as "localization" and "banding", these are discussed in detail in chapter II.

## Bibliography


Abu-Jdayil B (2011) Rheology of sodium and calcium bentonite-water dispersions: Effect of electrolytes and aging time. Int J Miner Process 98:208–213 . doi: 10.1016/j.minpro.2011.01.001

Bakker CW, Meyer CJ, Deglon DA (2010) The development of a cavern model for mechanical flotation cells. In: Minerals Engineering. pp 968–972

Benna M, Kbir-Ariguib N, Magnin A, Bergaya F (1999) Effect of pH on Rheological Properties of Purified Sodium Bentonite Suspensions. J Colloid Interface Sci

Boger D V. (2009) Rheology and the resource industries. Chem Eng Sci 64:4525–4536 . doi: 10.1016/j.ces.2009.03.007

Burdukova E, Becker M, Ndlovu B, et al (2008) Relationship Between Slurry Rheology and its Mineralogical Content. XXIV Int Miner Process Congr 2169–2178

Chegbeleh LP, Nishigaki M, Akudago JA, et al (2009) Laboratory Investigation of Ethanol / Bentonite Slurry Grouting into Rock Fractures : Preliminary Results. 14:23–28

Connelly D (2013) The Difficult Mineral Processing Issues with Clay Ores

Coussot P, Nguyen QD, Huynh HT, Bonn D (2002) Viscosity bifurcation in thixotropic, yielding fluids. J Rheol (N Y N Y) 46:1213–847 . doi: 10.1122/1.1459447

Doi M (2013) Soft Matter Physics, 1st edn. Oxford University Press., New York

Durán JDG, Ramos-Tejada MM, Arroyo FJ, González-Caballero F (2000) Rheological and Electrokinetic Properties of Sodium Montmorillonite Suspensions I. Rheological Properties and Interparticle Energy of Interaction. J Colloid Interface Sci 229:107–117 . doi: 10.1006

Farrokhpay S, Ndlovu B, Bradshaw D (2016) Behaviour of swelling clays versus non-swelling clays in flotation. Miner Eng 96–97:59–66 . doi: 10.1016/j.mineng.2016.04.011

Goh R, Leong YK, Lehane B (2011) Bentonite slurries-zeta potential, yield stress, adsorbed additive and time-dependent behaviour. Rheol Acta 50:29–38 . doi: 10.1007/s00397-010-0498-x

Gräfe M, Klauber C, McFarlane AJ, Robinson DJ (2017) Clays in the minerals processing value chain

Kelessidis VC, Tsamantaki C, Dalamarinis P (2007) Effect of pH and electrolyte on the rheology of aqueous Wyoming bentonite dispersions. Appl Clay Sci 38:86–96 . doi: 10.1016/j.clay.2007.01.011

Leistner T, Peuker UA, Rudolph M (2017) How gangue particle size can affect the recovery of ultrafine and fine particles during froth flotation. Miner Eng 109:1–9 . doi: 10.1016/j.mineng.2017.02.005

Luckham PF, Rossi S (1999) The colloidal and rheological properties of bentonite suspensions. Adv Colloid Interface Sci 82:43–92

Miyahara K, Adachi Y, Nakaishi K (1998) The viscosity of a dilute suspension of sodium montmorillonite in an alkaline state. Colloids Surfaces A Physicochem Eng Asp 131:69–75 . doi: 10.1016/S0927-7757(96)03961-1

Murray HH (2007) Applied Clay Mineralogy - Occurrences, Processing and Application of Kaolins, Bentonites, Palygorskite-Sepiolite, and Common Clays

Ndlovu B, Becker M, Forbes E, et al (2011) The influence of phyllosilicate mineralogy on the rheology of mineral slurries. Miner Eng 24:1314–1322 . doi: 10.1016/j.mineng.2011.05.008

Ndlovu B, Farrokhpay S, Bradshaw D (2013) The effect of phyllosilicate minerals on

mineral processing industry. Int J Miner Process 125:149–156 . doi: 10.1016/j.minpro.2013.09.011

Ndlovu B, Forbes E, Farrokhpay S, et al (2014) A preliminary rheological classification of phyllosilicate group minerals. Miner Eng 55:190–200 . doi: 10.1016/j.mineng.2013.06.004

Ovarlez G, Rodts S, Chateau X, Coussot P (2009) Phenomenology and physical origin of shear localization and shear banding in complex fluids. Rheol Acta 48:831–844 . doi: 10.1007/s00397-008-0344-6

Pecini EM, Avena MJ (2013) Measuring the isoelectric point of the edges of clay mineral particles: The case of montmorillonite. Langmuir 29:14926–14934 . doi: 10.1021/la403384g

Rand B, Melton IE (1977) Particle Interactions in Aqueous Kaolinite Suspensions I. Effect of pH and Electrolyte upon the Mode of Particle Interaction in Homoionic Sodium Kaolinite Suspensions. J Colloid Interface Sci 60:308–320

Raynaud JS, Moucheront P, Baudez JC, et al (2002) Direct determination by nuclear magnetic resonance of the thixotropic and yielding behavior of suspensions. J Rheol (N Y N Y) 46:709–732 . doi: 10.1122/1.1463420

Shabalala NZP, Harris M, Filho LSL, Deglon DA (2011) Effect of slurry rheology on gas dispersion in a pilot-scale mechanical flotation cell. doi: 10.1016/j.mineng.2011.07.004

Tadros TF (2010) Rheology of Dispersions: Principles and Applications

Tan X, Liu F, Hu L, et al (2017) Evaluation of the particle sizes of four clay minerals. doi: 10.1016/j.clay.2016.10.012

Taner HA, Onen V (2016) Control of clay minerals effect in flotation . A review. 2:6–11 . doi: 10.1051/e3sconf/20160801062

Tombacz E, Szekeres M (2004) Colloidal behavior of aqueous montmorillonite suspensions: The specific role of pH in the presence of indifferent electrolytes. Appl Clay Sci 27:75–94 . doi: 10.1016/j.clay.2004.01.001

Tombácz E, Szekeres M (2004) Colloidal behavior of aqueous montmorillonite suspensions: the specific role of pH in the presence of indifferent electrolytes. Appl Clay Sci. doi: 10.1016/j.clay.2004.01.001

van Olphen H (1954) Interlayer forces in bentonite. Clays Clay Miner 418–438

van Olphen H (1964) Internal mutual flocculation in clay suspensions. J Colloid Sci 19:313–322 . doi: 10.1016/0095-8522(64)90033-9

Vryzas Z, Kelessidis VC, Nalbantian L, et al (2017) Effect of temperature on the rheological properties of neat aqueous Wyoming sodium bentonite dispersions. Appl Clay Sci 136:26–36 . doi: 10.1016/j.clay.2016.11.007

Wang Y, Peng Y, Nicholson T, Lauten RA (2015) The different effects of bentonite and kaolin on copper flotation. doi: 10.1016/j.clay.2015.05.008

Zhang M, Peng Y (2015) Effect of clay minerals on pulp rheology and the flotation of copper and gold minerals. Miner Eng 70:8–13 . doi: 10.1016/j.mineng.2014.08.014

## I.V. Mix mineral systems

Naturally, mineral suspensions encountered in mineral extraction and processing industries are characterized with inhomogeneous composition of solid. It is common to encounter different mineral phases, polydispersity and various kinds of shapes within the same material flow stream. In the Fig. 14, the reader can see the zeta-potential vs pH curves of two minerals: quartz and hematite (Forbes and Franks 2013). Here, 25 °C curves are of interest (hollow symbols). These curves suggest, that once immersed in the solution with, let's say, pH 6, the charge of hematite particles becomes positive and of quartz particles - negative. As it was explained in the chapter I, part II "Inter-particle forces", when immersed in water, the minerals gain a charge and, if the charge is pH-dependent, an IEP. For oxide minerals (in contrary to sulfides) the IEP is generally situated around some fixed pH value above which the mineral is negatively charged and below which it is charged positively. For quartz, the IEP is situated around pH 3, and for hematite – generally, between pH 7 and 9 (Kosmulski 2016). That means, that once the particles of these minerals are immersed in the aqueous salt solution at pH between their IEPs they can aggregate due to the electrostatic attraction raising between them. Furthermore, inhomogeneously charged minerals, for example phyllosilicates (Durán et al. 2000; Ndlovu et al. 2014), can have one particle site attracting and another one – repelling from its neighbor-particle in polymineral suspension. It is very common to have minerals with different IEPs suspended together in the material flows.

In the system, where the force balance is simplified to the product of van der Waals and electrostatic interaction, heterocoagulation shall take place in two cases: 1) surfaces attract for they possess an opposite charge, 2) surface charge is of the same sign, but existing energy barrier is insufficient to resist attraction due to van der Waals force.

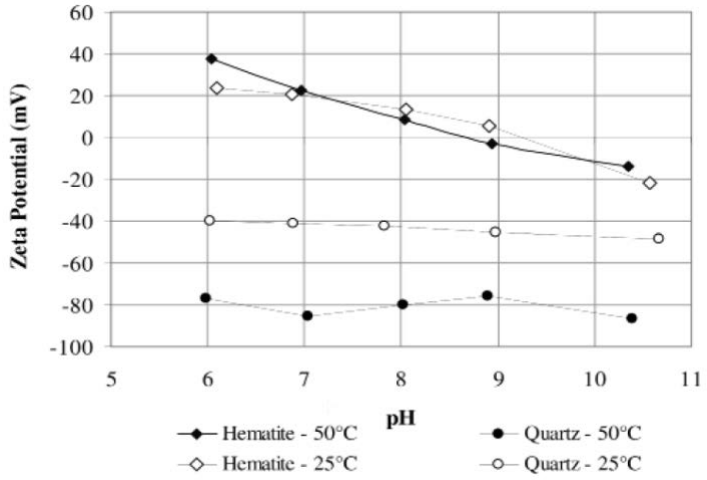


*Figure 14 - Zeta-potential of quartz and hematite as a function of pH (Forbes and Franks 2013).*

From the point of view of ideal system of non-interacting monodisperse spherical particles, an addition of smaller spheres to the voids occurring between the bigger spheres allows to increase the volume fraction of solids and, thus, to give raise to the suspension's viscosity (Tadros 2010). Polydisperse suspensions are known to allow high volume fractions and enhanced mechanical strength in comparison to suspensions with just one particle size. In the mineral streams, polydisperse solids are very common due to the properties of minerals and the grinding methods utilized. Different grindabillity of minerals involved in the same size reduction processes also contributes to polydispersity. A negative effect associated with polydispersity in concentrated systems is known as "crowding" – flow inhibition due to the close particle packing.

Shape of the particles plays an important role in behavior of the particle in the fluid flow. Flat particles, for example, tend to align with the flow (Grieger and Press 1996). Particle shape can significantly influence the maximum packing fraction of solids that suspension can accommodate (Barnes et al. 1989). It was shown that suspensions of particles of different shape do not perform rheologically in the same manner (Fig. 15, Clarke 1967).

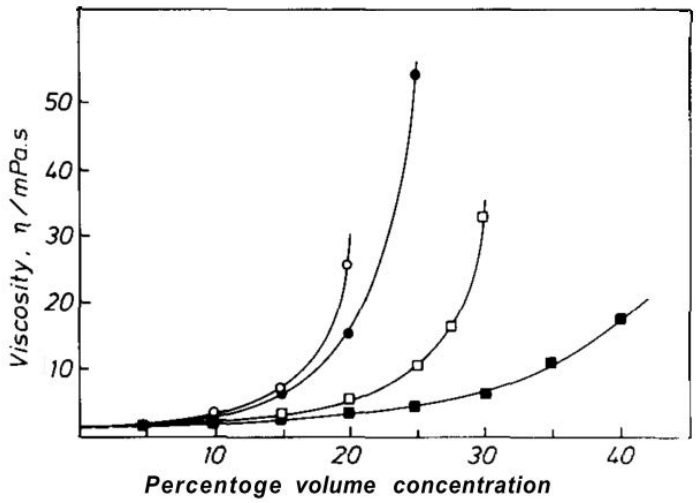


*Figure 15 - Viscosity as a function of particle shape (aqueous suspension measured at 300 $s^{-1}$); spheres (filled squares); grains (hollow squares); plates (filled circles); rods (hollow circles) (Clarke 1967; Barnes et al. 1989).*

All the above described characteristics attribute to the rheology of the mix mineral suspensions simultaneously, often yielding their significant rheological complexity. Rheology of heteroflocculated suspensions more and more attracts the attention of scientific community nowadays. Multiple works in this domain were dedicated to the charge-induced heteroflocculation of minerals with clays. In such works, authors often suggest their hypothesis of inter-particle organization that caused particular mechanical response. For example, Hilhorst et al. (2014) suggested the inter-particle organization occurring between the anionic or cationic silica and montmorillonite clay depicted in the Fig. 16a. On this image (Fig. 16a) the pH 5 case corresponds to attractive interaction between the clay and silica particles and pH 10 – to the repulsive interaction. In all cases (pH 5, 7 and 10) studied by Hilhorst et al. (2014) addition of anionic silica particles was found to weaken the gel yielding reduced rheology. On the other hand, Bailey et al. (2014) suggested an organization depicted in the Fig 16b for silica-montmorillonite system. They proposed that the resulting organization of silica particles and the montmorillonite gel of the same charge will depend on the concentration at which hydrodynamic radii of clay particles start to overlap. Below this concentration the precipitating heterocoagulated aggregates are formed and above – a reinforced heterocoagulated network is established (Fig. 16b).

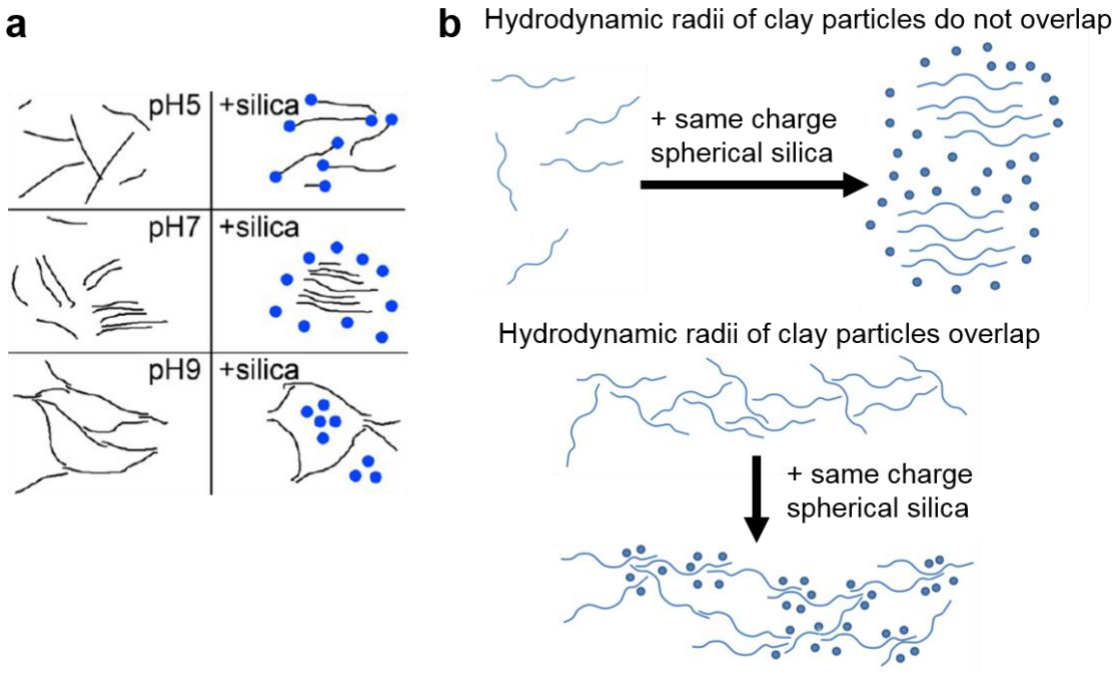


*Figure 16 - Charge-induced inter-particle organization between silica and montmorillonite suggested by (a) Hilhorst et al. (2014) and (b) Bailey et al. (2014).*

Tombácz et al. (2001) suggested that heterocoagulation of dissimilarly charged colloidal particles of clay and metal oxide at pH below 7 should look as depicted in the Fig. 17. Ji et al. (2004) provided schema of organization of montmorillonite and synthetic hematite particles depicted in the Fig. 18. They also suggested that the size of the synthetic hematite particles can be changed to manipulate the rheological properties of a resulting composite.

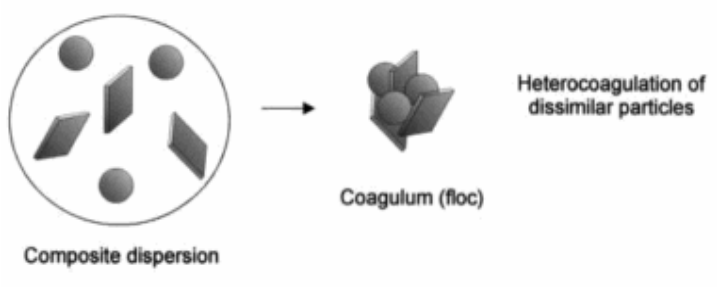


*Figure 17 - Schematic representation of heterocoagulated network formed between the clay particles and the particles of metal oxide (Tombácz et al. 2001).*

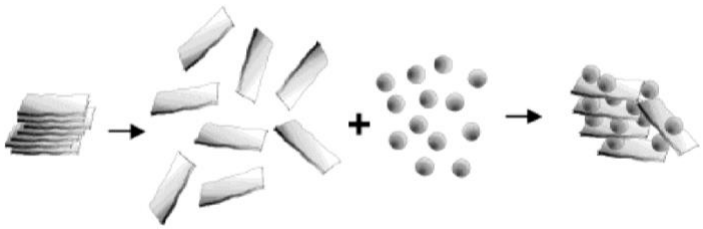

*Figure 18 - Schematic illustration of montmorillonite delamination and formation of the heteroflocculated association with hematite (Ji et al. 2004).*

A comprehensive study made by ten Brinke et al. (2007) conducted on charge- and shape-heterogeneous suspensions yielded some valuable conclusions. These are: 1) similarly charged particles of different shape added to the structured network disrupt it and provoke local packing changes (gel weakens), 2) oppositely charged particles of different shape added to the gel can enhance the strength of network through enhancing attractive interactions. Particle dimensions are suggested to be one of the primary parameters that define the network strength.

## Bibliography


Bailey L, Lekkerkerker HNWW, Maitland GC (2014) Rheology modification of montmorillonite dispersions by colloidal silica. Rheol Acta 53:373–384 . doi: 10.1007/s00397-014-0765-3

Barnes HA, Hutton JF, Walters K (1989) An Introduction to Rheology. Elsevier Science Publishers B.V.

Clarke B (1967) Rheology of Coarse Settling Suspensions. rans Inst Chem Eng 45:7251—7256

Durán JDGDG, Ramos-Tejada MMM, Arroyo FJJ, González-Caballero F (2000) Rheological and Electrokinetic Properties of Sodium Montmorillonite Suspensions. J Colloid Interface Sci 229:107–117 . doi: 10.1006/jcis.2000.6956

Forbes E, Franks G V (2013) Selective Separation of Hematite from Quartz By Flotation Using A Temperature Responsive Polymer. 12–14

Grieger S, Press W (1996) A diffraction technique to investigate the orientational alignment of anisotropic particles: studies of clay under flow. EPL 35:233

Hilhorst J, Meester V, Groeneveld E, et al (2014) Structure and rheology of mixed suspensions of montmorillonite and silica nanoparticles. J Phys Chem B 118:11816–11825 . doi: 10.1021/jp504217m

Ji Y-Q, Black L, Weidler PG, Janek MN (2004) Preparation of Nanostructured Materials by HeterocoagulationsInteraction of Montmorillonite with Synthetic Hematite Particles. Langmuir 20:9796–9806 . doi: 10.1021/la0495579

Kosmulski M (2016) Historical perspective Isoelectric points and points of zero charge of metal (hydr)oxides: 50 years after Parks' review. doi: 10.1016/j.cis.2016.10.005

Ndlovu B, Forbes E, Farrokhpay S, et al (2014) A preliminary rheological classification of phyllosilicate group minerals. Miner Eng 55:190–200 . doi: 10.1016/j.mineng.2013.06.004

Tadros TF (2010) Rheology of Dispersions: Principles and Applications

Ten Brinke AJW, Bailey L, Lekkerkerker HNW, Maitland GC (2007) Rheology modification in mixed shape colloidal dispersions. Part II: mixtures. doi: 10.1039/b713144e

Tombácz E, Csanaky C, Illés E (2001) Polydisperse fractal aggregate formation in clay mineral and iron oxide suspensions, pH and ionic strength dependence. Colloid Polym Sci 279:484–492 . doi: 10.1007/s003960100480

# Materials and methods

## Minerals

The minerals examined in the present work included: hematite from Brazil, quartz from Sigma-Aldrich and Kunipia-F sodium bentonite. Hematite from Brazil was obtained in various size ranges and processed according to the flowsheet given in the Fig. 19. Three stages of crushing were applied to conduct the primary reduction of hematite particle size: jaw and gyratory crushers, followed by a roll mill. These operations allowed to reduce the particle size to less than 1 mm. Subsequently, the grinding in a ball mill with steel grinding media was performed; it was followed by a wet sieving. Four sieves with the apertures of 300, 150, 75 and 40 μm were utilized. Hematite is considered as a "heavy" mineral (density of ~5.3 g/cm$^3$) and is known to sediment rapidly in the aqueous suspensions. It is evident, that an efficient electrostatic stabilization of -40 μm fraction is practically not possible. Finer PSD was achieved by grinding 75-150 μm fraction in an iron powderiser for 12 min.

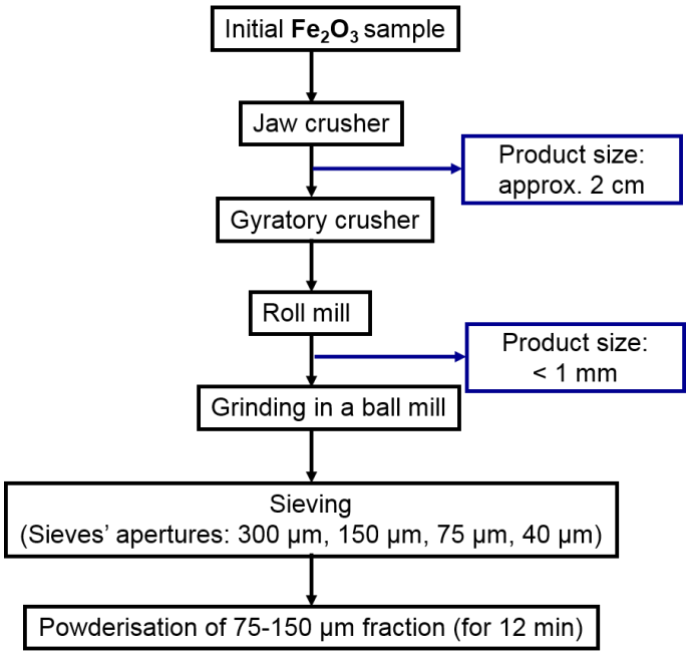


*Figure 19 - The size reduction flowsheet for hematite from Brazil.*

Particle size distributions of the minerals were obtained using the Mastrsizer 3000 (Malvern). The software allows to obtain a volumetric PSD, surface area-based PSD or PSD by number. In the work of Zhou et al. (1999), the concepts of volume, surface area and number average particle diameter were used to build predictive and descriptive rheological models of polydisperse suspensions. Within the framework of their yield stress modelling, it was suggested that the utilization of the volume average particle diameter yields in overestimated contribution of coarse particles and, thus, lower yield stresses comparing to the experimentally obtained values. On the other hand, the number average particle diameter resulted in the overestimation of fine particle contribution and higher yield stresses than those measured with the rheometer. Authors suggested that the surface area average particle diameter was the most suitable within their framework as it provided a balanced contribution of small and large particles and accurate estimation of the yield stress. Nevertheless, each distribution type (or average diameter) has its advantages and is preferred in different cases. In this chapter for the minerals studied, all three types of distributions shall be given.

To measure the PSD of non-swelling minerals, the dry mineral powders were suspended in the beaker of Mastrsizer in 500 ml of $1 \times 10^{-2}$ M $KNO_3$ at pH 10 for quartz, and of $1 \times 10^{-2}$ M $KNO_3$ at natural pH for hematite. Chemical conditions were chosen to achieve better particle dispersion. The agitation at 2000 rpm lasted for 15 min, including 2 min when the ultrasound was applied. Absorption indices were 0.042 and 0.01 for hematite and quartz, respectively. Refractive indices were 2,793 and 1.544 for hematite and quartz, respectively. Refractive index of the dispersing media was 1.33 (water) for all the measurements performed. Sphericity of particles was assumed. For each sample, 5 measurements were performed, with 30 sec interval between the measurements. Average of 5 measurements was taken to characterize the PSD of the minerals.

The PSD of hematite from Brazil after 12 min powderization is depicted in the Figs. 20-22. Silicon dioxide (quartz) from Sigma-Aldrich with density of 2.65 g/cm$^3$ and Kinipia-F sodium bentonite clay (Kunimine Industries Co., Ltd) with dry density of 2.6 g/cm$^3$ were used for suspension making as received (without any size reductive treatment). The PSD of quartz from Sigma-Aldrich can be found in the Figs. 20-22. The bars on the Figs. 20-22 represent the deviation given by eq.17:

$$\mathrm{dev} = \sqrt{\frac{\sum(x - \bar{x})^2}{n}} \qquad [17]$$

where $\bar{x}$ is an average volumetric, specific surface or number % of 5 measurements, corresponding to each size fraction; $x$ is the % obtained in a particular measurement for a particular size fraction; $n$ is the number of measurements.

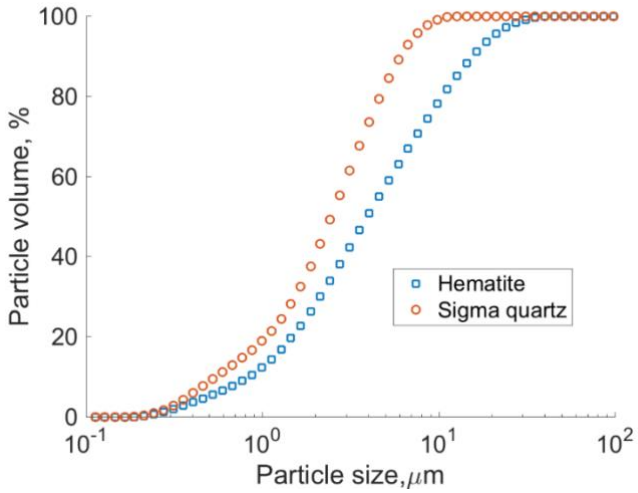


*Figure 20 - Cumulative volumetric PSD of hematite from Brazil and Sigma quartz.*

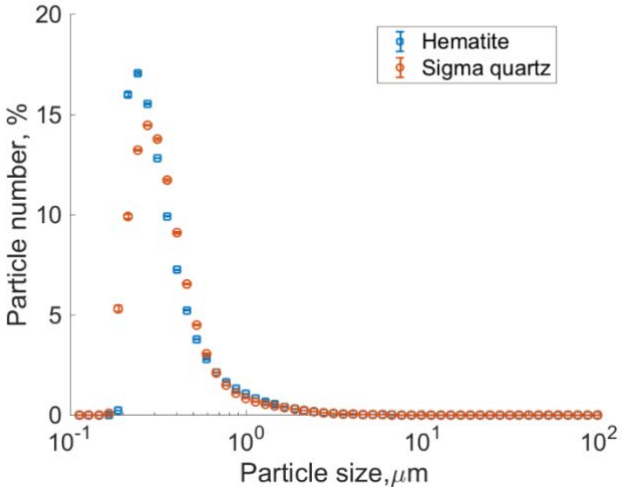


*Figure 21 - PSD by number of hematite from Brazil and Sigma quartz.*

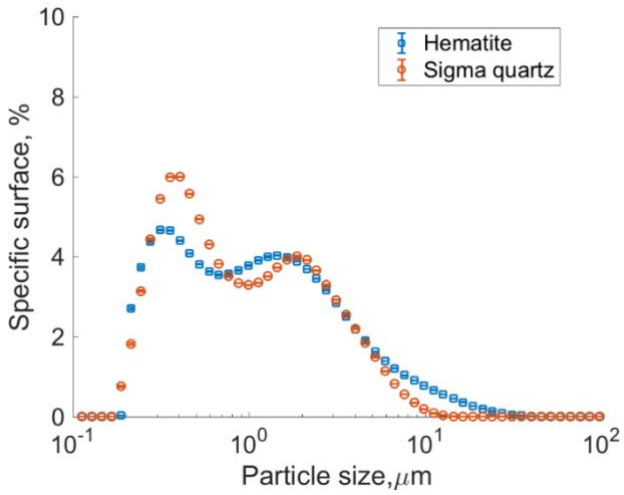


*Figure 22 - Specific surface area PSD of hematite from Brazil and Sigma quartz.*

Acquiring a representative PSD of the swelling clay, such as bentonite, is a challenging task for multiple reasons, including particle expansion, aggregation and exfoliation (Tan et al. 2017). To avoid erroneous results, the following steps were undertaken: 1) the particles were soaked in the salt solution ($1 \times 10^{-2}$ M $KNO_3$, pH 10) for 2 days prior to measurement, 2) soft ultrasound (US) was applied. Preference was given to the low US intensities during preparation to avoid (or, at very least, reduce) possible particle exfoliation. Sequence of 5 measurements with 30 s interval was repeated for each value of ultrasound tested, including: 0, 1, 2, 3 and 7 min. Refractive and absorption indices utilized were 1.5 and 0.01, respectively. Solid sample of bentonite was suspended in 500 ml of $1 \times 10^{-2}$ M $KNO_3$, pH 10 and left to age for 2 days. After 2 days of aging the pH of the suspension was measured and adjusted. Suspension then was poured in the beaker of the Mastersizer and agitated at 2000 rpm for 15 min. Particle size distributions obtained for Kunipia-F bentonite soaked in the aqueous salt solution ($1 \times 10^{-2}$ M $KNO_3$, pH 10) for 2 days at different US durations are given in the Figs. 23-25.

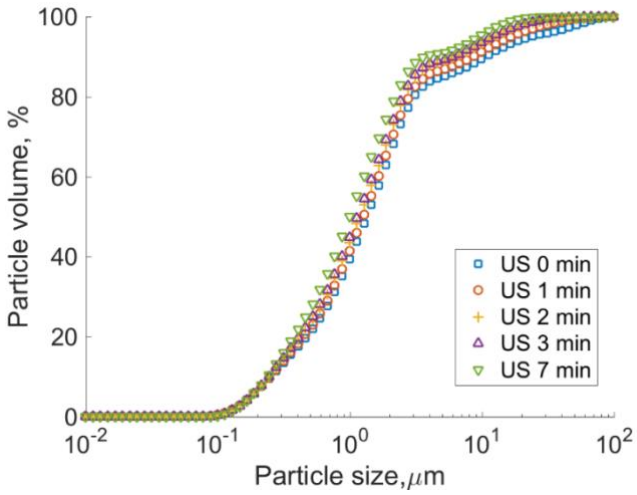


*Figure 23 - Cumulative volumetric PSD Kunipia-F bentonite in 1 × $10^{-2}$ M $KNO_3$, pH 10, after 2-day ageing.*

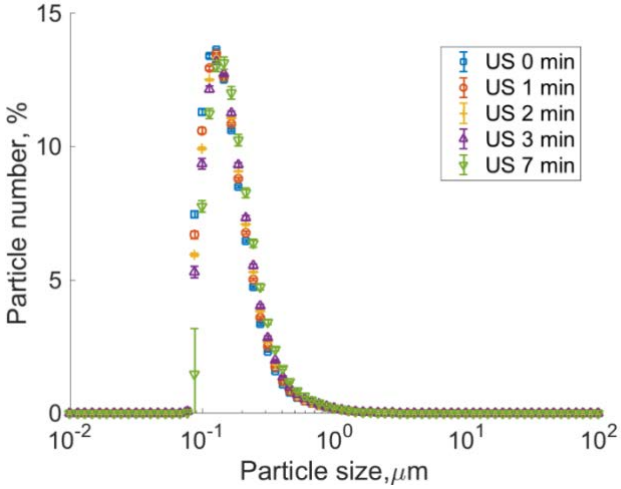


*Figure 24 - PSD by number of Kunipia-F bentonite in 1 × $10^{-2}$ M $KNO_3$, pH 10, after 2-day ageing.*

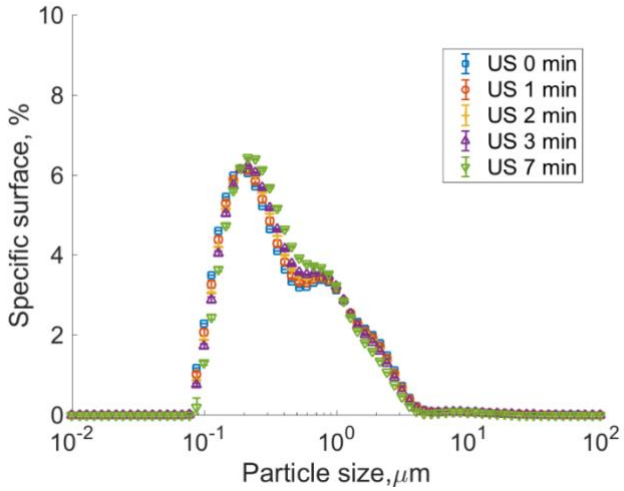


*Figure 25 - Specific surface area PSD Kunipia-F bentonite in 1 × $10^{-2}$ M $KNO_3$, pH 10, after 2-day ageing.*

It can be observed (Fig. 23) that few aggregates above 10 μm in size were formed in original suspension; these aggregates were entirely destroyed by the seventh min of ultrasonic treatment. As expected from this fine clay, majority of Kunipia-F bentonite particles are concentrated in the size class below 1 μm, where the majority of surface area is available.

For the flotation tests, the quartz from Fontainebleau and hematite from Brazil in -40 μm and 40-75 μm size fractions were utilized.

## Scanning electron microscopy (SEM)

Secondary electron (SE) SEM images of unique bentonite particles were obtained using MEB-FEG Hitachi S-4800. Kunipia-F bentonite powder was dispersed in ethanol (99.99% of $C_2H_6O$, Sigma Aldrich), the concentration of 0.1 vol% solid. A drop of suspension was placed onto the carbon-covered stage, which then was heated at 40 °C to provoke the evaporation of alcohol. In 30 min the sample was withdrawn from the heating plate and placed into the SEM sample holder. The technique allowed to provide high-quality images for the particles of the order of few microns and down to hundreds-tens of nanometers. Obtained images of individual bentonite particles can be found in the Fig. 26 below.

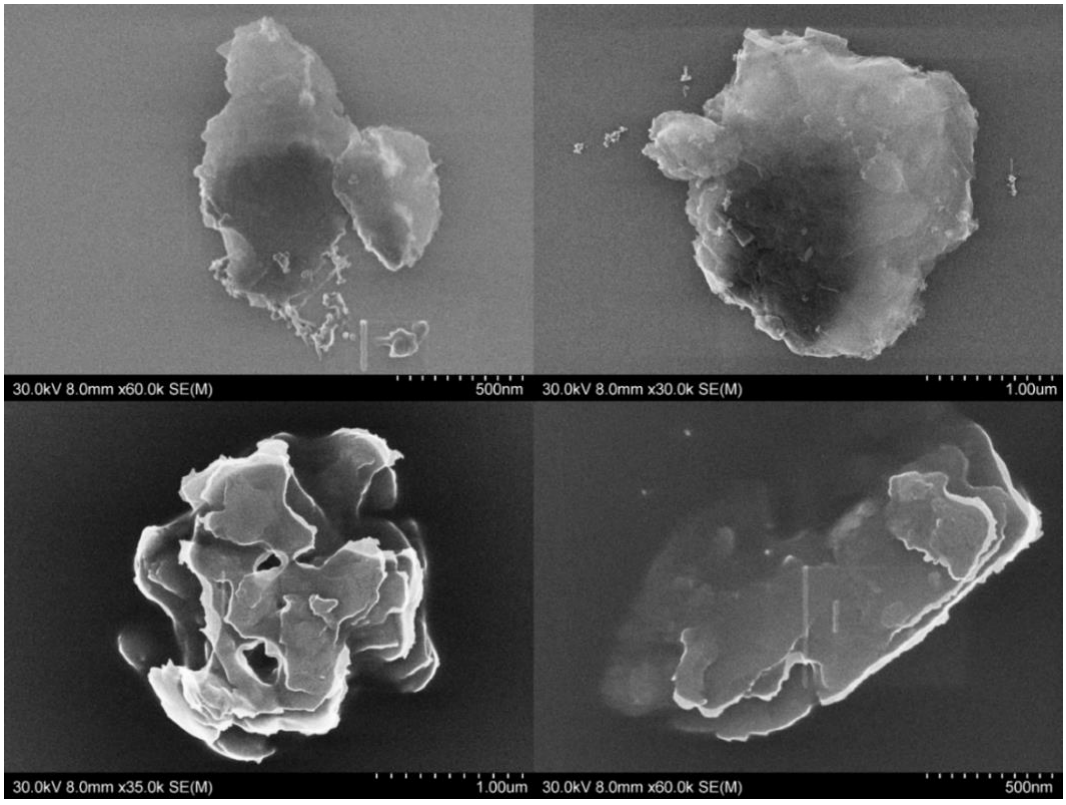


*Figure 26 - SEM SE images of Kunipia-F bentonite particles.*

SEM images of the mono- and polymineral particle networks (see chapter II and III) were acquired using TESCAN 218 VEGA3 SEM system.

## Reagents

All reagent solutions utilized in the present work were made with demineralized water. Salts utilized for the present research included potassium nitrate and sodium chloride, supplied by VWR. Base agent utilized for the pH adjustment – purified potassium hydroxide was purchased from LABOSI. Acids utilized for the pH adjustment were nitric acid (65%) and hydrochloric acid (37%), both purchaised from Sigma Aldrich. Acids and bases were used for pH adjustment in the form 1 M, 0.1 M and 0.01 M aqueous solutions. Corn starch (Sigma Aldrich) and dodecylammonium chloride were utilized for the flotation tests. Corn starch, prior to utilization, was mixed with KOH (1 M solution) in the proportion 1:4.5 (w/w), and the demineralized water was added. The mixture was then heated and agitated until becoming transparent. Dodecylammonium chloride ($C_{12}H_{28}ClN$) was obtained from dodecylamine ($CH_3(CH_2)_{11}NH_2$, 98%, Sigma Aldrich) and hydrochloric acid via reaction: $C_{12}H_{27}N+HCl \longrightarrow C_{12}H_{28}ClN$.

## Rheometry

Rheological measurements in the present work were performed with AR 1000 (coupled with Couette geometry, see chapter II) and AR 2000 (coupled with vane in grooved cup geometry, see chapter III) rotational rheometers from TA Instruments. Minimal measurable torque for these models was 0.1 μN.m. The rheometers were equipped with the Rheology Advantage software (TA instruments). Conversion of the torque ($T$) to the shear stress and angular velocity ($\Omega$) to the shear rate was performed using the shear stress ($F_\sigma$) and shear rate ($F_{\dot\gamma}$) factors, see eqs. 18 and 19.

$$\sigma = F_{\dot\gamma} T \qquad [18]$$

where $F_\sigma = \frac{R_{ext}^2 + R_{int}^2}{4\pi H R_{ext}^2 R_{int}^2}$.

$$\dot\gamma = F_{\dot\gamma} \Omega, \qquad [19]$$

where $F_{\dot\gamma} = \frac{R_{ext}^2 + R_{int}^2}{R_{ext}^2 - R_{int}^2}$.

Preparation procedure for mono- and polymineral suspensions for conventional rheometry and MRI velocimetry is described in chapters II and III, respectively.

## Flotation

Flotation experiments were performed to establish a problematic concentration of bentonite in the mineral pulp. The experiments consisted in conducting a reversed hematite flotation in the mixture of hematite (Brazil) and quartz (Fontainebleau) in the conditions of gradually increasing quantity of bentonite (0.05 vol%, 0.1 vol%, 0.3 vol%). The experiments were performed on two size fractions, -40 and 40-75 μm, with Kunipia-F bentonite, at pH 10 in $1 \times 10^{-2}$ M $KNO_3$. Corn starch (CS) was used as depressant for hematite, dodecylammonium chloride (DACl) was used as a quartz collector and frother. The flowsheets for both size fractions, -40 μm (Fig. 27) and 40-75 μm (Fig. 28), are given below.

In the flowsheets given in the Figs. 27, 28, the percent solid in the flotation cell before the bentonite addition was 10 vol% (30 wt%). Conditioning of mixture with the collector was performed in the head of the process to allow the attachment of amine cation onto the surface of quartz. Nevertheless, the report of bentonite particles to the foam is highly probable due to the particle charging favorable for $DACl^+$ physisorption at pH 10. Additional 20 $g/t_{SiO2}$ of collector were demanded to maintain the flotation process of the -40 μm mixture, due to higher surface area suggested by finer PSDs. For both size fractions, the foam hindering commences at 0.1 vol% of bentonite. Images of the foam can be found in the appendices I and II. It was concluded from the visual observation that the viscosity of pulp noticeably increased with the addition of even so little amount of sodium bentonite. It is known that starting from certain, often very low, solid concentration, hydrodynamic dimeters of clay particles come into contact. In other words, a particle during its rotation and rearrangement in such suspension with high probability will touch its neighbors. The 0.1 vol% bentonite suspensions were, thus, further analyzed in this work.

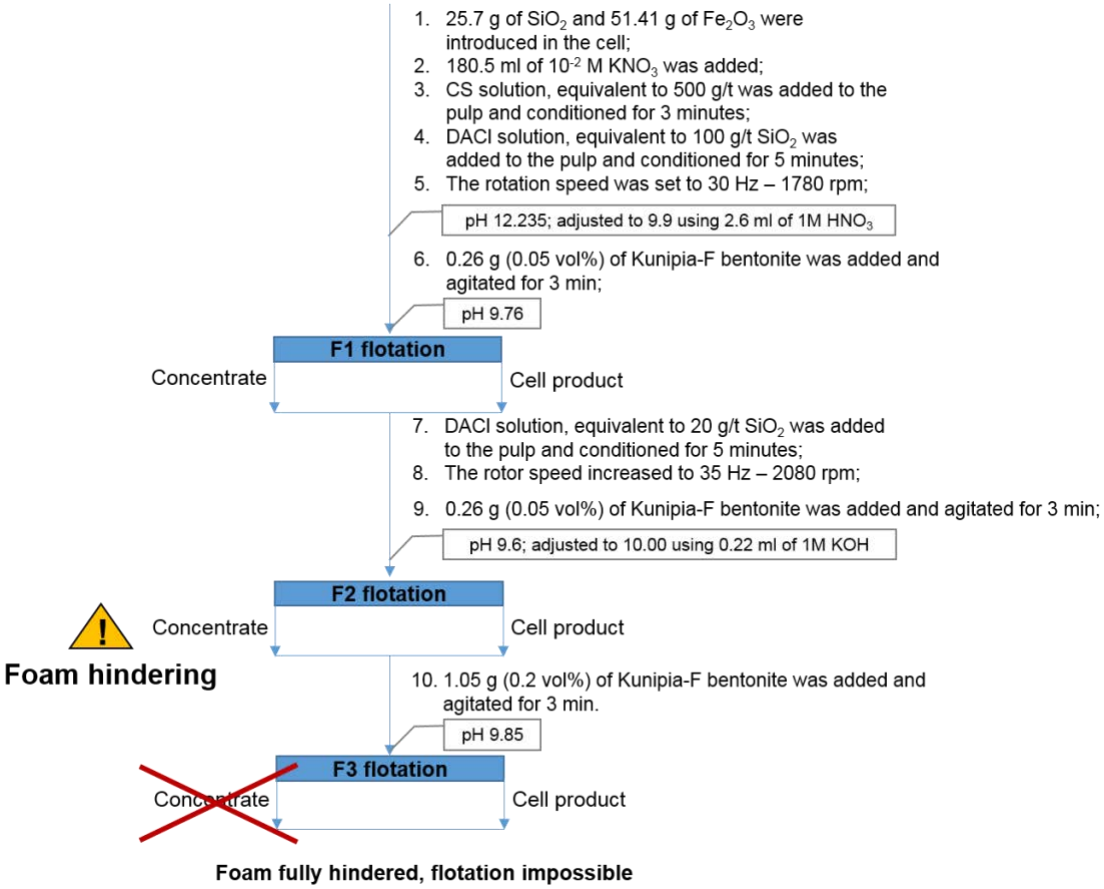


*Figure 27 - Flotation flowsheet, -40 µm mixture.*

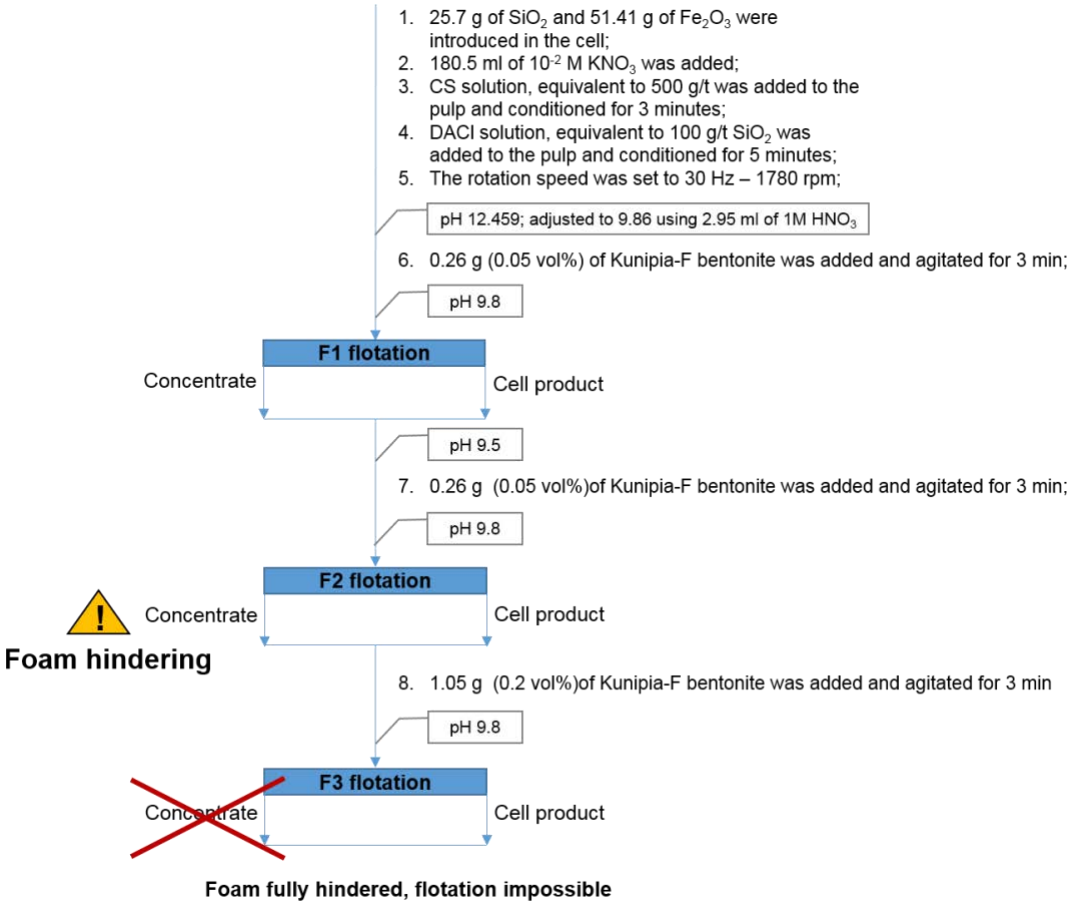


*Figure 28 - Flotation flowsheet, 40-75 µm mixture.*

## Bibliography

Tan X, Liu F, Hu L, et al (2017) Evaluation of the particle sizes of four clay minerals. doi: 10.1016/j.clay.2016.10.012

Zhou Z, Solomon MJ, Scales PJ, et al (1999) The yield stress of concentrated flocculated suspensions of size distributed particles. J Rheol (N Y N Y) 43:651 . doi: 10.1122/1.551029

# Chapter II – Dynamic behavior of dilute bentonite suspensions under different chemical conditions studied via magnetic resonance imaging velocimetry

Article published in *Colloids and Interfaces*

Olga Chernoburova [1,*], Mathieu Jenny [2], Sébastien Kiesgen De Richter [2], Maude Ferrari [2] and Akira Otsuki [1]

[1] GeoRessources Laboratory, Université de Lorraine, UMR7359, BP10162, Vandoeuvre-lés-Nancy, France; akira.otsuki@univ-lorraine.fr

[2] LEMTA, CNRS, Université de Lorraine, UMR 7563, F-54500, Vandoeuvre-lés-Nancy, France; mathieu.jenny@univ-lorraine.fr (M.J.), sebastien.kiesgen@univ-lorraine.fr (S.K.D.R.), maude.ferrari@univ-lorraine.fr (M.F.)

[*] Correspondence: O.Chernoburova@gmail.com; Tel.: +33-760-283-514

Received: 16 August 2018;

Accepted: 25 September 2018;

Published: 27 September 2018

## Résumé

Cette étude examine les suspensions aqueuses diluées de particules de bentonite par la vélocimétrie par imagerie par résonance magnétique (IRM). Quatre conditions chimiques différentes sont testées pour étudier l'influence du pH et du type d'électrolyte monovalent sur le comportement rhéologique local des suspensions de bentonite. Les résultats indiquent la bande de cisaillement dans une suspension diluée de 0,1% de solide en volume en raison de la formation d'un réseau tridimensionnel de particules dans un certain environnement chimique (c'est-à-dire, pH 4 dans $1 \times 10^{-2}$ M $KNO_3$). Ce réseau est responsable de l'existence de la contrainte d'écoulement dans cette suspension diluée. Les changements structurels induits par la modification de la chimie des suspensions sont examinés par microscopie électronique à balayage. Une méthode, déjà établie, basée sur le traitement des couples obtenus via une mesure rhéométrique conventionnelle, est également appliquée comme un moyen alternatif de récupérer des informations de flux locaux. Dans la plage du taux de cisaillement couverte par la vélocimétrie IRM, les résultats des deux méthodes concordent. Cette étude suggère que l'existence d'une «master curve» (ou courbe d'écoulement globale) pour les suspensions diluées, dépend de l'organisation des particules de bentonite dans la suspension. Cette organisation est influencée par la chimie de solution et l'historique des contraintes précédentes.

## Abstract

This study investigates dilute aqueous suspensions of bentonite particles using magnetic resonance imaging (MRI) velocimetry. Four different chemical conditions are tested to investigate the influence of pH and type of monovalent electrolyte on the local rheological behavior of bentonite suspensions. The results indicate the shear banding in a dilute suspension of 0.1 vol.% solid due to the formation of a continuous three-dimensional particle network under a certain chemical environment (i.e., pH 4 in $1 \times 10^{-2}$ M $KNO_3$). This network is responsible for the existence of the yield stress in that dilute suspension. Structural changes induced by modification of suspensions' chemistry are examined via scanning electron microscopy. A previously established method based on processing the torques acquired via conventional rheometric measurement is also applied as an alternative way to recover local flow information. Within the shear rate range covered by our MRI velocimetry, the results of both methods show good agreement. This study suggests that the existence of a master curve (or global flow curve) for dilute suspensions is dependent on the bentonite particle organization, which is influenced by the suspension chemistry and the previous flow history.

**Keywords:** local rheology; shear banding; shear localization; monovalent salts; pH

## Introduction

Suspension rheology is a broad domain of soft matter science that studies flow properties of liquid-solid dispersions. Clay suspensions gained a lot of interest in the domain of granular and colloidal suspensions due to their unique properties, such as high aspect ratio, spatial chemical inhomogeneity, ion exchange capacity and swelling (Otterstedt and Brandreth 1998). Certain clays, for example bentonite, have found their broad applications in multiple industries, including pelletization (Forsmo et al. 2006), filtration and purification (Mopoung et al. 2014), medicine (Nones et al. 2015), hydraulic barriers and radioactive waste disposal (Sun et al. 2009). Swelling and absorbing properties of bentonite justify its wide use. Bentonite (or montmorillonite) suspensions are often handled in mineral beneficiation (Farrokhpay et al. 2016), drilling (Mahto and Sharma 2004), and mineral waste disposal (Boger 2009) processes.

Bentonite is an aluminum phyllosilicate clay, composed mostly of montmorillonite, classified as a dioctahedral smectite. Each particle of montmorillonite consists of sandwich-like sheets held together via the van der Waals force. A single sheet is constructed with three layers: an octahedral alumina layer sandwiched between two tetrahedral silica layers. The distance between the $SiO_2$-$Al2O_3$-$SiO_2$ sheets is the order of 10 Å (van Olphen 1954) and can accommodate some water molecules and exchange cations such as $K^+$, $Na^+$, $Ca^{2+}$, $Mg^{2+}$ (Huertas et al. 2001). Dominating exchange cation defines the extent and the reversibility of clay swelling. The highest swelling capacity is usually associated with the monovalent strongly hydrated interlayer cations of small ionic radius, such as $Li^+$ or $Na^+$. For theoretical explanations and modelling, bentonite particles are often approximated as rectangular sheets or disks. The nature of this mineral leads its spatial chemical inhomogeneity. The particle edge and face possess different chemical properties, and, thus, exhibit different physical properties (Otterstedt and Brandreth 1998; Luckham and Rossi 1999).

Rheological behavior of aqueous bentonite suspensions depends on various parameters, including type of bentonite or $Na^+/Ca^{2+}$ ratio (Abu-Jdayil 2011), solid concentration (Abu-Jdayil 2011; Choo and Bai 2015), aging time (Abu-Jdayil 2011; Choo and Bai 2015), temperature (Vryzas et al. 2017), pressure (Alderman et al. 1988) and solution chemistry (Luckham and Rossi 1999).

Once a bentonite particle is immersed in an aqueous salt solution, it gains a so-called electrical double layer (EDL)—an ionic structure built through the electrostatic attraction of ions to a charged particle surface. EDL can be divided into two parts: (1) fixed layer—ions densely adsorbed onto a surface of an opposite sign (also called Stern layer) and (2) a diffuse part—a loose cloud of ions and counter ions attracted from the bulk solution (Hunter 1986). An imaginary border that splits the EDL onto mobile and stationary parts is called a shear plane; it is thought to be situated in the diffuse part of the EDL. Isomorphous substitutions are responsible for charge occurrence on bentonite particle face. The face charge has greater influence on bentonite particle EDL than that of the edge. The EDL on the edge originates from the crystal lattice disruption and potential-determining ions attracted to broken chemical bonds (Luckham and Rossi 1999). EDL of the edge strongly depends on the solution chemistry, in particular, solution pH. In acidic environment particle edge gains positive charge, whereas alkaline environment generates negative charge. On the other hand, the face remains negative along all the pH range. The pH corresponding to no net electrical charge on the shear plane is called an "isoelectric point" (IEP). It was proposed that the edges of sodium bentonite particles possess IEP around pH 7–8 (Benna et al. 1999; Durán et al. 2000). Once the EDL repulsion is suppressed, the resulting particle-particle interaction is governed by the van der Waals force, causing particles to attract, according to the DLVO (Derjaguin–Landau–Verwey–Overbeek, Hunter 1986) theory.

Opposite charging of bentonite particle edges and faces in aqueous suspensions laid the foundation of the charge-based structuring theories. In sufficiently concentrated bentonite suspension, particles are situated close enough to interact with each other. In this case, they organize in a way that oppositely charged particle sites attract while similarly charged sites repel. In an acidic suspension, such organizations result in a structure that was described as "cubic card house" (van Olphen 1964) used to explain the gel formation in bentonite suspensions (Fig. 29).

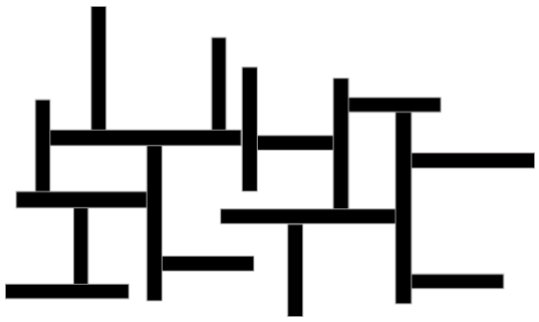

*Figure 29 - Schematic cubic card house structure.*

There are several other particle association models suggested to justify the bentonite gel formation (e.g., Norrish 1954); but the “card house” appears to be the most firmly established. In the card house structure, the “edge-to-face” (E-F) particle association is dominant. “Edge-to-edge” (E-E) accompanied by E-F particle association becomes highly probable at the IEP of the edges. In suspensions with moderate alkaline pH, all particle sites are negatively charged and mutually repel, and thus no structure will be formed (Tombácz and Szekeres 2004). On the other hand, there are reports suggesting repulsion-promoted E-F arrangement in highly alkaline environment (Benna et al. 1999). Arrangement of “face-to-face” (F-F) type is predominantly associated with double layer compression at high salt concentrations (Luckham and Rossi 1999; Tombácz and Szekeres 2004); it was also reported to be pH-independent (Durán et al. 2000). These association models were employed to explain the difference in rheological behavior of bentonite suspensions under various chemical environments. It was found experimentally that the suspensions exhibited higher shear stresses and yield stresses in the acidic pH below IEP, than in basic pH above IEP (Benna et al. 1999; Tombácz and Szekeres 2004). Also, several studies showed the general trend of lower shear stresses and yield stresses corresponding to increased ionic strength of the solution (Kelessidis et al. 2007; Abu-Jdayil 2011). Rheological studies of bentonite suspensions infrequently consider the ionic radius of salt cation, despite its importance.

Thixotropy is another feature of bentonite suspensions linked to the particle structuring. Tadros (2010) defined thixotropy as a reversible time-dependent decrease in viscosity that results from: (a) a spatial rearrangement of molecules or particles in a non-Newtonian system or (b) change of the structure in the system, under an applied shear. Once the yield stress of the internal structure is exceeded, it collapses and the suspension

flows. Its recovery does not happen instantaneously after the load is removed, resulting in a modified rheological response for some time. That temporary change of the rheological behavior is usually characterized with the hysteresis in the flow curve. Tombácz and Szekeres (2004) estimated the highest thixotropic loop area corresponding to their lowest tested pH (i.e., pH 5, within the range of pH 5–8).

Swelling of bentonite clay is a property that is characterized with a certain kinetics that affects the rheological behavior of the suspension. Aging time is a period during which the bentonite is exposed to the excess water available for the inter-sheet hydration and physicochemical transformations. Thixotropy and the yield stress of bentonite suspensions can enhance with aging time (Luckham and Rossi 1999; Abu-Jdayil 2011). It was reported that the major changes occurred within first 24 h while later the transformations were less significant (Goh et al. 2011; Abu-Jdayil 2011; Choo and Bai 2015). It is common to use Bingham or Herschel–Bulkley rheological models to describe the flow behavior of bentonite suspensions (Luckham and Rossi 1999; Benslimane et al. 2016).

Most studies listed above used global rheology alone to characterize mechanical properties of bentonite suspensions. On the other hand, for the fluids that are characterized with non-linear behavior or perturbation effects, it is useful to investigate the local rheology. Acquiring velocity profile at a controlled stress distribution allows to assign a local stress to a local velocity and deduce a constitutive law of the matter on the local scale (Coussot 2005).

Nowadays, different scattering and signal attenuation techniques aimed to extract the velocity field in flowing matters have become available. Among many others, magnetic resonance imaging (MRI) velocimetry gained popularity in the field of mechanics of complex fluids, as a technique based on direct excitation of materials' constituents. MRI is non-destructive and non-invasive, suitable for non-transparent matters technique based on nuclear magnetic resonance (NMR) spectroscopy. The theory behind NMR spectroscopy and MRI velocimetry can be found elsewhere (Callaghan 1999; Coussot 2005).

MRI velocimetry can be used to recover the velocity distribution in the gap of the concentric cylinder geometry. In a steady Couette flow, the shear stress ($\tau$) on an inner rotating cylinder is related to the torque ($\mathrm{T}$) via

$$\tau(\mathrm{R}) = \frac{\mathrm{T}}{2\pi \mathrm{h} \mathrm{R}^2}, \qquad [20]$$

where $\mathrm{R}$ is the radial distance from the axis, and $\mathrm{h}$ is the immersed heights of the cylinder. The torque on the inner cylinder is extracted from the global rheological measurement. Local shear rate $\dot{\gamma}(\mathrm{R})$ is obtained from MRI velocimetry, as a function of measured local velocity ($\mathrm{V}$):

$$\dot{\gamma}(\mathrm{R}) = \frac{\mathrm{V}}{\mathrm{R}} - \frac{\partial \mathrm{V}}{\partial \mathrm{R}}. \qquad [21]$$

Combining the above data allows to access local rheology.

Some typical velocity profiles recovered in the gap of the rotational rheometer are depicted in Fig. 30. Thick solid line corresponds to a profile expected for a Newtonian fluid in a wide-gap Couette geometry, where the ratio of internal to external cylinder radii is smaller than one. The thin solid line corresponds to a shear thinning fluid, dashed line represents “localization”, and dash-dotted line—“banding”. Banding and localization are yield stress fluid phenomena, whose distinctive feature is simultaneous coexistence of flowing and static zones of material. There is some controversy over the definition of banding in literature, thus its signification and definition will be specified below. It was suggested (Coussot et al. 2009; Ovarlez et al. 2009) that the major difference between banding and localization concerns the manner of shear and stress distribution at the interface between solid and flowing regions.

Banding is a discontinuity in a sheared complex fluid, characterized with the coexistence of two adjacent regions with different velocities (shear rates, $\dot{\gamma}$) but insignificantly different shear stresses ($\tau$). The shear rate on one side of the interface between the regions equals to the critical shear rate ($\dot{\gamma}_c$), and on the other side it is zero, with $\tau \approx \tau_c$ (with $\tau_c$ being a yield stress) for both sides. The banding effect was found in pastes (Jarny et al. 2005), micellar solutions (Perge et al. 2014), emulsions (Salmon et al. 2003), gels (Ovarlez et al. 2013). Localization is characterized with the coexistence of flowing and static regions due to continuous spatial variation of both, velocity (shear rate) and shear stress. The value of shear rate progressively decreases from some finite value to zero, where the flow stops. In a Couette cell, due to the character of shear stress

distribution, the fluid flows until the value of stress at certain distance from the rotating cylinder falls below $\tau_c$, and then the flow stops. Ideally, corresponding transition between the different velocity regions (smooth for localization and abrupt for banding, see Fig. 30) should be distinguishable at any scale of observation that is large enough to respect the continuum equation. More detailed information about banding and localization phenomena can be found in (Olmsted 2008; Ovarlez et al. 2009; Divoux et al. 2015). Experimental techniques used to access these local phenomena are well summarized in (Manneville 2008).

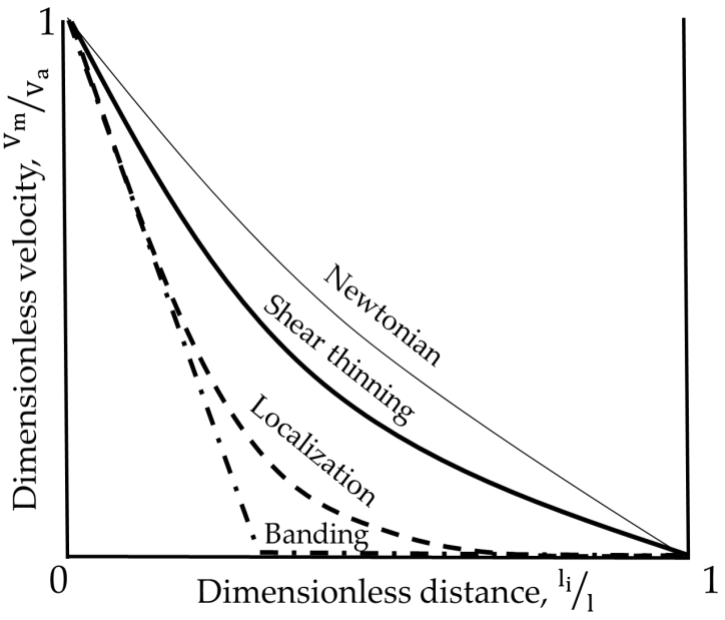


*Figure 30 - Schematic velocity distributions observed for fluids in a wide-gap Couette geometry; $l_i$ is the distance from the inner cylinder wall, $l$ is total length of the gap, $V_m$ is the measured velocity of fluid in the gap, $V_a$ is the applied rotational velocity.*

In the absence of MRI velocimetry, one can recover local flow information by processing the output of conventional rheometric measurement alone. In a Couette cell, where the shear stress distribution is well-known, local shear rate at the inner cylinder can be recovered. This method was described in (Coleman et al. 1966; Coussot 2005) and successfully applied by (Ovarlez et al. 2008; Coussot et al. 2009). It suggests the summation of successively decreasing torques differing one from another by $k=R_{int}^2/R_{ext}^2$,

where $R_{int}$ is internal and $R_{ext}$ is external cylinder radii of the Couette geometry. This allows the elimination of shear rate on the external cylinder at each summation step, see eq. 22,

$$\dot{\gamma}(\tau) = \sum_{i=0}^{\infty} \left(2T \frac{\partial \Omega}{\partial T}\right)_{k^i \tau}, \qquad [22]$$

where $\Omega$ is the angular velocity.

Once computed shear stress falls below the yield stress, the summation stops. The method has shown to give accurate predictions for some localizing fluids but must be treated with caution when material slippage occurs (Coussot 2005). Some aspects of local rheological behavior of bentonite suspensions with modest to high solid concentrations were reported in the past. Coussot et al. (2002a, b,c), for example, indicated the velocity bifurcation and dependency of suspensions' local properties on the time of rest following the load. Roussel et al. (2004) studied the validity of thixotropy modelling under different flow conditions at different scales (local and global). Raynaud et al. (2002) monitored behavior of bentonite suspensions in transient flows, fluid restructuring under the load and at rest. They demonstrated the dependency of steady state on the flow history and suggested that simple power-law approximation of the flowing region is appropriate.

The aim of this study, on the other hand, was to apply the MRI velocimetry to dilute bentonite suspensions to study the linkage between the solution chemistry and the local rheological performance. To the authors' best knowledge, there is yet no study in this regard. In the first place, the difference in velocity profiles of bentonite suspensions prepared under different chemistry was discussed and explained from the perspective of electrostatic interactions and particle structuring. Scanning electron microscopy was applied to visualize structural differences in those suspensions. Secondly, the rheological curves obtained using different means were compared and discussed. Finally, the question of existence of a master curve (or, otherwise, global flow curve) for each type of suspension was addressed.

## Materials and methods

Dilute (0.1 vol.%) suspensions were prepared using the Kunipia-F sodium bentonite (Kunimine Industries Co., Ltd.). The average size of the bentonite particles was measured using Mastersizer 3000 (Malvern). The particles were suspended in aqueous salt solution ($1 \times 10^{-2}$ M $KNO_3$) at pH 10, and soft ultrasound was applied to disperse the particles. Measurement yielded an average particle size of 0.5–1 μm (≈ face diameter). For the MRI velocimetry and conventional rheological measurements, suspensions were prepared using $1 \times 10^{-2}$ M $KNO_3$ or NaCl aqueous salt solution made with demineralized water. After introducing the solids to a salt solution, 5 min agitation with magnetic stirrer was applied, followed by the pH adjustment. The sample was then agitated with a magnetic stirrer for additional 15 min, and the pH adjustment was repeated. The pH of suspensions with $KNO_3$ was regulated using $HNO_3$ or KOH, while pH of suspension with NaCl was regulated with HCl. Once the desired pH value was achieved the sample was left to age. After 48 h, the pH was measured and adjusted one final time. Four bentonite suspension samples were prepared for the tests: pH 4, 8 and 10 in $1 \times 10^{-2}$ M $KNO_3$ solution and pH 4 in $1 \times 10^{-2}$ M NaCl solution.

The velocity profile acquisition was carried out with Bruker Avance III 600 wide bore spectrometer (14.1 T, 600 MHz proton resonance frequency) coupled with Rheo-NMR accessory from Magritek. The setting with indication of its major elements is given in Fig. 31. Micro-imaging probe (MicWB57) was a 40 mm quadrature resonator manufactured by Bruker, with 45 G/cm gradient system. Image acquisition was performed using the flow encoding spin-echo sequence.

Concentric cylinder geometry with radial dimensions of internal ($R_{int}$) and external ($R_{ext}$) cylinders, and immersed heights ($h$) was used to conduct the measurement (see the insert of Fig. 31). The inner cylinder of the geometry was roughened with glass beads of 150–250 μm diameter to prevent slipping. The field of view with the length ($a$), width ($b$), and section thickness ($c$) was analysed (see Fig. 31). Matrix of 512 × 64 pixels allowed the velocity profile spatial resolution of 78 μm. Only one side of the cell was analyzed as the profile symmetricity was assumed. The estimated error of a velocity measurement with our MRI velocimetry was 5%.

In this work, there was no opportunity to conduct MRI velocimetry and rheometry simultaneously in one machine; thus, the torque measurements were performed separately, using the AR 1000 rheometer (TA Instruments) assembled with the Couette geometry identical to the one used for MRI experiments. Steady state measurements were conducted for the range of angular velocities increasing from $1 \times 10^{-3}$ to 100 rad/s. The rheometer was equipped with Rheology Advantage software that used eq. 23 to calculate the shear rate from the angular velocity.

$$\dot{\gamma} = F_{\dot{\gamma}}\Omega, \qquad [23]$$

where $F_{\dot{\gamma}}=(R_{ext}^2+R_{int}^2)/(R_{ext}^2-R_{int}^2)$.

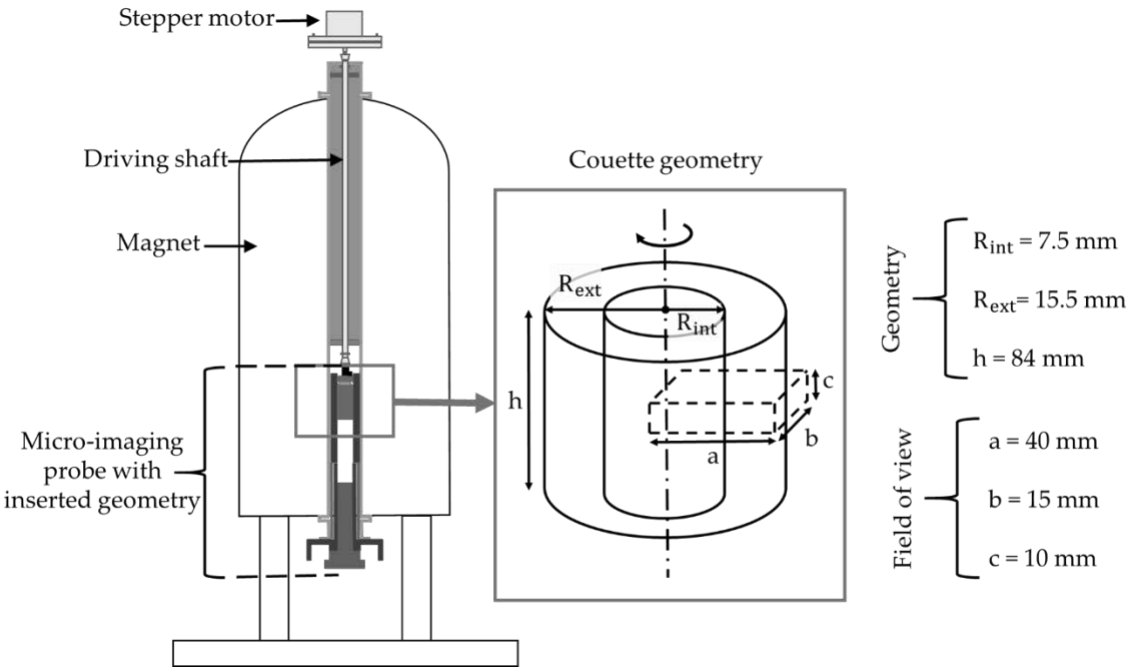


*Figure 31 - Schematic diagram of Brucker Rheo-NMR setting (left, Callaghan and Fischer 2001) and Couette geometry with spatial designations (right).*

Throughout whole experimental program the pH deviation from its initial values was carefully monitored and controlled; the deviation was found to be negligible. Swelling after 48 h (included in sample preparation) was significantly limited as agreed with literature (Goh et al. 2011; Abu-Jdayil 2011; Choo and Bai 2015). The evaporation was prevented by sealing the sample container with plastic paraffin film during its storage

period. Temperature was set to 20 °C and did not deviate significantly from this value for all conducted measurements. It was ensured that each sample has same shear rate history prior to the measurements.

Scanning electron microscopy (SEM) images of all four suspensions were taken using TESCAN VEGA3 SEM system. One drop of each suspension was placed on an Al sample stub and left to dry over the night at room temperature. The dried sample was then carbon-coated and placed in the TESCAN VEGA3 chamber. Secondary electron (SE) detector was used to image the samples.

## Results

Dimensionless velocity profiles for the suspensions with different solution pH in $1 \times 10^{-2}$ $KNO_3$ are shown in Fig. 32. In all cases given below, the dimensionless velocity represents the ratio of the applied velocity to the velocity measured through MRI. The solid line on the images corresponds to a velocity profile expected for a Newtonian fluid in a wide-gap Couette cell.

The wall slip could not be fully prevented and is estimated to cause the velocity loss up to 10–15% (maximum) from the imposed value (Fig. 32). A sharp slope discontinuity (banding) at low velocity was observed only in suspension with pH 4 (Fig. 32a) and not pH 8 (Fig. 32b) or 10 (Fig. 32c), with the same solid volume fraction.

It is a coherent question whether banding is established as a stationary phenomenon. The pH 4 in $1 \times 10^{-2}$ M $KNO_3$ suspension was tested after 48 and 96 h of aging (Fig. 33a). As shown in the Fig. 33a, there was no significant influence of aging time on the positioning of the banding point after the first 48 h of exposure to the aqueous salt solution. The apparent slip corresponding to the 96-h curve is a sequence of instrumental-related uncertainty in the proximity of the inner cylinder. The stationarity of banding under the load for the 96-h aged pH 4 in $1 \times 10^{-2}$ M $KNO_3$ suspension was investigated in the 6–24 rpm range of applied velocities (Figs. 33b, c). Fig. 33b shows the average of 14 velocity profiles collected during 2.5 h of experiment, after 96 h aging in total. The applied velocities were 6, 9, 12, 15, 18, and 21 rpm, with the minimum of two acquisitions (at 5 and 20 min) performed per each applied velocity. As seen from the standard deviation, these profiles exhibited minor difference. In other words, the location of the banding point in the gap did not change within the 6–21 rpm velocity range. Fig. 33c demonstrates the establishment of a stationary localized profile for the 96-h aged pH 4 in $1 \times 10^{-2}$ M $KNO_3$ sample. Upon increasing the applied velocity from 21 to 24 rpm, the conditional border between the solid and liquid regions lost its sharpness. The interface between solid and liquid regions advanced towards the external cylinder wall until a stationary localized profile (i.e., 40 min (24 rpm), Fig. 33c) was established.

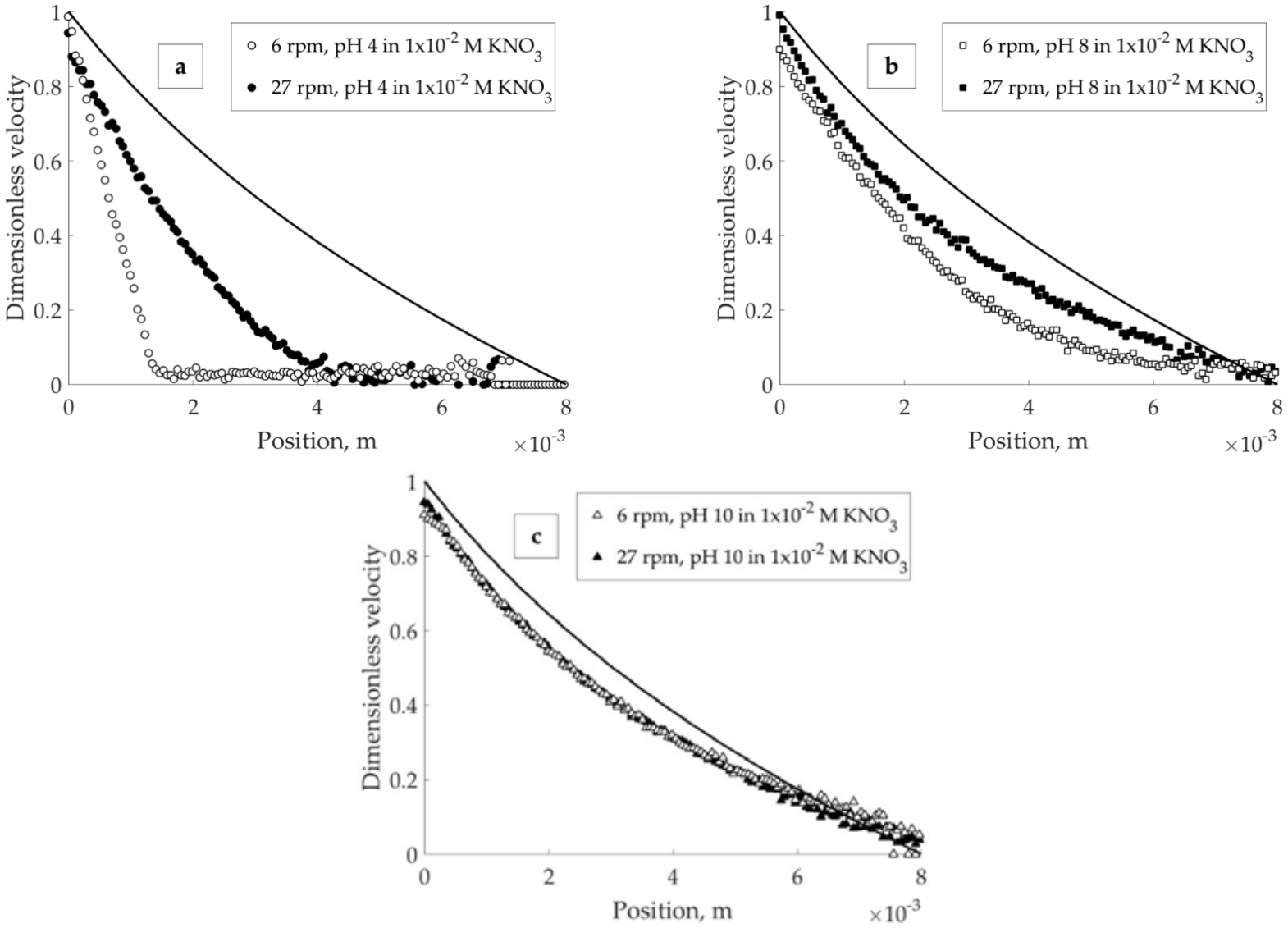


*Figure 32 - Dimensionless velocity profiles for suspensions at: (a) pH 4; (b) pH 8; (c) pH 10; in 1 × $10^{-2}$ M $KNO_3$, for 6 and 27 rpm rotational velocity.*

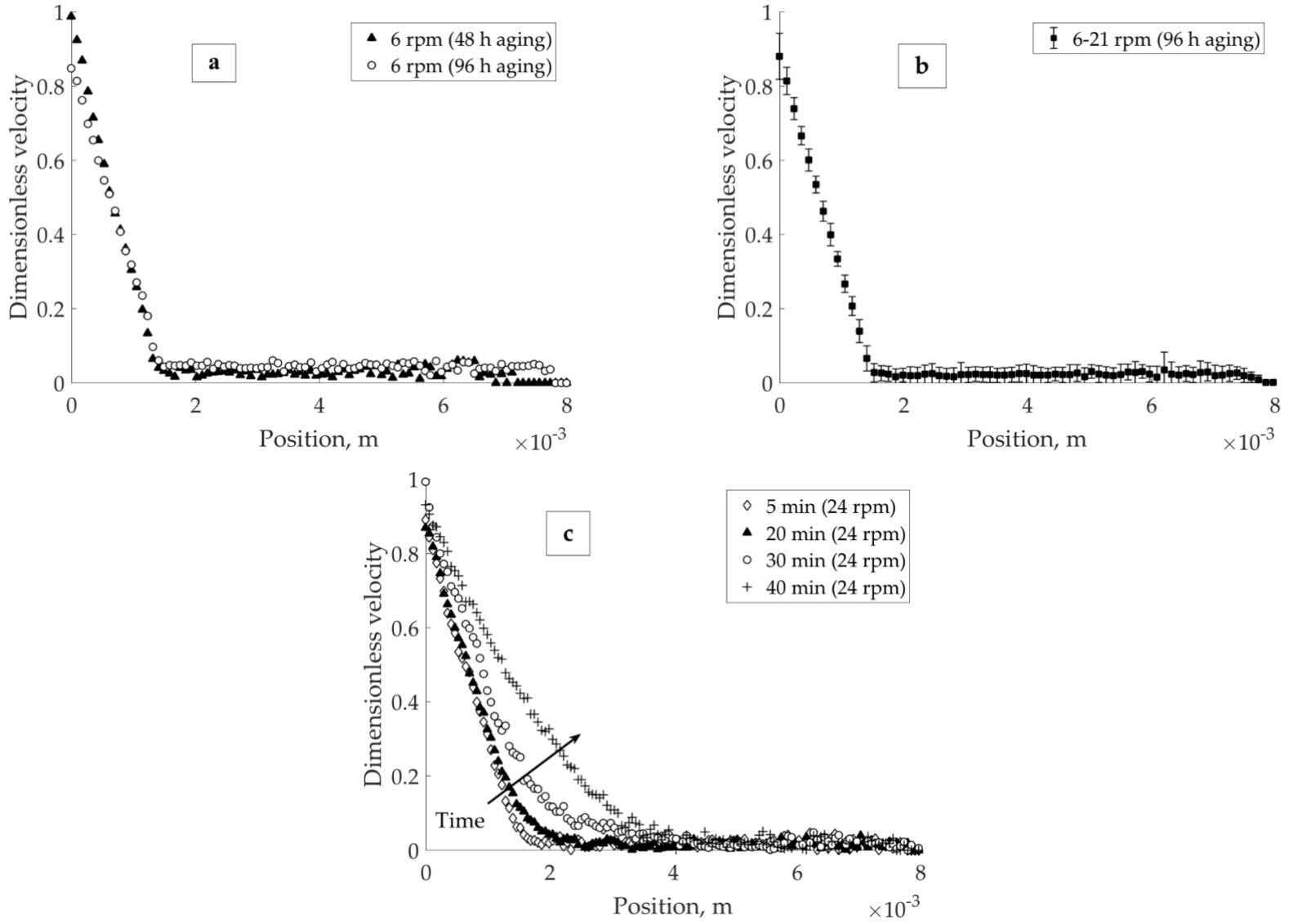


*Figure 33 - Dimensionless velocity profiles for pH 4 in 1 × $10^{-2}$ M $KNO_3$ sample: (a) comparison of velocity profiles after 48 and 96 h of aging, 6 rpm; (b) after 96 h of aging, the average of 14 profiles collected at 6, 9, 12, 15, 18, and 21 rpm during 2.5 h; (c) achievement of a steady localized profile after loss of banding, 24 rpm.*

To observe the recovery of the network under mild load after the breakage, the pH 4 in 1 × $10^{-2}$ M $KNO_3$ bentonite suspension was subjected to high-speed agitation (27 rpm) followed by an immediate velocity decrease to 6 rpm. The network recovery process was investigated during 12 h at the constant applied velocity of 6 rpm (see Fig. 34). The location of banding points found from network recovery tests (0.7 × $10^{-3}$ m, Fig. 34) and shearing the original suspension (1.5 × $10^{-3}$ m, Fig. 33a) mismatched.

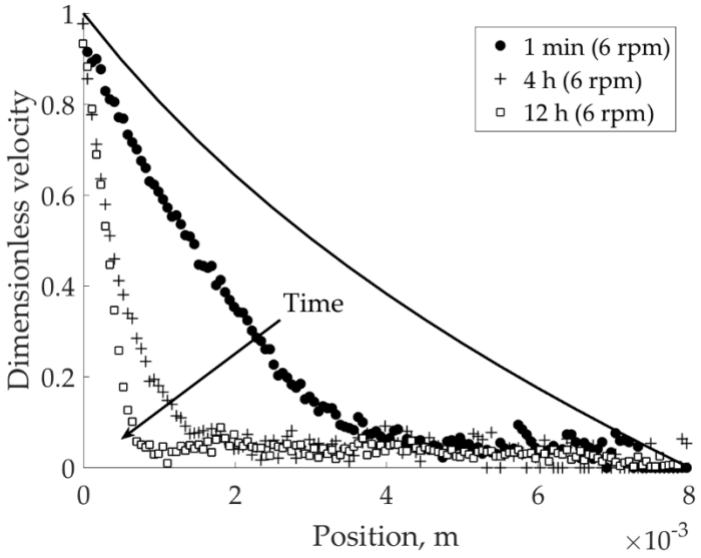


*Figure 34 - Recovery of shear banding under the load in the pH 4 in 1 × $10^{-2}$ M $KNO_3$ suspension, after agitation at 27 rpm.*

Suspension at pH 4 in 1 × $10^{-2}$ M NaCl was subjected to a constant load of 9 rpm for 40 min, to investigate the effect of salt type on suspension flow behavior. It was found that the stationary state for this sample at low shear rate is rather localization than banding (see Fig. 35a). The interface between solid and flowing regions lost its sharpness already after 10 min of the experiment; after 40 min the stationary localized profile was recorded (40 min (9 rpm), Fig. 35a). Furthermore, agitating the suspension 27 rpm and leaving it to recover the network at 6 rpm during 31.5 h resulted in the recovery of a localized profile (Fig. 35b).

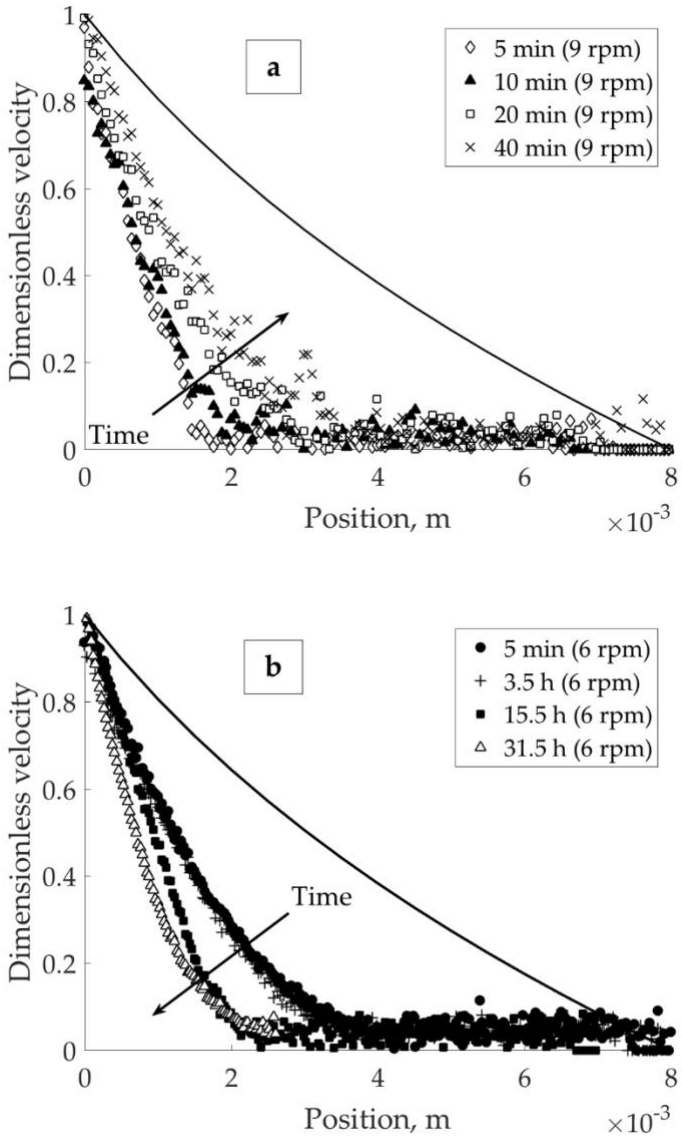


*Figure 35 - Velocity profiles of pH 4 in 1 × $10^{-2}$ M NaCl bentonite suspension: (a) achievement of a steady localized profile after loss of banding at 9 rpm; (b) recovery of the localized profile under the load, after agitation at 27 rpm.*

SEM was used to visualize the differences between the networks formed in suspensions prepared under different chemistries. The SE images of all four samples are given in Fig. 36. The observed structures represent the organization of particle aggregates in different chemical environments.

It can be observed that the aggregate networks formed in different salt solutions ($KNO_3$ in Fig. 36a, and NaCl in Fig. 36b) were noticeably different in size. Thicker aggregates were obtained with NaCl-based bentonite suspension at pH 4. At pH 8 and $1 \times 10^{-2}$ $KNO_3$ bentonite suspension, some long chains of aggregates were identified, an example of such chain is indicated with an arrow on the Fig. 36c. No significant particle network differences between the suspensions at pH 4 (Fig. 36a) and 10 (Fig. 36d) in $1 \times 10^{-2}$ M $KNO_3$ were observed up to 5000 times magnification.

To deduce the local rheology, we accessed to the global rheological data (Fig. 37), which in this study was collected using a regular rotational rheometer. The seeming inconsistency of pH 4 suspensions behaviour in low shear rate range (below 0.1 $s^{-1}$) can occur due to the transient flows. It was also suggested that such inconsistency may occur due to the wall slip, as it happens, for example, in the suspensions of synthetic swelling laponite clay, see work of Divoux et al. (2013).

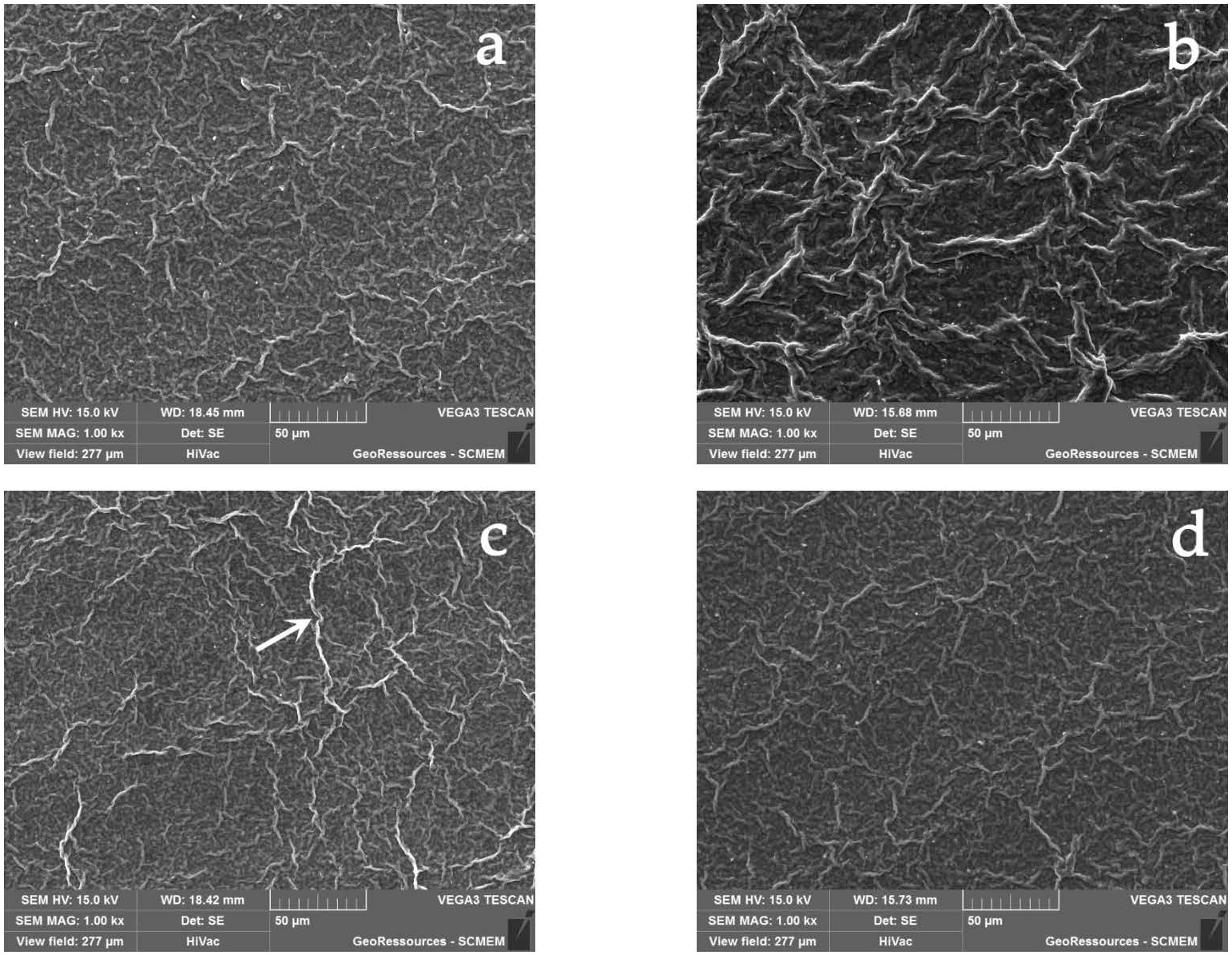


*Figure 36 - SEM images of bentonite suspension prepared at (a) pH 4 in 1 × $10^{-2}$ M $KNO_3$, (b) pH 4 in 1 × $10^{-2}$ M NaCl, (c) pH 8 in 1 × $10^{-2}$ M $KNO_3$, and (d) pH 10 in 1 × $10^{-2}$ M $KNO_3$, and deposited on Al stubs followed by drying and carbon coating.*

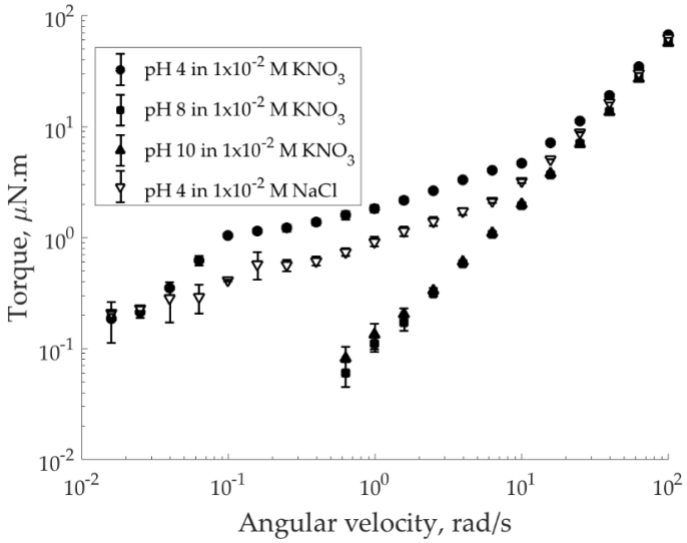


*Figure 37 - Global rheology of bentonite suspensions measured with a rotational rheometer.*

Two methods were used to obtain the local rheology of the suspensions. The first one requires only measurement with a conventional rheometer (Coleman et al. 1966; Coussot 2005; Ovarlez et al. 2008; Coussot et al. 2009). The second method uses MRI velocimetry (e.g., Coussot et al. 2009). For the first method, the procedure summarized in eq. 22 allows to compute the local shear rate on the inner cylinder of a Couette geometry and assign a value of shear stress calculated by eq. 20 to this spatial point. This method was applied to treat flow curves of viscous pH 4 suspensions, which are characterized with pronounced yield stress (see Fig. 38). The calculation outcome was fitted with the Herschel–Bulkley model, eq. 24.

$$\tau = \tau_c + \kappa\dot{\gamma}^n, \qquad [24]$$

where $\kappa$ is the consistency index and $n$ is the flow index.

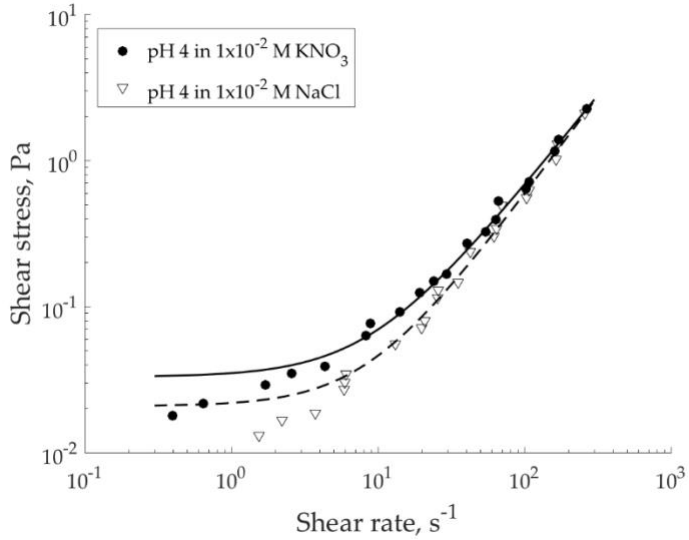


*Figure 38 - Local rheology computed using eq. 22, with Herschel–Bulkley fit for: pH 4 in 1 × $10^{-2}$ M $KNO_3$ (filled symbols, solid line, $K$ = 0.0020 Pa.s, $n$ = 1.25, $\tau_0$ = 0.033 Pa), and pH 4 in 1 × $10^{-2}$ M NaCl (hollow symbols, dashed line, $K$ = 0.0011 Pa.s, $n$ = 1.35, $\tau_0$ = 0.021.*

Local shear rates calculated using the model, eq. 22, and bulk shear rates provided by the rheometer are of the same order of magnitude at high applied velocities (not depicted); at the low velocities, these shear rates significantly differ. The model suggests that apparent shear rates obtained from the rheological measurement are underestimated. Such result makes sense in localized or banded flows in a Couette cell. This method is applied when MRI velocimetry is not available, and has limited application in case of material slippage. To investigate how much the slippage perturbed the shear rate estimation using eq. 22, the result was compared with the one obtained using MRI velocimetry.

Local rheology obtained using MRI velocimetry is shown in Fig. 39. For the sequence of velocity measurements resulting in overlapping shear rates it is normal to have a dispersion of associated local stress values. This happens due to the difference of the initial state of the matter at the beginning of each measurement.

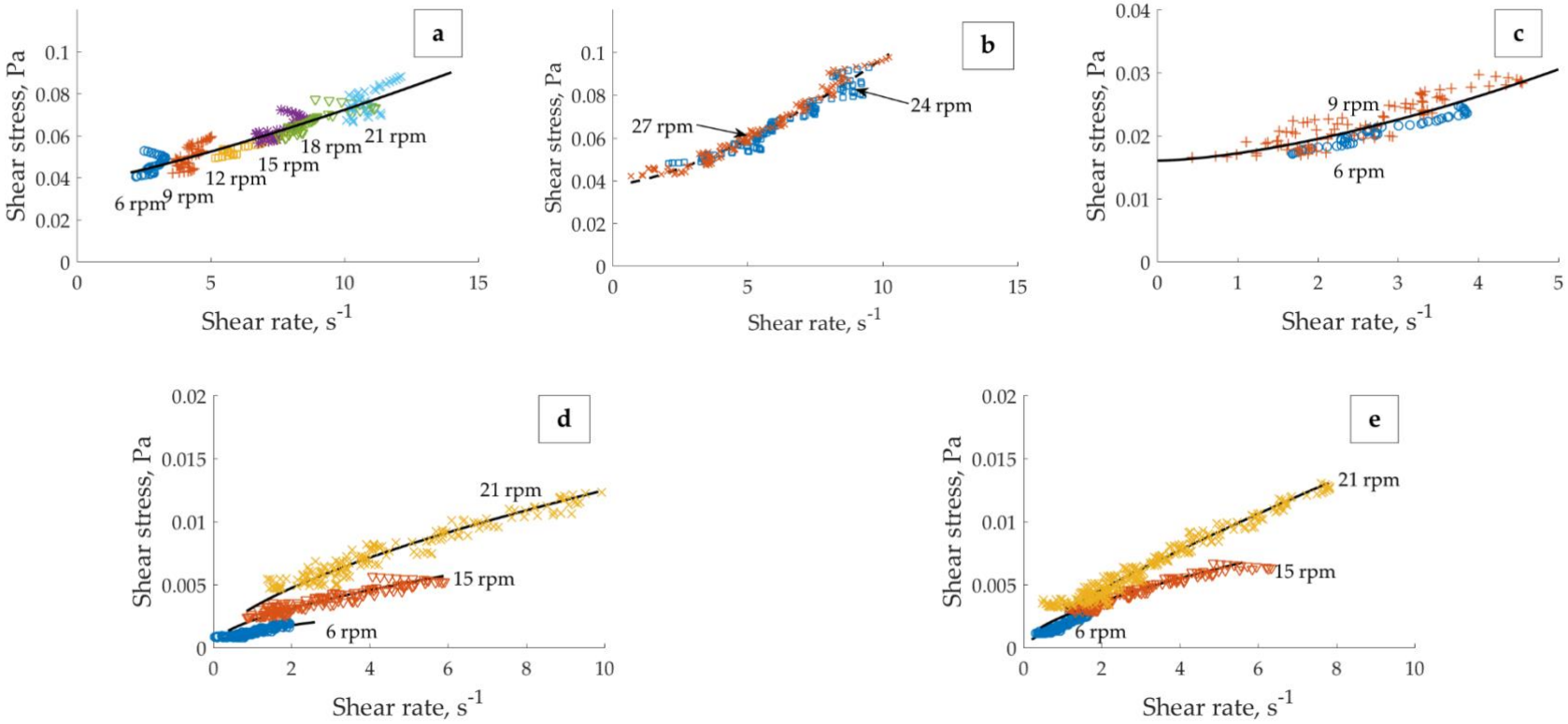


*Figure 39 - Local rheology (calculated from MRI velocimetry) for suspensions prepared under different chemistry, with Herschel–Bulkley fit for: (a) pH 4 in 1 × $10^{-2}$ M $KNO_3$, 6–21 rpm (solid line: $K$ = 0.002 Pa.s, $n$ = 1.24, $\tau_0$ = 0.038 Pa); (b) pH 4 in 1x$10^{-2}$ M $KNO_3$, 24, 27 rpm (dashed line: $K$ = 0.002 Pa.s, $n$ = 1.47, $\tau_0$ = 0.038 Pa); (c) pH 4 in 1x$10^{-2}$ M NaCl (solid line, $K$ = 0.0012 Pa.s, $n$ = 1.56, $\tau_0$ = 0.016 Pa); (d) pH 8 in 1x$10^{-2}$ M $KNO_3$, (e) pH 10 1x$10^{-2}$ M $KNO_3$.*

For the pH 4 in $1 \times 10^{-2}$ M $KNO_3$ suspension two major trends were observed. They are depicted in the Fig. 39a (all curves result from the banded profiles) and Fig. 39b (both curves result from the localized profiles). The yield stress corresponding to the $KNO_3$-based suspension (0.038 Pa, Fig. 39a) was twice that of NaCl-based suspension (0.016 Pa, Fig. 39c). For suspensions at pH 8 (Fig. 39d) and 10 (Fig. 39e) in $1 \times 10^{-2}$ M $KNO_3$, the low shear rate viscosities acquired using MRI velocimetry are about the viscosity of water, which causes respective torques to approach the lowest limit of the rheometer. This fact complicates the proper evaluation of the yield stress which seems to be very small, or, even inexistent for these suspensions, explaining the absence of yield-stress related phenomena. The apparent stratification of the curves at different applied velocities in Figs. 39d, e is, thus, assigned to the measurement-related uncertainty. Full set of local rheological curves (6, 9, 12, 15, 18 and 21 rpm) for pH 8 in $1 \times 10^{-2}$ M $KNO_3$ can be found in the appendix III.

## Discussion

The difference between the suspensions with different pH observed in Fig. 32 can be explained by the formation of a three-dimensional particle network in the acidic environment. At pH 4 (Fig. 32a) the faces and edges of the particles possess opposite surface charge which allows the formation of continuous E-F network in the suspension. Once the applied load exceeds the yield stress of this fragile network, it breaks, and the particles follow the flow direction assigned by the movement of the internal cylinder. The structure collapses abruptly so that the shear rate cannot advance accordingly, and the suspension exhibits banding. Coexistence of solid and liquid phases in more concentrated (around 3–5 vol.% solid, i.e., 30-50 times higher concentration than the one investigated in this study) bentonite suspensions was previously reported by (Raynaud et al. 2002; Coussot et al. 2002c). Those studies were conducted on the suspensions made with tap or distillate water at, presumably, natural pH (no value reported) which is usually slightly basic for bentonite suspensions. In these conditions, the particles mutually repel, and the formation of a three-dimensional network is hindered. Coussot et al. (2002c) related the thickness of solid region to the degree of jamming. In their system with repulsive electrostatic interactions, jamming may also explain simultaneous occurrence of flowing and static regions in their suspensions. Fig. 32b features the velocity profile in the suspension where bentonite particle edges are close to their IEP. In this case, absolute value of potential energy of interaction of E-F type is less (meaning, the attraction is reduced) comparing to that at pH 4; interaction between the edges, on contrary, is enhanced (Durán et al. 2000). At pH 8, for both association types (E-F and E-E), the potential barrier that must be exceeded for dispersion of the aggregated particles is small compared to that at pH 4. Decrease in the attractive E-F interaction between the particles with increasing pH yields an easy-flowing system without any obvious localized discontinuities in the gap. Figure 32c demonstrates the velocity profile of bentonite suspension at pH 10. In this environment, all particle sites carry negative charge and, thus, mutually repel. Therefore, the suspension at pH 10 flows easily, giving a response close to one of Newtonian fluid. Above mentioned electrostatic interactions between the bentonite particles suggest that in dilute aqueous bentonite suspensions coexistence of static and flowing zones of material is related to the formation of continuous three-dimensional network.

In acidic bentonite suspensions under the load, there is a constant confrontation between the building and breaking of the three-dimensional particle network. It is expected that as soon as the load is removed or decreased significantly, the re-structuring of the network in the lowest shear zone will commence and continue progressing as far as possible with respect to the local shear rate in the gap. Figure 34 demonstrates the recovery of the three-dimensional particle network under the mild load (6 rpm). Intensive recovery took place in first four hours after the velocity decrease from 27 rpm while after 12 h the shear banding was recovered. Mismatch in banding points found from network recovery tests (Fig. 34) and shearing the original suspension (Fig. 33a) could be explained by favoured due to previous shear-induced particle alignment recovery mechanism. Alternatively, the application of shear rate from zero velocity to 6 rpm (e.g., Fig. 33a) provides impulsive cracking that possesses a semi-steady nature, and at higher timescales the banding point eventually converges to that found at 12 h (Fig. 34).

From the results presented on the Fig. 35, it is clear that the local rheology of acidic bentonite suspensions is affected by the type of monovalent electrolyte available in the solution. There are several ways in which the chosen salt can influence the mechanical strength of the particle network. First, the size of an elementary unit of the network (meaning, the bentonite particle) is known to depend on the degree of swelling. Having $K^+$ instead of $Na^+$ in aqueous bentonite suspensions was found to limit the particle swelling (Norrish 1954; Luckham and Rossi 1999). In other words, the size of the network elementary unit is a function of the type of cation introduced with the salt. Secondly, the strength of the interaction between those elementary units can be influenced through the EDL formed around the particles by changing the type and concentration of salt introduced in the suspension. Niriella and Carnahan (2006) measured the zeta potential (electric potential at the shear plane of EDL) of bentonite particles in various electrolyte solutions. For $1 \times 10^{-2}$ M electrolyte concentration, zeta potential of -22 mV in NaCl against -15.6 mV in KCl was reported at pH 4 and 200 mg/L of solid. It was suggested that due to less cation hydration, EDL formed with $K^+$ is thinner than the one formed with $Na^+$, with higher portion of ions representing the Stern layer (Shainberg and Kemper 1966; Di Maio 1996). Bentonite lamellae are composed of the $SiO_2$-$Al_2O_3$-$SiO_2$ sheets; the chemistry of these oxides and the character of their interaction with the salt define the properties of the bentonite particles' EDL. Therefore, we shall take a look at the chemistries and surface properties of silica ($SiO_2$) and alumina ($Al_2O_3$). Some studies indicated the preferential adsorption of $K^+$ ion (over $Na^+$) onto the silanol groups, relating it to the bare ion size, and

suggested that the cation adsorbability is not influenced by the ionic hydrated radius (Dishon et al. 2011). It was reported earlier (Dishon et al. 2009) that the decay of electrostatic repulsion between two silica surfaces is more pronounced in the solution of KCl than in that of NaCl. Thus, considering the same distance between the surfaces, the van der Waals attraction is more influential in KCl solution. The effect of anion identity (e.g., $Cl^-$ or $NO_3^-$) on surface charge density and surface potential of silica was proven to be insignificant in the range of pH values above pH 3 (Gmür et al. 2016). Measurements performed on alpha-alumina showed no significant difference in the adsorption tendencies, behaviour in EDL, and thus, no significant change in zeta potentials for $Cl^-$ and $NO_3^-$ anions (Johnson et al. 1999; Franks et al. 1999). The influence of type of cation on electrochemical properties of alpha-alumina was found to be negligible at moderate ($1 \times 10^{-2}$ mol/L) electrolyte concentration and was only manifested at a high (1 mol/L) electrolyte concentration, with the preferential binding of $Na^+$ over $K^+$ (Johnson et al. 1999). From the above points, one may conclude that the difference in the EDL of bentonite particles in different salt solutions is largely dictated by the type of cation and its interaction with the $SiO_2$ layers of bentonite particles. The anion identity in this case is expected to have from no to minor effect on the electrochemical properties of the bentonite particles. In summary, the above-described phenomena are responsible for difference in particle network formed in presence of $K^+$ and $Na^+$, and its mechanical resistance against loading. Some recent advances in the customization of non-Newonian fluids also suggest manipulation of the salt type and concentration as a mean of control of viscoelastic properties of polyelectrolyte solutions (Turkoz et al. 2018).

SEM images presented in Figs. 36a, b suggest that the size of the aggregates depends on the type of the salt utilized. The aggregates found in the suspension prepared with $1 \times 10^{-2}$ M NaCl (Fig. 36b) were larger and thicker than those found in the suspension prepared with $1 \times 10^{-2}$ M $KNO_3$ (Fig. 36a). Larger aggregates can explain why the network does not collapse abruptly (shear banding) that happened to the suspension prepared in $1 \times 10^{-2}$ $KNO_3$ at pH 4; but it rather flows in a continuous manner (shear localization). Long chains of aggregates found at pH 8 (around IEP of bentonite edges) in $1 \times 10^{-2}$ $KNO_3$ bentonite suspension (Fig. 36c) are attributed to the decrease in the electrostatic repulsion between bentonite particle edges and, thus, increased weak E-E attraction due to the van der Waals force. This attraction, however, is not significantly influential to lead shear banding or localization (Fig. 33b).

From the global rheological curves presented on the Fig. 37, it is clear that pH 4 suspensions in different salt solutions do not flow in the same manner. Significant effect of $K^+$ ion on the rheological properties of sodium montmorillonite was previously reported (Güngör and Dilmac 1997). Suspensions at pH 10 and pH 8 (both in $1 \times 10^{-2}$ M $KNO_3$) flow in very similar manner. This happens due to repulsive interactions between the particles at pH 10 and weak particle interaction at pH 8; both cases result in easy-flowing system. It is important to state that the result is valid for dilute suspensions in this study.

Shear rate is related to the velocity gradient in the gap of the rheometer. An equation used by the rheometer software for the shear rate calculation, eq. 23, contains coefficient ($F_{\dot{\gamma}}$) that ignores the stagnant regions in the cell. In contrast, the MRI velocimetry allows to identify the critical radius, observe the velocity distribution, detect slipping and quantify its degree. Identifying the border between "solid" and "liquid" region is crucial for correct estimation of shear rate in a suspension characterised with banding or localization. This explains the underestimation of the shear rate by means of conventional rheometry.

Despite the slipping, two methods used to recover the local rheology of pH 4 suspensions agreed in the overlapping range of shear rates (Figs. 38 and 39a–c). The yield stress difference between the $KNO_3$-based suspension (Fig. 39a) and NaCl-based suspension (Fig. 39c) is assigned to the influence of the type of monovalent electrolyte on the strength of the three-dimensional particle network formed at pH 4. Suspensions not possessing a continuous three-dimensional E-F network (Figs. 39d, e) behaved in a manner similar to one another, each overlapping with or being very close to the global curve (obtained via conventional rheometry). Despite the absence of a continuous E-F three-dimensional particle network in the suspensions with solely repulsive interactions (e.g., pH 10 in $1 \times 10^{-2}$ M $KNO_3$), the (reversible) particle re-organisation still can occur under the shear. Specifically, the particles can align with the flow under the load, resulting in re-arrangement, which is not necessary charge-favourable. When the load is removed, particles must reorganise again, to increase the distance between similarly charged sites.

The existence of a master curve for the suspensions in this study depends on the chemistry of the suspending media. For pH 8 and 10 in $1 \times 10^{-2}$ M $KNO_3$, the establishment of master curve is possible due to the simplicity of the global rheological curve and its good agreement with local rheology (within the range of shear rates acquired via MRI velocimetry). Narrow range of data acquired for pH 4 in $1 \times 10^{-2}$ M NaCl sample (Fig. 39c)

did not allow us to confidently conclude the existence of master curve — further research is required. Nevertheless, it is worth mentioning that all the steady state local rheological curves obtained for this suspension collapse on the curve depicted in Fig. 39c. For the pH 4 in $1 \times 10^{-2}$ M $KNO_3$, the establishment of a master curve suitable for whole shear rate range at any scale and flow history with a single set of parameters does not seem to be possible (Figs. 39a, b). Similar conclusion was drawn by (Salmon et al. 2003) when comparing local and global behaviour of concentrated emulsions. The behaviour of the acidic suspensions in the flowing zone can be described by a simple power-law model (e.g., Herschel–Bulkley). It was also the case for more concentrated suspensions with non-interfered chemistry (Raynaud et al. 2002; Coussot et al. 2002c). Nevertheless, the velocity profile for a given applied load is a function of suspension's history of shear and time of rest (as agreed with the previous report by Raynaud et al. 2002). As an evidence of true thixotropy, the existence of several different structure-dependent states for a single value of the shear rate was demonstrated. Each of these states is characterised by its own local curve that reflects the degree of system's destruction. That leads to complexity of relevant description of suspension's flow behaviour via a single simple model with just one set of parameters.

Some of the observations made in the present work agree with those conducted on the aqueous suspensions of laponite, such as occurrence of banding (Divoux et al. 2013) and localization (Gibaud et al. 2009), or the shear rate-shear stress plateau found in the global flow curve, in the shear rate range corresponding to banding (Divoux et al. 2013).

## Conclusions

Coussot et al. (2002a) reported that the structured fluids at low and moderate shear rates cannot flow homogeneously, which complicates conduction of meaningful measurement via conventional viscometric methods. Present study investigates flow inhomogeneities in such fluids. In our study, the card house concept was used to explain the differences among the local flow behaviors of dilute bentonite suspensions prepared under different solution chemistry. Using the MRI velocimetry, it was found that banding and localization were manifested in the clay suspensions with a low volumetric concentration of solids (0.1 vol.%), under chemical conditions favorable for the three-dimensional particle network formation (e.g., pH 4 in $1 \times 10^{-2}$ $KNO_3$ and NaCl salt solutions). Mechanical strength of E-F network was controlled through the particle swelling and the EDL of the particle surfaces, hence, the pH and type of salt used to make a suspension had a crucial influence. It was demonstrated that in dilute aqueous bentonite suspensions banding could be significantly hindered by: (a) increasing the suspension pH to close to or above the IEP of bentonite particle edge, (b) adding cations with smaller bare radius from monovalent salt to the suspension. In the latter case, formation of aggregates of different size with different monovalent salt was observed by means of SEM. The later findings suggest that in case of necessity to maintain a certain acidity in a stirred tank it is not essential to compromise the pH to eliminate the banding; but changing the type of electrolyte could help to diminish the banding effect. For instance, coexistence of stagnant and agitated volumes in the stirred tanks (otherwise known as “caverns”) is an actual problem in mineral processing industry, that is often related to presence of phyllosilicates (Bakker et al. 2009, 2010).

The absence of shear banding or localization in the suspensions at pH 8 and 10, both in $1 \times 10^{-2}$ M $KNO_3$ is due to very low or no yield stress present in these samples. Weak attractive particle interactions at pH 8 and repulsive interactions at pH 10 result in easy-flowing systems.

A method consisting in the recovery of local flow curve using the output of conventional rheometer (Coleman et al. 1966; Coussot 2005; Ovarlez et al. 2008; Coussot et al. 2009) was applied to the dilute acidic bentonite suspensions (pH 4 in $1 \times 10^{-2}$ $KNO_3$ and NaCl salt solutions). Within the range of shear rates tested, the result

of calculation was found to be in a good agreement with the local rheology obtained via the MRI velocimetry, despite the slipping.

A master curve with a single set of parameters can be established for the dilute suspensions without a continuous three-dimensional particle network (meaning, pH 8 and 10 in $1 \times 10^{-2}$ M $KNO_3$). It is possible due to their simple behaviour under the load and low sensitivity to the history of shear. Suspension at pH 4 in $1 \times 10^{-2}$ M $KNO_3$ is characterised with a card house network and banded velocity profile; strong history-dependence of its flow properties justifies the existence of several flow curves, each correspondent to a particular state of the material. A concept of simple power-law master curve with a single set of parameters is inapplicable in this case, and a more complex model will be considered.

## Author Contributions

Data Curation and Validation, M.J., S.K.D.R, O.C., A.O. and M.F., Investigation, O.C., M.F. and A.O., Resources, A.O., S.K.D.R. and M.F., Supervision, A.O., S.K.D.R., and M.J., Writing-Review & Editing, O.C., A.O. and M.J., Visualization, O.C. and A.O.

## Funding

The financial support of Ministry of Higher Education, Research and Innovation of France is acknowledged.

## Acknowledgments

Prof. Jean-Marc Montel from Université de Lorraine is acknowledged for his helpful comments. The authors also thank the technical support from GeoRessources.

## Conflicts of Interest

The authors declare no conflict of interest.

## Bibliography


Abu-Jdayil B (2011) Rheology of sodium and calcium bentonite–water dispersions: Effect of electrolytes and aging time. International Journal of Mineral Processing 98:208–213. doi: 10.1016/j.minpro.2011.01.001

Alderman N, Gavignet A, Guillot D, Maitland G (1988) High-Temperature, High-Pressure Rheology of Water-Based Muds

Bakker CW, Meyer CJ, Deglon DA (2010) The development of a cavern model for mechanical flotation cells. Minerals Engineering 23:968–972. doi: 10.1016/j.mineng.2010.03.016

Bakker CW, Meyer CJ, Deglon DA (2009) Numerical modelling of non-Newtonian slurry in a mechanical flotation cell. Minerals Engineering 22:944–950. doi: 10.1016/j.mineng.2009.03.016

Benna M, Kbir-Ariguib N, Magnin A, Bergaya F (1999) Effect of pH on Rheological Properties of Purified Sodium Bentonite Suspensions. Journal of Colloid and Interface Science 218:442–455. doi: 10.1006/jcis.1999.6420

Benslimane A, Bekkour K, François P, Bechir H (2016) Laminar and turbulent pipe flow of bentonite suspensions. Journal of Petroleum Science and Engineering 139:85–93. doi: 10.1016/j.petrol.2015.12.020

Boger DV (2009) Rheology and the resource industries. Chemical Engineering Science 64:4525–4536. doi: 10.1016/j.ces.2009.03.007

Callaghan PT (1999) Rheo-NMR: nuclear magnetic resonance and the rheology of complex fluids. Reports on Progress in Physics 62:599–670. doi: 10.1088/0034-4885/62/4/003

Callaghan PT, Fischer E (2001) Rheo-NMR: a New Application for NMR Microscopy and NMR Spectroscopy. 5

Choo KY, Bai K (2015) Effects of bentonite concentration and solution pH on the rheological properties and long-term stabilities of bentonite suspensions. Applied Clay Science 108:182–190. doi: 10.1016/j.clay.2015.02.023

Coleman BD, Markovitz H, Noll W (1966) Special Viscometric Flows. In: Viscometric Flows of Non-Newtonian Fluids. Springer, Berlin, Heidelberg, pp 34–55

Coussot P (2005) Rheometry of Pastes, Suspensions, and Granular Materials: Applications in Industry and Environment. John Wiley & Sons

Coussot P, Nguyen QD, Huynh HT, Bonn D (2002a) Viscosity bifurcation in thixotropic, yielding fluids. Journal of Rheology 46:573–589. doi: 10.1122/1.1459447

Coussot P, Nguyen QD, Huynh HT, Bonn D (2002b) Avalanche Behavior in Yield Stress Fluids. Phys Rev Lett 88:175501. doi: 10.1103/PhysRevLett.88.175501

Coussot P, Raynaud JS, Bertrand F, et al (2002c) Coexistence of Liquid and Solid Phases in Flowing Soft-Glassy Materials. Physical Review Letters 88:. doi: 10.1103/PhysRevLett.88.218301

Coussot P, Tocquer L, Lanos C, Ovarlez G (2009) Macroscopic vs. local rheology of yield stress fluids. Journal of Non-Newtonian Fluid Mechanics 158:85–90. doi: 10.1016/j.jnnfm.2008.08.003

Di Maio C (1996) Exposure of bentonite to salt solution: osmotic and mechanical effects. Géotechnique 46:695–707. doi: 10.1680/geot.1996.46.4.695

Dishon M, Zohar O, Sivan U (2011) Effect of Cation Size and Charge on the Interaction between Silica Surfaces in 1:1, 2:1, and 3:1 Aqueous Electrolytes. Langmuir 27:12977–12984. doi:

10.1021/la202533s

Dishon M, Zohar O, Sivan U (2009) From Repulsion to Attraction and Back to Repulsion: The Effect of NaCl, KCl, and CsCl on the Force between Silica Surfaces in Aqueous Solution. Langmuir 25:2831–2836. doi: 10.1021/la803022b

Divoux T, Fardin M-A, Manneville S, Lerouge S (2015) Shear Banding of Complex Fluids. Annual Review of Fluid Mechanics 48:. doi: 10.1146/annurev-fluid-122414-034416

Divoux T, Grenard V, Manneville S (2013) Rheological Hysteresis in Soft Glassy Materials. Physical Review Letters 110:. doi: 10.1103/PhysRevLett.110.018304

Durán JDG, Ramos-Tejada MM, Arroyo FJ, González-Caballero F (2000) Rheological and Electrokinetic Properties of Sodium Montmorillonite Suspensions: I. Rheological Properties and Interparticle Energy of Interaction. Journal of Colloid and Interface Science 229:107–117. doi: 10.1006/jcis.2000.6956

Farrokhpay S, Ndlovu B, Bradshaw D (2016) Behaviour of swelling clays versus non-swelling clays in flotation. Minerals Engineering 96–97:59–66. doi: 10.1016/j.mineng.2016.04.011

Forsmo SPE, Apelqvist AJ, Björkman BMT, Samskog P-O (2006) Binding mechanisms in wet iron ore green pellets with a bentonite binder. Powder Technology 169:147–158. doi: 10.1016/j.powtec.2006.08.008

Franks GV, Johnson SB, Scales PJ, et al (1999) Ion-Specific Strength of Attractive Particle Networks. Langmuir 15:4411–4420. doi: 10.1021/la9815345

Gibaud T, Barentin C, Taberlet N, Manneville S (2009) Shear-induced fragmentation of laponite suspensions. Soft Matter 5:3026. doi: 10.1039/b906274b

Gmür TA, Goel A, Brown MA (2016) Quantifying Specific Ion Effects on the Surface Potential and Charge Density at Silica Nanoparticle–Aqueous Electrolyte Interfaces. J Phys Chem C 120:16617–16625. doi: 10.1021/acs.jpcc.6b02476

Goh R, Leong Y-K, Lehane B (2011) Bentonite slurries—zeta potential, yield stress, adsorbed additive and time-dependent behaviour. Rheol Acta 50:29–38. doi: 10.1007/s00397-010-0498-x

Güngör N, Dilmac S (1997) The effect of some salts and (NaPO3)n polymer on viscosity of na-montmorillanite slurry. Journal of the Chemical Society of Pakistan 19:14–19

Huertas FJ, Carretero P, Delgado J, et al (2001) An Experimental Study on the Ion-Exchange Behavior of the Smectite of Cabo de Gata (Almería, Spain): FEBEX Bentonite. Journal of Colloid and Interface Science 239:409–416. doi: 10.1006/jcis.2001.7605

Hunter RJ (1986) Foundations of colloïd science. Oxford (GB) : Clarendon Press. 1986.

Jarny S, Roussel N, Rodts S, et al (2005) Rheological behavior of cement pastes from MRI velocimetry. Cement and Concrete Research 35:1873–1881. doi: 10.1016/j.cemconres.2005.03.009

Johnson SB, Scales PJ, Healy TW (1999) The Binding of Monovalent Electrolyte Ions on α-Alumina. I. Electroacoustic Studies at High Electrolyte Concentrations. Langmuir 15:2836–2843. doi: 10.1021/la980875f

Kelessidis VC, Tsamantaki C, Dalamarinis P (2007) Effect of pH and electrolyte on the rheology of aqueous Wyoming bentonite dispersions. Applied Clay Science 38:86–96. doi: 10.1016/j.clay.2007.01.011

Luckham PF, Rossi S (1999) The colloidal and rheological properties of bentonite suspensions. Advances in Colloid and Interface Science 82:43–92. doi: 10.1016/S0001-8686(99)00005-6

Mahto V, Sharma VP (2004) Rheological study of a water based oil well drilling fluid.

Journal of Petroleum Science and Engineering 45:123–128. doi: 10.1016/j.petrol.2004.03.008

Manneville S (2008) Recent experimental probes of shear banding. Rheol Acta 47:301–318. doi: 10.1007/s00397-007-0246-z

Mopoung S, Sriprang N, Namahoot J (2014) Sintered filter materials with controlled porosity for water purification prepared from mixtures with optimal ratio of zeolite, bentonite, kaolinite, and charcoal. Applied Clay Science 88–89:123–128. doi: 10.1016/j.clay.2013.11.035

Niriella D, Carnahan RP (2006) Comparison Study of Zeta Potential Values of Bentonite in Salt Solutions. Journal of Dispersion Science and Technology 27:123–131. doi: 10.1081/DIS-200066860

Nones J, Riella HG, Trentin AG, Nones J (2015) Effects of bentonite on different cell types: A brief review. Applied Clay Science 105–106:225–230. doi: 10.1016/j.clay.2014.12.036

Norrish K (1954) The swelling of montmorillonite. Discussions of the Faraday Society 18:120. doi: 10.1039/df9541800120

Olmsted PD (2008) Perspectives on shear banding in complex fluids. Rheol Acta 47:283–300. doi: 10.1007/s00397-008-0260-9

Otterstedt J-E, Brandreth DA (1998) Clays and Colloidal Silicas. In: Small Particles Technology. Springer, Boston, MA, pp 155–183

Ovarlez G, Cohen-Addad S, Krishan K, et al (2013) On the existence of a simple yield stress fluid behavior. Journal of Non-Newtonian Fluid Mechanics 193:68–79. doi: 10.1016/j.jnnfm.2012.06.009

Ovarlez G, Rodts S, Chateau X, Coussot P (2009) Phenomenology and physical origin of shear localization and shear banding in complex fluids. Rheol Acta 48:831–844. doi: 10.1007/s00397-008-0344-6

Ovarlez G, Rodts S, Ragouilliaux A, et al (2008) Wide-gap Couette flows of dense emulsions: Local concentration measurements, and comparison between macroscopic and local constitutive law measurements through magnetic resonance imaging. Phys Rev E 78:036307. doi: 10.1103/PhysRevE.78.036307

Perge C, Fardin M-A, Manneville S (2014) Surfactant micelles: Model systems for flow instabilities of complex fluids. The European Physical Journal E 37:. doi: 10.1140/epje/i2014-14023-4

Raynaud JS, Moucheront P, Baudez JC, et al (2002) Direct determination by nuclear magnetic resonance of the thixotropic and yielding behavior of suspensions. Journal of Rheology 46:709–732. doi: 10.1122/1.1463420

Roussel N, Le Roy R, Coussot P (2004) Thixotropy modelling at local and macroscopic scales. Journal of Non-Newtonian Fluid Mechanics 117:85–95. doi: 10.1016/j.jnnfm.2004.01.001

Salmon J-B, Bécu L, Manneville S, Colin A (2003) Towards local rheology of emulsions under Couette flow using Dynamic Light Scattering. The European Physical Journal E 10:209–221. doi: 10.1140/epje/i2002-10110-5

Shainberg I, Kemper WD (1966) Hydration Status of Adsorbed Cations. Soil Science Society of America Journal 30:707. doi: 10.2136/sssaj1966.03615995003000060017x

Sun D, Cui H, Sun W (2009) Swelling of compacted sand–bentonite mixtures. Applied Clay Science 43:485–492. doi: 10.1016/j.clay.2008.12.006

Tadros TF (2010) Rheology of Dispersions: Principles and Applications. Wiley

Tombácz E, Szekeres M (2004) Colloidal behavior of aqueous montmorillonite suspensions: the specific role of pH in the presence of indifferent electrolytes. Applied Clay Science 27:75–94. doi: 10.1016/j.clay.2004.01.001

Turkoz E, Perazzo A, Arnold CB, Stone HA (2018) Salt type and concentration affect the viscoelasticity of polyelectrolyte solutions. Applied Physics Letters 112:203701. doi: 10.1063/1.5026573

van Olphen H (1954) Interlayer forces in bentonite. 418–438

van Olphen H (1964) Internal mutual flocculation in clay suspensions. Journal of Colloid Science 19:313–322. doi: 10.1016/0095-8522(64)90033-9

Vryzas Z, Kelessidis VC, Nalbantian L, et al (2017) Effect of temperature on the rheological properties of neat aqueous Wyoming sodium bentonite dispersions. Applied Clay Science 136:26–36. doi: 10.1016/j.clay.2016.11.007

# Chapter III – Rheology of mineral mixtures

Article in preparation

Olga Chernoburova [1], Akira Otsuki [1], Mathieu Jenny [2], Jean-Marc Montel [3]

[1] GeoRessources Laboratory, Université de Lorraine, UMR7359, BP10162, Vandoeuvre-lés-Nancy, France; akira.otsuki@univ-lorraine.fr

[2] LEMTA, CNRS, Université de Lorraine, UMR 7563, F-54500, Vandoeuvre-lés-Nancy, France;

[3] ENSG, GeoRessources laboratory, OTELo, Université de Lorraine F-54500 Vandoeuvre-lès-Nancy, France

## Résumé

Ce travail est dédié à l'étude des propriétés rhéologiques de suspensions mélangées de trois minéraux: le quartz, l'hématite et la Na-bentonite, avec différentes propriétés de charge de surface. Les courbes d'écoulement des suspensions aqueuses des minéraux et de leurs mélanges ont été obtenues à l'aide d'un rhéomètre à rotation à géométrie «vane-in-cup». La manipulation de la composante électrostatique de la balance de force inter-particules, en modifiant le pH du milieu de suspension, a permis de contrôler l'homo- et l'hétérocoagulation des particules dans la suspension. La microscopie électronique à balayage a été utilisée pour visualiser les différences d'orientation des particules de bentonite dans les systèmes minéraux à quartz-bentonite et hématite-bentonite. Les résultats ont indiqué l'existence de différentes orientations préférées dépendantes de la charge des particules de bentonite à la surface du quartz et de l'hématite. L'orientation des constituants de la matrice de bentonite et leur zone de contact avec la phase minérale introduite ont une forte influence sur les propriétés d'écoulement de la suspension. Plusieurs modèles d'association de particules ont été proposés pour expliquer le comportement des suspensions de minéraux mélangés sous la charge appliquée.

## Abstract

This work studied rheological properties of mix mineral suspensions of three minerals: quartz, hematite and Na-bentonite, with different surface charging properties. Flow curves of aqueous suspensions of the minerals and their mixtures were obtained using a rotational rheometer with a vane and grooved cup geometry. Manipulation of the electrostatic component of inter-particle force balance, achieved by changing the pH of the suspending media, allowed to control particle homo- and heterocoagulation in the suspension. Scanning electron microscopy was used to visualize the differences in the bentonite particle orientation in quartz-bentonite and hematite-bentonite mineral systems. The results indicated the existence of different preferred charge-dependent orientations of bentonite particles on the surface of quartz and hematite. The orientation of the bentonite matrix constituents and their area of contact with the introduced mineral phase has a strong influence on the flow properties of the suspension. Several particle association models were proposed to explain the behavior of the mix mineral suspensions under the applied load.

**Key words**: Homocoagulation, heterocoagulation, isoelectric point, yield stress, pH

## Introduction

Rheology of mineral suspensions has been extensively studied, with particular attention focused on the mechanical properties of fine particle suspensions. Its importance has been highlighted by multiple scientists, in diverse areas, including: pharmaceutics (Aguzzi et al. 2013), mineral processing, in particular - mineral flotation (Ndlovu et al. 2011, 2013; Farrokhpay 2012), drilling fluids (Mahto and Sharma 2004), hydraulic barriers (Barast et al. 2017) and waste management (Boger 2009). Due to their complex behavior under the load, these suspensions may promote formation of caverns in agitation tanks, as it happens, for example, in presence of fine phyllosilicate particles in flotation cells (Bakker et al. 2009, 2010; Ndlovu et al. 2013). It is well-known that aqueous clay suspensions often offer non-Newtonian response to the applied load.

Bentonite is an aluminum phyllosilicate clay, composed mostly of montmorillonite (some other minerals such as quartz or other oxides are also present, in low amounts); it is one the most widely studied swelling clays of smectite group. Its structure consists of sheets (or unit layers) held together via the van der Waals force. Each sheet (unit layer) is built of two tetrahedral silica layers and an octahedral alumina layer sandwiched between them (Luckham and Rossi 1999). Interlayer galleries between the sheets can accommodate some hydrated exchange cations, such as $Na^+$, $Ca^{2+}$, $Mg^{2+}$ (Huertas et al. 2001). Dominating exchange cation defines the type of bentonite. Smaller monovalent cations, such as $Li^+$ or $Na^+$ are usually associated with higher swelling capacity (Norrish 1954; Luckham and Rossi 1999). When ground, this clay breaks down into fine plate-like particles that are characterized with spatial chemical inhomogeneity; it affects charge development on the particle surface. Charge on the faces originates from the isomorphs substitutions present in crystal lattice. This mechanism of charging is not pH-dependent (Durán et al. 2000; Pecini and Avena 2013) and is responsible for permanent net negative charge of particles in aqueous salt solutions. On the edges, where the broken chemical bonds are exposed, the charge is developed due to the adsorption of potential-determining ions and can be positive or negative depending on the pH. The isoelectric point (IEP) of bentonite edges is commonly thought to fall between pH 7 and 8 (Benna et al. 1999; Durán et al. 2000). On the other hand, some reports also suggest the IEP of bentonite edges at pH 4-5.3 (Pecini and Avena 2013). Electrical double layer (EDL) compression was found at 0.1 M NaCl (Tombácz and Szekeres 2004). The concept of “visibility” of EDL of the

edges of montmorillonite was suggested by Tombácz and Szekeres (2004). It implies that until a certain salt concentration (0.01 M NaCl) the EDL induced by the edge of particles is covered by the EDL of the face. Above the threshold of electrolyte concentration, the EDL of the montmorillonite particle becomes “visible” to other particles; in case of oppositely charged edge and face, mutual attraction between neighboring platelets shall take place. A continuous three-dimensional arrangement resulting from such attraction is commonly referred to as “house of cards” (see Fig. 40). Originally, this organization type was suggested by van Olphen (1964) to explain the gel formation in bentonite suspensions.

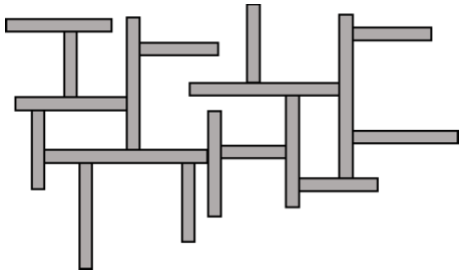

*Figure 40 - “House of cards” arrangement.*

Mechanical properties of bentonite suspensions are known to depend on significant amount of parameters, such as: percent solid (Abu-Jdayil 2011; Choo and Bai 2015), aging time (Abu-Jdayil 2011; Goh et al. 2011; Choo and Bai 2015), chemical environment: pH, salt type and concentration (Luckham and Rossi 1999; Tombácz and Szekeres 2004; Kelessidis et al. 2007; Goh et al. 2011), temperature (Vryzas et al. 2017), previous flow history (Luckham and Rossi 1999; Tombácz and Szekeres 2004). Latter is often referred to as “thixotropy” – a reversible time-dependent viscosity decrease that occurs under the applied load due to structural rearrangements in the system (Tadros 2010). Rheological response of bentonite suspensions can be described using Bingham or Herschel–Bulkley models (Luckham and Rossi 1999; Kelessidis et al. 2007; Abu-Jdayil 2011; Choo and Bai 2015).

Significant amount of comprehensive studies about bentonite homocoagulation was published. Interaction of bentonite (or montmorillonite) with other minerals also gained attention in scientific community. Bailey et al. (2014) studied the effect of addition cationic and anionic silica to montmorillonite dispersions (10:1 montmorillonite to silica ratio, 2.4 and 3.2 wt% solid) and found that mixing relatively small amounts of cationic silica with

the anionic montmorillonite particles results in the formation of a strong heteroflocculated gel. By contrast, result of mixing anionic silica with anionic montmorillonite was dependent on the $c^*$ - solid concentration at which the effective hydrodynamic volumes of the particles begin to overlap. At concentrations below $c^*$, the addition of anionic silica to the anionic montmorillonite results in decrease of the rheological performance of the complex fluid due to destruction of its original structure. On the other hand, above the $c^*$ the mixture of the same components gives gel (Bailey et al. 2014). Later, Hilhorst et al. (2014) used rheology and cryo-TEM to investigate the structural changes in the montmorillonite suspensions with spherical silica particles at different pH, in solution of NaCl. The silica to clay w/w ratios of 0, 0.1 and 0.5 with 2.6-3.4 wt% of clay were studied. It was reported that the addition of silica to montmorillonite suspension results in lowering the yield stress at all pH values tested (pH 5, 7 and 9). Cyro-TEM results evidenced weak mutual attraction between positive clay edges and negatively charged silica particles at pH 5, microphase separation at pH 7, and homogeneous distribution of silica particles throughout the water pockets formed by clay platelets at pH 9. Works performed on silica-kaolinite mixtures with varying size of silica particles (7, 12, 22 nm) evidenced mixture solidification at lower solid concentrations for smaller silica particles. It was found that solidification occurs at lower percent solid for increased salt concentration (in 0.1-0.7 M NaCl range, Baird and Walz 2006). In addition, introduction of silica particles to kaolinite suspension resulted in partial stabilization against sedimentation. Rheological examination of these mixtures suggested that at fixed percent solid, higher yield stresses corresponds to the suspensions with smaller silica particles and higher electrolyte concentrations (Baird and Walz 2007).

The formation of heterocoagulated network in mixed iron oxide and montmorillonite clay systems, below the IEP of the montmorillonite particle edges and above the IEP of iron oxide (hematite or magnetite), is very likely (Tombácz et al. 2004; Tombácz et al. 2001). In such gels, the original montmorillonite particle network gains in strength with addition of iron oxide particles thanks to their adhesive action. However, above certain concentration limit of iron oxide in the suspension (0.2g/100g, as was reported by Tombácz et al. 2001), the structure begins to weaken. These conclusions were drawn for montmorillonite suspension containing 0.01 M of NaCl at pH 4, with 1:15 iron oxide to clay w/w ratio. Structural organization and coagulation in these systems (alike in pure montmorillonite suspensions) has pronounced dependency from the electrolyte concentration, especially under acidic conditions. It has been reported (Tombácz et al. 2001) that heterocoagulation of dissimilar, oppositely charged particles in acidic conditions

(pH ~4) is triggered at significantly lower salt concentration (about 0.01 M NaCl for magnetite-montmorillonite system) than homocoagiulation of each mineral independently (0.035 M for montmorillonite and 0.150 M for magnetite). Electrostatic charge-based associations of non-swelling clays and iron oxide particles that can be manipulated through the pH of continuous media were also reported (e.g., kaolinite (Ohtsubo 1989) and illite (Ohtsubo et al. 1991; Ji et al. 2004).

A valuable input in the study of the relation between the particle shape and rheological performance of the mix component systems was brought by ten Brinke et al. (2007). In this work, the charged lath-, sphere-, plate- or rod-shaped particles were mixed together, and the strength of resulting network was investigated. The study yielded some general conclusions that can be extended to systems of similar nature. On one hand, addition of *similarly charged* particles of different shape to the structured network disrupts it and provokes local packing changes, which weakens the gel. On the other hand, addition of the *oppositely charged* particles of different shape to the gel may enhance the strength of network through enhancing attractive interactions. Particle dimensions are expected to be one of the primary parameters defining the strength of the network, which goes in agreement with the works published by (Baird and Walz 2007; Chernoburova et al. 2018). Under the load electrostatically stabile colloidal suspension (with repulsive interactions between the particles) is expected to behave as Newtonian fluid, whereas aggregated system usually gives plastic or pseudoplastic response (Firth 1976; Firth and Hunter 1976; Tombácz et al. 2004). Nevertheless, it has to be kept in mind that even in the system with solely repulsive electrostatic interactions the mechanical response is a function of particle-particle physical contacts and time required for internal rearrangements under the load.

Majority of studies discussed above suggest surface charging as a mean of manipulating mechanical properties of the mix mineral suspensions. Despite variety of works published in the domain, there is still a place for research, e.g., polydisperse systems, more complex mineralogical composition. In this work, the rheology of polydisperse mix mineral suspensions of sodium bentonite clay, non-spherical quartz and hematite was studied. Different chemical conditions were examined to manipulate the electrostatic component of particle-particle interaction. Several particle association models were proposed to explain the behavior of the mix mineral suspensions under the load.

## Materials and methods

Mineral powders utilized in this study were Kinipia-F sodium bentonite clay (Kunimine Industries Co., Ltd), silicon dioxide (quartz, Sigma-Aldrich), hematite (Brazil). Particle size distributions (PSDs) of the materials were measured using Mastersizer 3000 laser diffraction particle size analyzer (Malvern); the results are presented in the Fig. 41. Sodium bentonite and quartz were suspended in $1 \times 10^{-2}$ M $KNO_3$ aqueous solution at pH 10 to provoke repulsive interaction between the particles for better dispersion. Hematite was suspended in $1 \times 10^{-2}$ M $KNO_3$ aqueous solution at natural pH (approx. 6.3). Measuring the PSD of swelling clays can be challenging (Tan et al. 2017). Thus, the following steps were undertaken to avoid erroneous result: 1) the particles were soaked in the solution ($1 \times 10^{-2}$ M $KNO_3$, pH 10) for 2 days prior to measurement, 2) soft ultrasound (US) was applied. Preference was given to the low US intensities during preparation to avoid possible particle exfoliation.

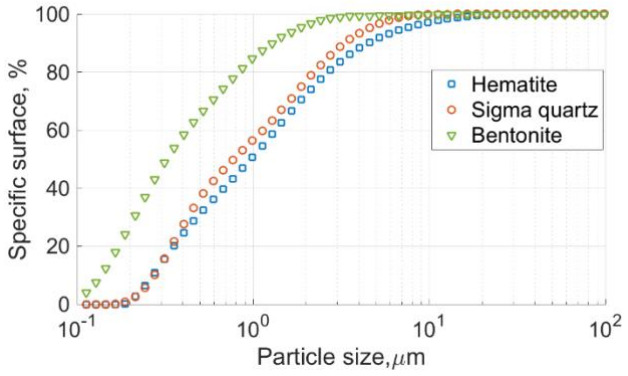


*Figure 41 - PSD of mineral powders.*

Dilute suspensions of this bentonite clay exhibit a wall slip in a Couette concentric cylinder geometry (Chernoburova et al. 2018). In the current study, a reduced slip geometry was thus used to perform the rheological measurements. The flow curve acquisition was conducted using the AR 2000 rheometer (TA Instruments), assembled with vane and cup geometry. Grooved cup was installed in the Peltier concentric cylinder temperature system (TA Instruments) and set to 20°C. Figure 42 displays the utilized geometry with dimensions; it was equivalent to a cylindrical Couette geometry with an

internal cylinder equivalent diameter of 22 mm. The volume of specimen fed into the gap was 45 ml. Steady state measurements were conducted in the shear rate range from 0.01 to 100 $s^{-1}$.

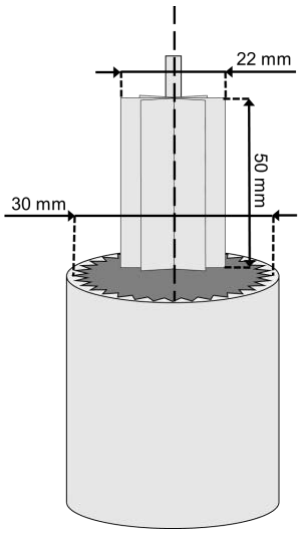


*Figure 42 - Vane and grooved cup geometry.*

Suspensions for rheological measurements were prepared by dispersing the mineral(s) at desired volume percent solid in 1 × $10^{-2}$ M $KNO_3$ aqueous solution and adjusting the pH to 4 (using 1 M and 0.1 M solutions of $HNO_3$) or 10 (using 1 M and 0.1 M solutions of KOH). All bentonite-based suspensions were left to age for 48 h, with another pH-adjustment prior to rheological measurement. Same history of shear for all bentonite-containing specimens was achieved via fixed duration and speed of agitation applied at every conditioning step.

List of specimens prepared for rheological measurements is given in the Table 2. The preparation procedure is explained using specimen 1 as an example. The amount of quartz equal to 0.5 vol% solid was introduced in the 1 × $10^{-2}$ M $KNO_3$ aqueous solution, followed by adjustment to pH 4. Suspension then was placed in the cup of the rheometer and the measurement was performed. Then, another 0.5 vol.% addition of quartz to the total 1 vol% solid was made and the pH was adjusted to maintain the pH 4. The rheological measurement was performed again. Same steps were repeated for the 2.5, 3, 5, 8, and 10 vol% solid. For the specimens 5, 6, 13 and 14 at each step both, quartz and hematite, were added at the same time in 1:1 volume proportion. Last column of the Table 2 contains

the references to the figures depicting the results of rheological measurements that correspond to the given specimen conditions.

*Table 2 - List of specimens and their specification*

| Specimen number | Mineralogical composition, vol% (calculated from the dry mass) | | | pH | Figure |
|---|---|---|---|---|---|
| | Bentonite | Quartz | Hematite | | |
| 1 | - | 0.5, 1, 2.5, 3, 5, 8, 10 | - | 4 | 3 |
| 2 | - | 0.5, 1, 2.5, 3, 5, 8, 10 | - | 10 | 4 |
| 3 | - | - | 0.5, 1, 2.5, 3, 5, 8, 10 | 4 | 5 |
| 4 | - | - | 0.5, 1, 2.5, 3, 5, 8, 10 | 10 | 6 |
| 5 | - | 0.5/0.5, 1/1, 2.5/2.5, 3/3, 5/5 | | 4 | 7 |
| 6 | - | 0.5/0.5, 1/1, 2.5/2.5, 3/3, 5/5 | | 10 | 8 |
| 7 | 0.1 | - | - | 4 | 9 |
| 8 | 0.1 | - | - | 10 | 9 |
| 9 | 0.1 | 0, 0.05, 0.1, 0.15, 0.2, 0.4, 0.6, 0.8, 1, 2, 2.5, 3, 4, 5, 6, 8, 10 | - | 4 | 10 |
| 10 | 0.1 | 0, 0.5, 1, 3, 5, 8, 10 | - | 10 | 11 |
| 11 | 0.1 | - | 0, 0.05, 0.1, 0.2, 0.4, 0.6, 0.8, 1, 1.5, 2, 3, 4, 5, 6, 8, 10 | 4 | 12 |
| 12 | 0.1 | - | 0.5, 1, 3, 5, 8, 10 | 10 | 13 |
| 13 | 0.1 | 0/0, 0.5/0.5, 1/1, 2.5/2.5, 3/3, 5/5 | | 4 | 14 |
| 14 | 0.1 | 0/0, 0.5/0.5, 1/1, 2.5/2.5, 3/3, 5/5 | | 10 | 15 |

Dissolution of iron species influences surface charging and particle-particle interactions (Tombácz et al. 2004). A significant dissolution of iron oxides occurs only below pH4 (Tombácz et al. 2004; Cornell and Schwertmann 2004), meaning that the present study does not suffer from this issue.

Scanning electron microscopy (SEM) was performed using TESCAN VEGA3 SEM system. For image acquisitions, coarse size fractions (40-75 μm) of hematite or quartz were suspended at 0.1 vol% in bentonite matrix (also 0.1 vol%). For each specimen studied, a droplet of suspension was placed onto a standard SEM aluminum stub and left to dry over a night at room temperature. After the carbon coating, secondary electron (SE) images of the specimens were acquired.

## Results

Along with the experimental data, it is common to suggest a simple mathematical equation describing the general shear rate ($\dot{\gamma}$) - shear stress ($\sigma$) relationship (e.g. Hershel-Bulkley model, eq. 25). Such equation, even though arguably representative of real physical values, gives a set of parameters that allows to compare the flow curves to one another using just few values, namely, the value of yield stress ($\sigma_y$), consistency ($k$) and flow indices ($n$).

$$\sigma = \sigma_y + k\dot{\gamma}^n. \qquad [25]$$

If $n > 1$ the fluid is dilatant, if $n < 1$ it is pseudoplastic and if $n = 1$ the fluid is called "Bingham plastic". A case where $\sigma_y = 0$ and $n = 1$, with $k$ being a constant, shear rate-independent value, corresponds to a Newtinoan fluid.

In the Figs. 43-44 and 46-48, the error bars assigned to each point correspond to the percent tolerance set for the torque during the rheological measurement (10%). The data below the torque limit of the rheometer (0.1 μN.m) is not depicted. Shear rate – shear stress curves for quartz suspended in $1 \times 10^{-2}$ M $KNO_3$ aqueous solution, at pH 4 and 10 are given in the Figs. 43a and b, respectively. At low volumetric fractions of solid (0.5, 1 vol%), both pH 4 and pH 10 suspensions behave in the same way – flow in a log-log linear manner, with no clear yield stress observed. In the Fig. 43a, the change in the flow behavior of pH 4 suspension with increasing volume fraction is evident. Upon the addition of solids, the suspension develops a yield stress and changes behavior to Bingham plastic, with and $\sigma_y$ and $k$ reaching 0.1 Pa and 0.02 Pa.s, respectively, for 10 vol% solid

It was found (Fig. 43b) that all the flow curves for the pH 10 suspension fall onto the same line, suspensions behave dilatant, with the $k$ and $n$ being 0.002 and 1.35, respectively.

The flow curves for the suspensions of hematite at pH 4 and 10 in $1 \times 10^{-2}$ M $KNO_3$ are shown in the Figs. 43c and 43d, respectively. As in the case of quartz suspensions, at low solid volume fractions (i.e., 0.5 and 1 vol%) hematite suspensions behave log-log linear, and give more complex rheological behavior only starting from 2.5 vol% solid. In both cases, pH 4 and pH 10, increasing the percent solid results in enhanced rheology. For equivalent volumetric concentration of solid, hematite suspensions at pH 10

give higher stresses than those at pH 4 (for 2.5-10 vol% solid). The behavior of these suspensions can be described using Hershel-Bulkley model. For 10 vol% hematite suspension at pH 4 Hershel-Bulkley fit was characterized with $\sigma_y$=0.24 Pa, $k$=0.26 Pa.s and $n$=0.41, against $\sigma_y$=0.46 Pa, $k$=0.28 Pa.s and $n$=0.42 at pH 10 (also 10 vol%).

Figures 44a and b show rheological behavior of quartz-hematite mixtures at pH 4 and 10 in 1 × $10^{-2}$ M $KNO_3$, respectively. Volumetric proportion of quartz to hematite in these suspensions was set to 1:1. The flow curves of quartz-hematite suspensions at pH 4 and 10 show no difference between 0.5/0.5 vol% fractions; higher stresses were attributed to pH 4 at 1/1, 2.5/2.5 and 3/3 vol% and difference falling into an error bar at 5/5 vol%. Next, suspension of quartz-hematite mixture at pH 4 (Fig. 44a) was compared with single mineral suspensions at pH 4 with the same total volume percent solid (see Fig. 43a for quartz and Fig.43d for hematite). No difference was found between the flow curves of 1 vol% quartz and hematite suspensions (pH 4) and 0.5/0.5% of quartz-hematite mixture (pH 4); all curves demonstrated the same log-log linear trend. The 2.5/2.5 vol% quartz-hematite mixture at pH 4 gave higher stresses than hematite suspended at 5 vol% (pH 4) and much higher stresses than quartz suspended at 5 vol% (pH 4). The 5/5 vol% quartz-hematite mixture at pH 4 exhibited higher stresses than 10 vol% quartz suspension (pH 4) and was comparable (difference within the error bar) with 10 vol% hematite suspension (pH 4).

Flow curves of the mix mineral suspension at pH 10 (depicted in the Fig. 44b) were compared with those of single mineral suspensions with same total volume percent solid at pH 10 (see Fig. 43b for quartz and Fig. 43d for hematite). No difference was found between the 1 vol% quartz and hematite suspensions and 0.5/0.5 vol% quartz-hematite mixture; all curves have shown the same log-log linear trend. However, raising the solid concentration above total 1 vol% solid yielded significant difference of flow curves obtained for quartz-hematite mixture and quartz suspension at pH 10, with more complex rheology attributed to the mixture. Comparison between the quartz-hematite mixture at 2.5/2.5 vol% and 5/5 vol% with 5 and 10 vol% hematite suspensions, respectively, resulted in lower stresses attributed to the mixture at pH 10.

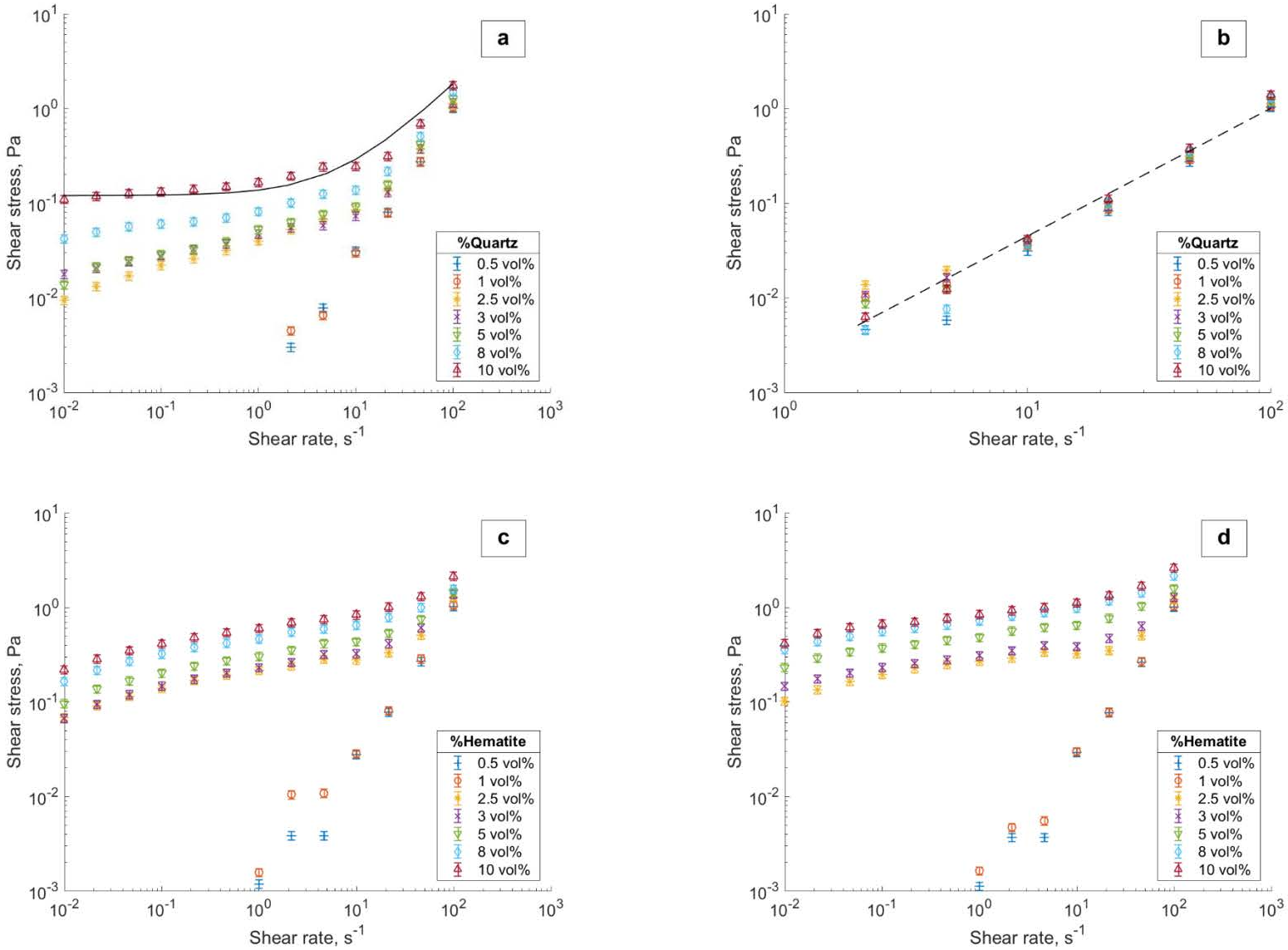


*Figure 43 – Aqueous 1 × $10^{-2}$ M $KNO_3$ suspensions of quartz at (a) pH 4 and (b) pH 10 and hematite at (c) pH 4 and (d) pH 10.*

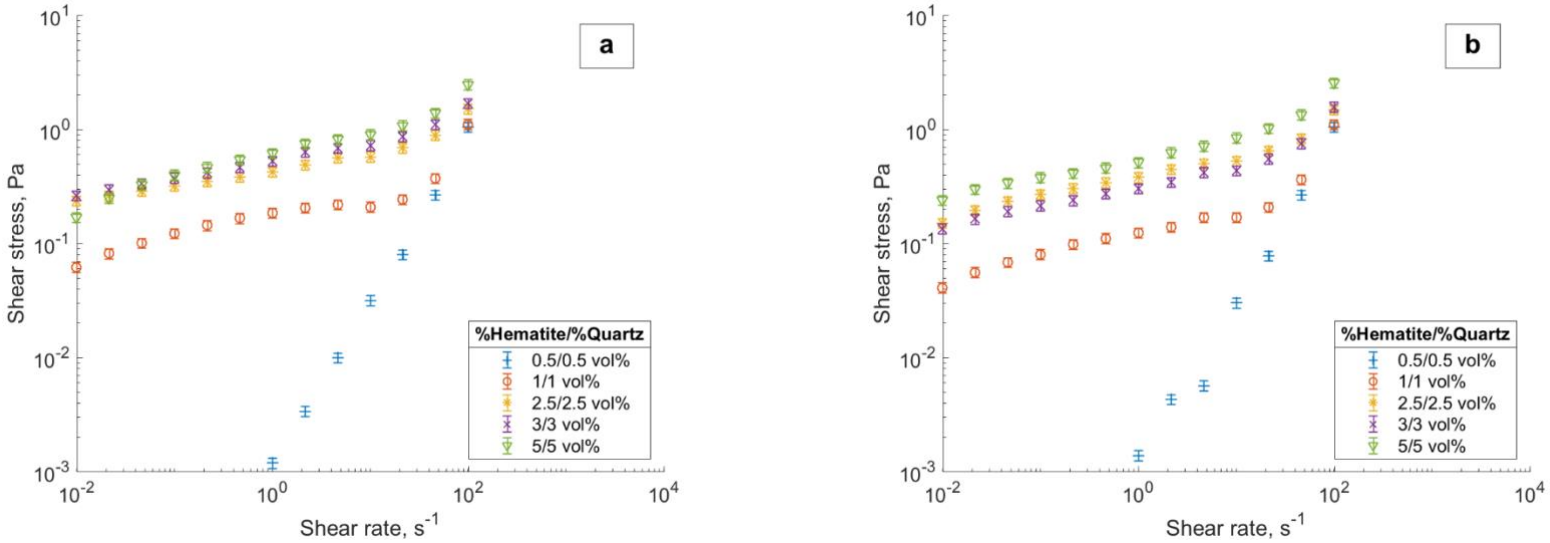


*Figure 44 - Quartz and hematite in volumetric proportion 1:1 at (a) pH 4 and (b) pH 10 in 1 × $10^{-2}$ M $KNO_3$ aqueous solution.*

In the Fig. 45, the flow curves of 0.1 vol% Na-bentonite suspensions at pH 4 and 10 in 1 × $10^{-2}$ M $KNO_3$ are given. Each curve is an average of three measurements, with the bars to each point representing the standard deviation. Low shear rate viscosities measured for the pH 10 bentonite suspension corresponded to the lowest measurable torque of the rheometer, which explains the large deviation from the mean at low shear rates applied. Fig. 45 evidences higher stresses and complexity of rheological behavior attributed to bentonite suspension at pH 4 in 1 × $10^{-2}$ M $KNO_3$ than that at pH 10 in 1 × $10^{-2}$ M $KNO_3$. These results are in agreement with the ones previously published for the same kind of suspensions (Chernoburova et al. 2018).

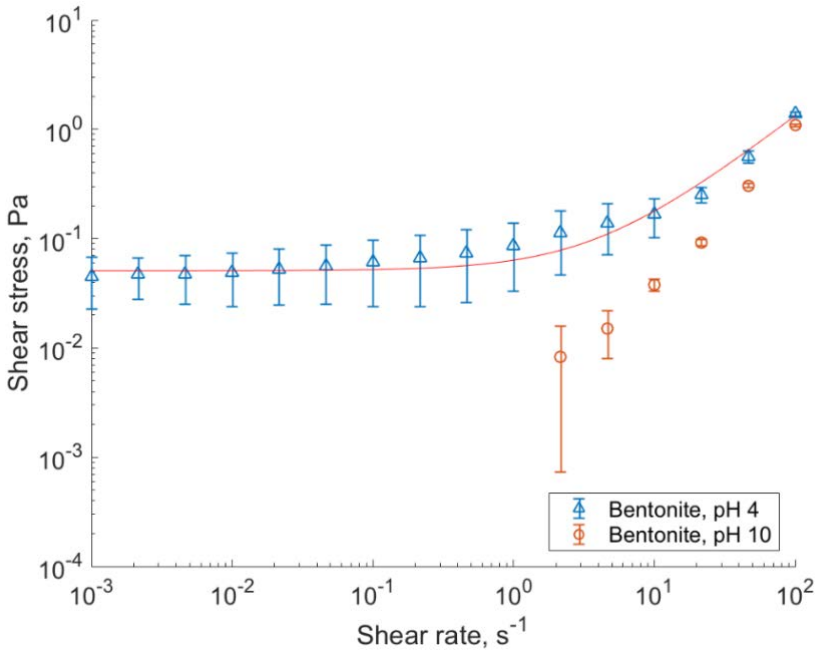


*Figure 45 - Bentonite (0.1 vol%) at pH 4 (triangles) and 10 (circles) in 1 × $10^{-2}$ M $KNO_3$ aqueous solution; the solid line represents a Bingham fit with $\sigma_y$ = 0.05 Pa and $k$ = 0.013 Pa.s.*

The dilute (0.1 vol%) bentonite suspension at pH 4 characterized with the house of cards particle arrangement was used as matrix for quartz and hematite particles. The flow curves of bentonite suspensions with various content of quartz at pH 4 and 10 (in solution of $1 \times 10^{-2}$ M $KNO_3$) are given in the Figs. 46a and b, respectively. In order to avoid the figure overcrowding with the flow curves representing the low volumetric fractions, the reduced representation of these curves is given in the insert in the Fig. 46a. In comparison with the suspension of pure quartz at pH 4, the quartz-containing matrices at pH 4 exhibited higher shear stresses and yield stresses. The flow curves of pH 4 quartz-containing matrices can be fit with the Bingham model. For the bentonite matrix containing 10 vol% of quartz (pH 4) Bingham fit parameters were $\sigma_y$= 0.73 Pa and $k$ = 0.022 Pa.s, against $\sigma_y$ = 0.1 Pa and $k$ = 0.02 Pa.s for 10 vol% quartz suspension (pH 4, see Fig. 43a).

In otherwise even conditions, the flow curves of quartz-containing matrices at pH 4 were found to exhibit higher shear stresses and yield stresses than quartz-containing bentonite suspensions at pH 10. The latter flow in a manner significantly different from both, bentonite and quartz single mineral suspensions at pH 10. Starting from 1 vol% of quartz in the bentonite suspension (pH 10) a sharp difference from 1 vol% single mineral quartz suspension (pH 10) becomes noticeable. Bentonite suspension at pH 10 containing 10 vol% of quartz develops a Bingham yield stress of 0.24 Pa, with 0.023 Pa.s consistency index. On the other hand, 10 vol% quartz suspensions at pH 10 were not found to exhibit the yield stress and behaved dilatant ($n$=1.35).

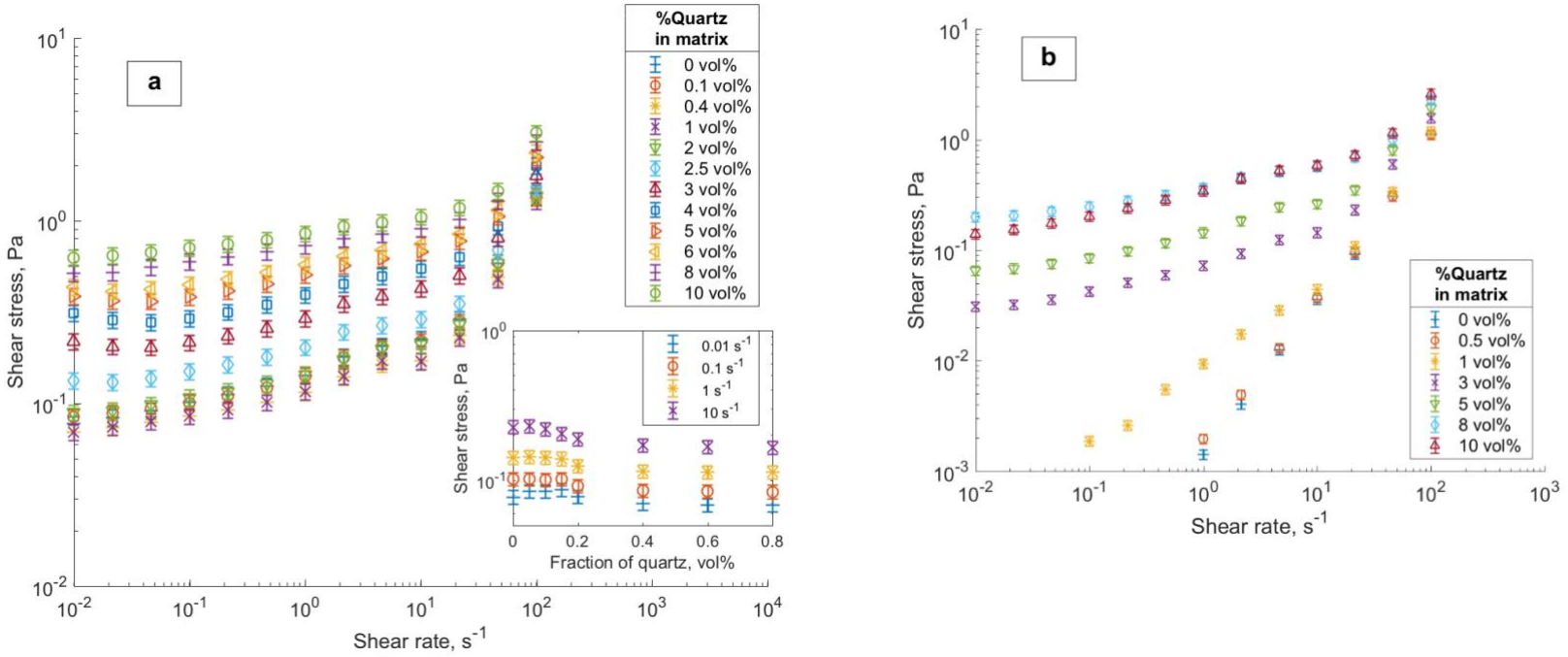


*Figure 46 - Quartz dispersed in (a) bentonite matrix at pH 4 and (b) bentonite suspension at pH 10 in 1 × $10^{-2}$ M $KNO_3$ aqueous solution.*

The rheological curves of bentonite suspensions with various content of hematite in solution of $1 \times 10^{-2}$ M $KNO_3$ can be found in the Figs. 47a (pH 4) and 13 (pH 10). For the facility of comparison, the preference was given to the volume fraction vs shear stress representation. Insert in the Fig. 47a gives better insight into the behavior of hematite-containing matrices with low volumetric concentrations of hematite.

The flow curves of hematite-containing matrices at pH 4 were fit with Hershel-Bulkley model. At pH 4, the hematite-containing matrices change their behavior from dilatant ($n>1$) at low volume fractions of hematite to shear thinning ($n<1$) at high volume fractions of hematite suspended in the bentonite matrix. Flow index of $n=1.02$ (with $k=0.013$ Pa.s and $\sigma_y=0.08$ Pa) corresponded to 0.6 vol% of hematite suspended in the bentonite matrix. Yield stress was found to increase with volume fraction of hematite particles suspended in the bentonite matrix at pH 4, reaching Hershel-Bulkley yield stress of 0.89 Pa (with $k=0.53$ Pa.s and $n=0.31$) at 10 vol% of added hematite. That is, against $\sigma_y=0.24$ Pa, $n=0.41$, and $k=0.26$ Pa.s found for 10 vol% pure hematite suspension at pH 4. It could be observed (Fig. 47a), that from approximately 1.5 vol% of hematite in bentonite matrix its rheological response did not change significantly with the volume fraction of hematite.

Unlike the hematite-containing matrix at pH 4, at pH 10 the hematite-containing bentonite suspension exhibited a consistent increase of the stress response with increasing hematite concentration. The flow curves obtained for hematite dispersed in bentonite suspension at pH 10 were characterized with Hershel-Bulkley fit, with flow index of $n>1$ for 0.5-3 vol%, $n=1.09$ at 5 vol% and $n<1$ for 8 and 10 vol% of hematite. At the same volumetric fraction of hematite pH 10, the suspension gave lower stresses than that at pH4. In comparison to pure hematite suspensions at pH 10, the hematite-containing bentonite suspensions (pH 10) yielded higher shear stresses at the same volumetric concentrations of hematite.

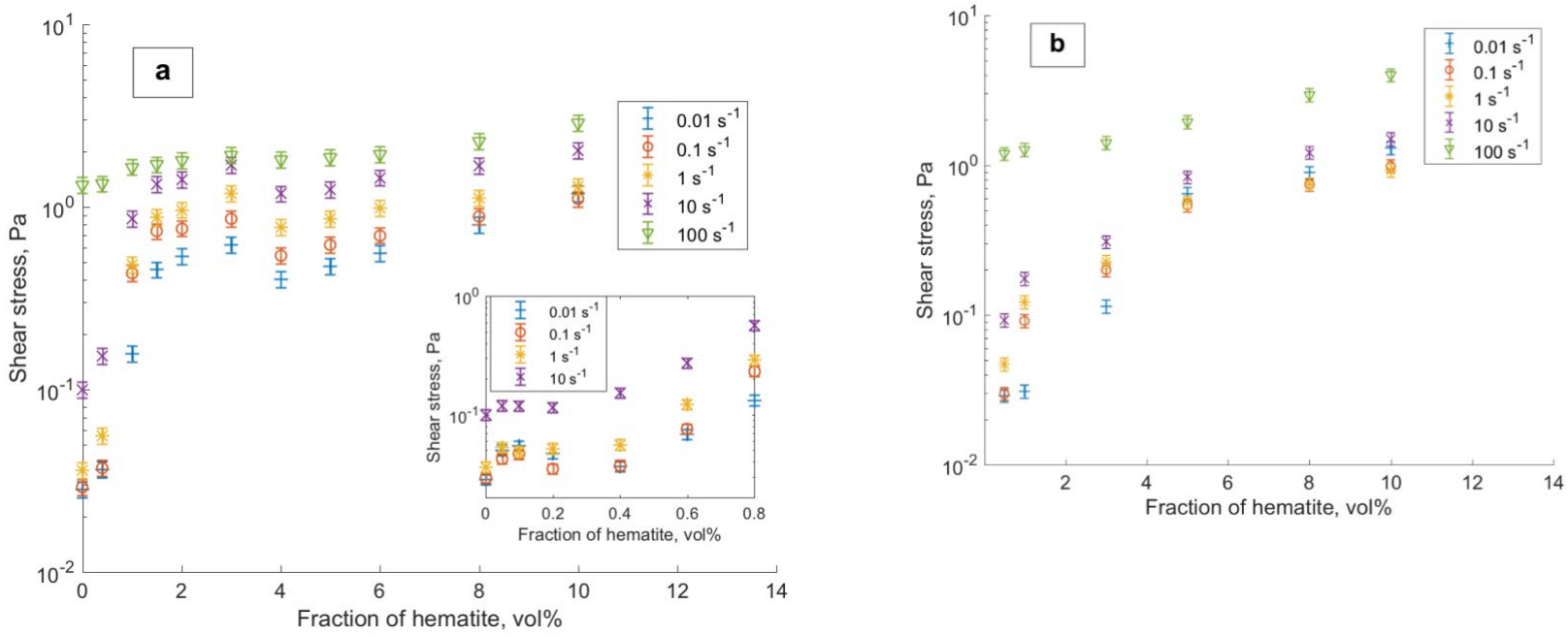


*Figure 47 - Hematite dispersed in (a) bentonite matrix at pH 4 and (b) bentonite suspension at pH 10 in 1 × $10^{-2}$ M $KNO_3$ aqueous solution.*

The flow curves of bentonite suspensions with various content of quartz-hematite mixture at pH 4 and 10, in solution of $1 \times 10^{-2}$ M $KNO_3$ are given in the Figs. 48a and b, respectively. Volumetric proportion of quartz to hematite in these suspensions was set to 1:1. In the first place, a clear difference between the flow curves obtained for low volumetric fractions (0.5/0.5 vol%) of quartz-hematite mixture with (Fig. 48a) and without (Fig. 44a) bentonite can be observed. Quartz-hematite mixture (0.5/0.5 vol%) suspended in bentonite matrix at pH 4 develops a yield stress and more complex, Bingham flow behavior than the 0.5/0.5 vol% quartz-hematite mixture without bentonite. Generally, the behavior of quartz-hematite mixture suspended in the matrix is characterized with higher shear stresses and yield stresses than the behavior of the mixture without bentonite. Considering the same total volume percent of solid, hematite suspended in bentonite matrix at pH 4 gives higher shear stresses and yield stresses than the quartz-hematite mixture suspended in bentonite matrix at pH 4. Quartz suspended in bentonite matrix at pH 4 (at the same total volumetric concentration of solid) gives lower shear stresses and yield stresses than the quartz-hematite mixture suspended in bentonite matrix at pH 4.

Between quartz-hematite mixture dispersed in bentonite suspension at pH 4 and 10 the latter is characterized with lower shear and yield stresses at the same total volume percent solid. Unlike in the case of pH 4, quartz-hematite mixture dispersed in bentonite suspension at pH 10 gave generally lower shear stresses than the quartz-hematite mixture without bentonite at pH 10 (considering the same volumetric fraction of quartz and hematite). The exception was 0.5/0.5 vol% quartz-hematite mixture dispersed in bentonite suspension at pH 10, which gave higher shear stresses and more complex flow behavior than the 0.5/0.5 vol% quartz-hematite mixture without bentonite (pH 10). In comparison to the quartz-containing bentonite suspension at pH 10, the quartz-hematite dispersion in bentonite suspension at pH 10 gave higher yield stresses and shear stresses at low and moderate shear rates. The shear stresses and yield stresses attributed to the hematite dispersed in bentonite suspension at pH 10 were higher than that found for the mixture dispersed in bentonite suspension (pH 10).

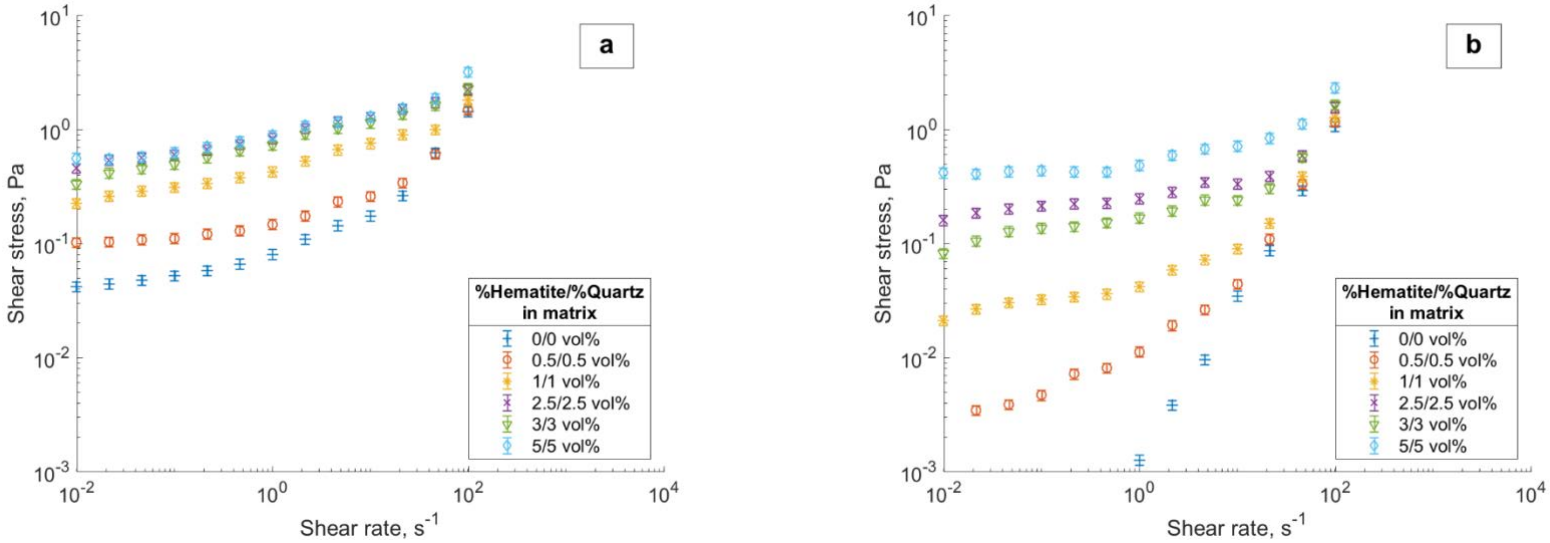


*Figure 48 - Quartz and hematite in volumetric proportion 1:1 dispersed in (a) bentonite matrix at pH 4 and (b) bentonite suspension at pH 10 in 1 × $10^{-2}$ M $KNO_3$ aqueous solution.*

SEM images of coarse fractions of iron-free quartz and hematite suspended at 0.1 vol% in bentonite matrix (also 0.1 vol% solid) at pH 4 in $1 \times 10^{-2}$ $KNO_3$ are given in the Figs. 49 and 50, respectively. Coarse size fractions and their low volumetric concentration allowed better visualization of differences in organization of bentonite aggregates and particles around another mineral phase. General view of the dried suspensions are given in the Figs. 49a and 50a; magnified image depicting the organization of the bentonite aggregates around quartz and hematite particles is given in the Figs 49b and 50c, d. Figure 49c depicts the quartz particle surface with unique bentonite lamellae attached onto it. Figure 50b shows coarse hematite particles without added bentonite. The dense coating of bentonite particles surrounding hematite particles at pH 4 (Figs. 50a, c, d) was not found around the quartz particles at pH 4 (Figs. 49a, b).

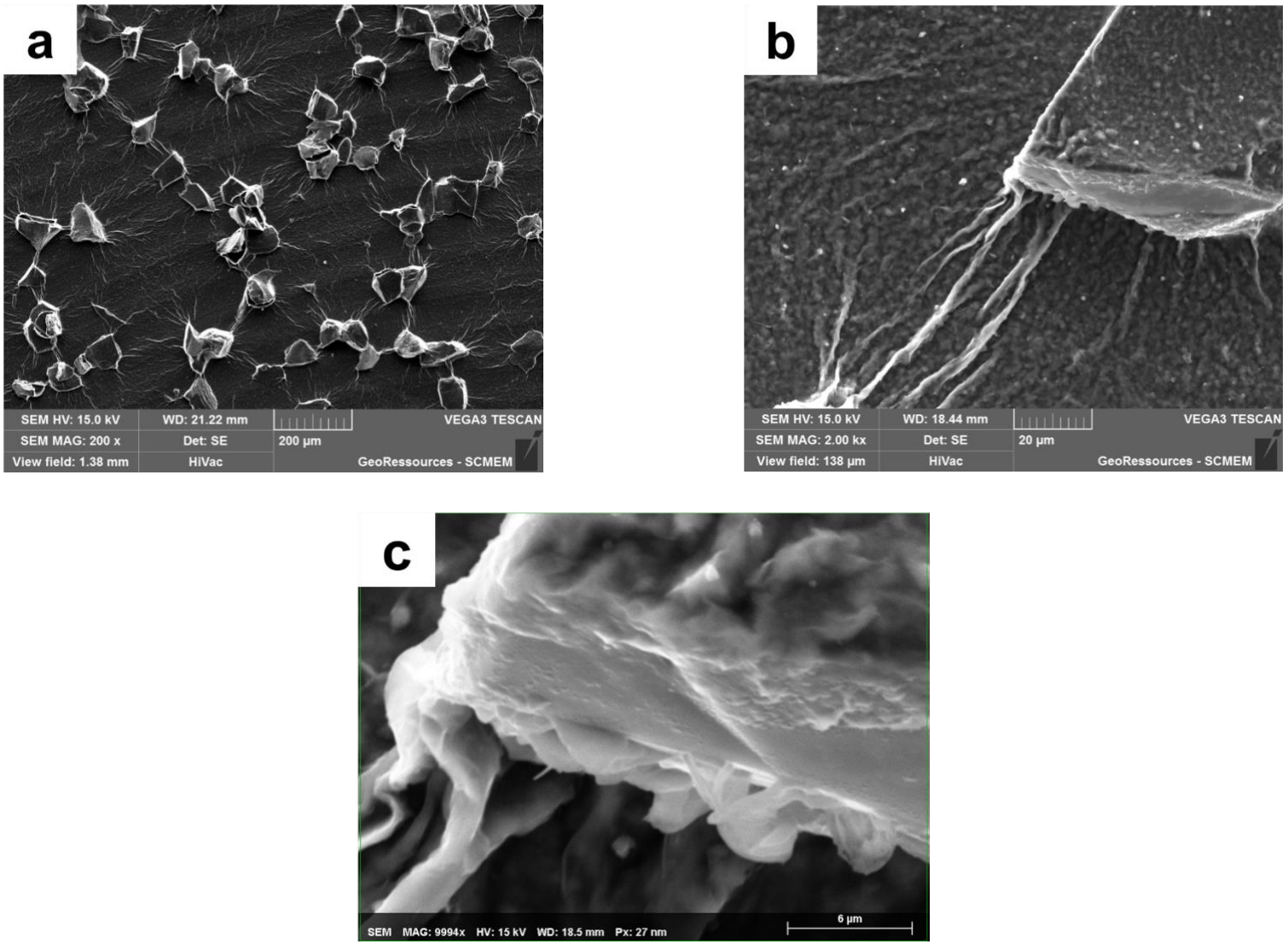


*Figure 49 - SEM images of quartz-bentonite suspension prepared at pH 4 in 1 × $10^{-2}$ M $KNO_3$ aqueous solution. Suspension droplets were deposited on Al stubs, dried and carbon-coated prior to image acquisitions.*

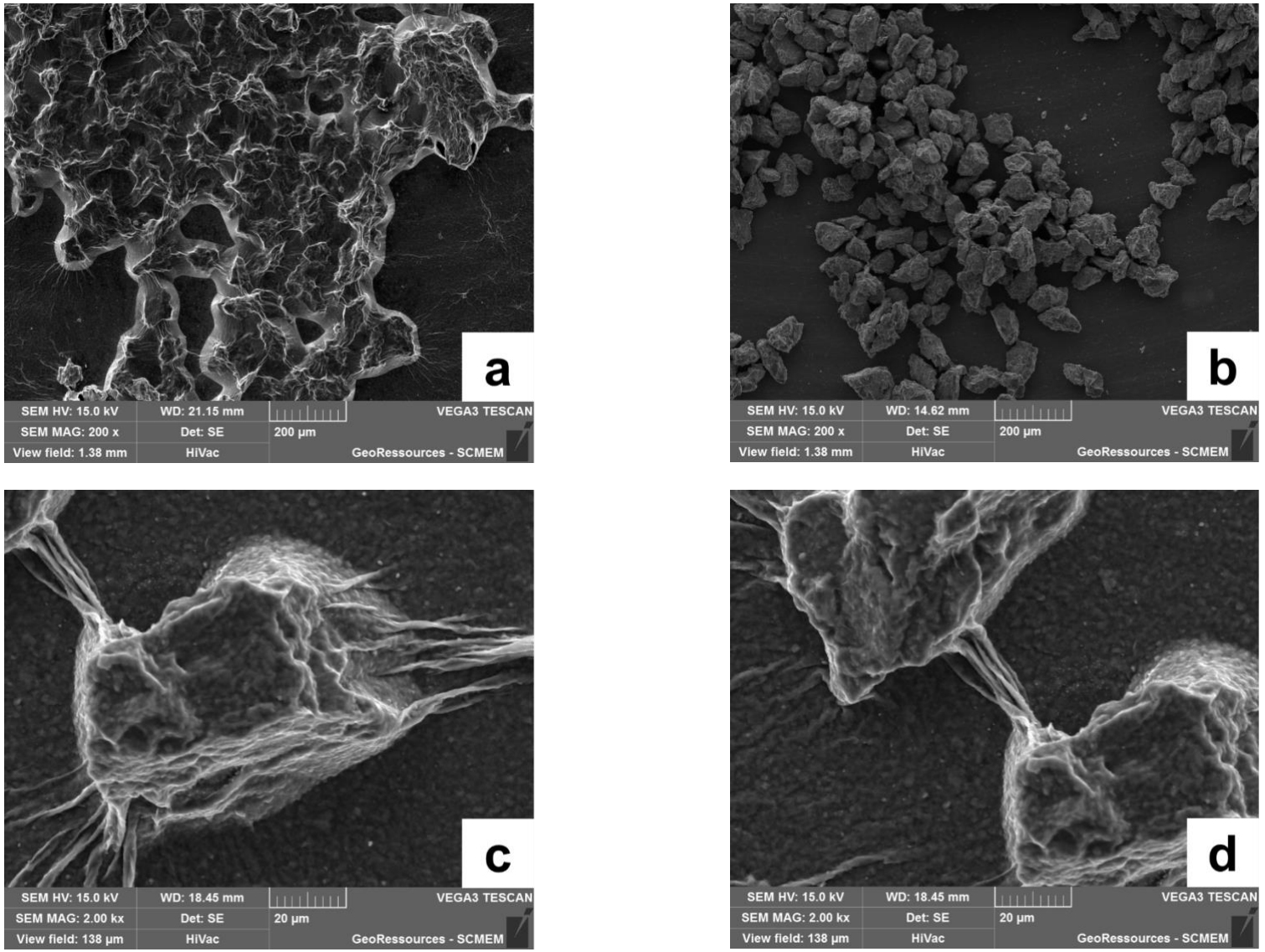


*Figure 50 - SEM images of: (a) hematite-bentonite suspension prepared at pH 4 in 1 × $10^{-2}$ M $KNO_3$ aqueous solution, general view, (b) coarse fraction of hematite, (c), (d) hematite-bentonite suspension prepared at pH 4 in 1 × $10^{-2}$ M $KNO_3$ aqueous solution, high magnification. Suspension droplets were deposited on Al stubs, dried and carbon-coated prior to acquisition.*

## Discussion

Rheological curves obtained for the suspensions with a single mineral phase at pH 4 and 10 are presented in the Figs. 43a and b for quartz, Figs. 43c and 43d for hematite and Fig. 45 for bentonite. Homocoagulation for homogeneously charged minerals occurs when the repulsive electrostatic force between the particles is weak and the van der Waals attraction dominates the force balance. Reduced electrostatic repulsion is observed in the proximity of minerals IEP. From the review of (Kosmulski 2016) it is safe to conclude the IEP of hematite between pH 7 and 9 and silicon dioxide – below pH 3. That explains the enhanced rheology of pH 4, 2.5-10 vol% quartz suspensions (Fig. 43a) relative to the rheology of pH 10 quartz suspensions (Fig. 43b). The repulsion between particles at pH 4 is lower due to the proximity of the IEP, thus, the van der Waals attraction leads particle aggregation. Due to necessity of aggregate breakage, the pH 4, 2.5-10 vol% quartz suspensions require higher stresses to initiate the flow; they also exhibit a noticeable yield stress, unlike the suspensions of dispersed particles (i.e., pH 10). It is known that dilute, electrostatically stabile colloidal suspensions flow in a Newtonian manner, which implies the flow index in the eq. 25 to be $n$=1 for pH 10 quartz suspension (Fig. 43b). However, the recovered flow index was $n$=1.35 (meaning, shear thickening). Viscosities recorded below 2 $s^{-1}$ are of the order of the viscosity of water, and, thus were not depicted in the Fig. 43b due to the insufficient precision. Such systems were discussed in the work of Barnes (1989), where it was concluded that almost any dispersion of non-aggregating solid particles suspended in Newtonian media will display dilatancy at sufficiently high shear rate. Thus, authors suggest Newtonian behavior close to the behavior of suspending media at low shear rates and dilatancy at high shear rates for pH 10 quartz suspensions under the study. Hematite suspensions of 2.5-10 vol% at pH 10 demonstrated higher stresses than that of pH 4. At pH 10 the mutual repulsion between the hematite particles is smaller and the van der Waals attraction dominates. Hematite suspensions at pH 10 (2.5-10 vol% solid) are partly aggregated and thus give higher shear stresses than that at pH 4. Quartz and hematite suspensions of 0.5 and 1 vol% solid are not concentrated enough to exhibit noticeable rheological complexity; in such suspensions particles are situated far from one another and the effects related to particle aggregation due to colloidal forces are minor.

Physicochemical properties of bentonite are more complex due to the charge-heterogeneity of its particles. The faces of particles do not change their charge with the pH and are negatively charged at both pH values tested (i.e., pH 4 and 10). On the other hand, the charge on the particles' edges is pH-dependent, with IEP situated around pH 7-8 (Benna et al. 1999; Durán et al. 2000). That is to say that at pH 4 the edges are positively charged, and at pH 10 they are charged negatively. Meaning, that the occurrence of a house of cards arrangement is possible at pH 4 and shall not take place at pH 10. For this reason, at pH 10 the bentonite suspension flows almost Newtonian but gives more complex, significantly different from Newtonian, rheological response at pH 4 (Fig. 45). Homocoagulation at pH 4 is promoted by two elastic colloidal forces: electrostatic and van der Waals (both attractive). These forces are also responsible for occurrence of the yield stress in the pH 4 bentonite suspension (Fig. 45).

In the suspensions with more than one mineral phase, the charge-induced heterocoagulation can take place. It occurs when two or more colloidal mineral particles with surface charge of an opposite sign are brought close enough to interact. Table 3 summarizes expected qualitative pair interaction (resulting from the electrostatic and van der Waals forces) between the minerals used in this work, at pH 4 and 10 in $1 \times 10^{-2}$ M $KNO_3$. At $1 \times 10^{-2}$ M $KNO_3$ the particles' EDL is not compressed.

*Table 3 - Qualitative pair interaction between the minerals at pH 4 and 10 in $1 \times 10^{-2}$ M $KNO_3$*

| Mineral pair | pH 4 | pH 10 |
|---|---|---|
| Hematite-bentonite edge | repulsive | weakly attractive to repulsive |
| Hematite-bentonite face | attractive | weakly attractive to repulsive |
| Quartz-hematite | attractive | weakly attractive to repulsive |
| Quartz-bentonite edge | attractive | repulsive |
| Quartz-bentonite face | repulsive | repulsive |

At pH 4 hematite particles are positively charged, whereas the quartz particles are slightly negatively charged, close to their IEP. Such chemical conditions favor the heterocoagulation in the sufficiently concentrated mix mineral suspensions (i.e., 1/1 - 5/5 vol% quartz/hematite, Fig. 44a). On the other hand, at pH 10 the quartz particles are strongly negatively charged, and the hematite particles are slightly negatively charged, close to their IEP. Such chemical conditions allow less intense heterocoagulation and, thus, yield lower shear stresses and yield stresses for quartz-hematite suspension at pH 10 (Fig. 44b) than for that at pH 4 (Fig. 44a). Heterocoagulated quartz-hematite suspensions at pH 4 (Fig. 44a) gave generally higher stresses than the suspensions with single mineral phase at pH 4 (Figs. 43a and 43c). This is explained by an additional attractive interaction arising due the electrostatic force between the oppositely charged particles. Higher affinity of aggregated particles towards one another explains higher stresses obtained for the mixture (in comparison to homocoagulated suspensions of quartz or hematite). The attraction between quartz and hematite particles is weaker at pH 10 than at pH 4. However, this attraction, accompanied by the mutual attraction of hematite particles to each other, is sufficient to change the behavior of the suspension from quartz-like log-log linear (pH 10, Fig. 43b) to more complex hematite-like yield stress flows (Figs. 43d and 44b), at the same total volumetric concentration of solid. In other words, replacing half of quartz for hematite in sufficiently concentrated suspension at pH 10 yields an aggregated suspension with more complex rheology than that of pure quartz suspension at pH 10. In comparison to homocoagulated hematite suspensions at pH 10, the quartz-hematite mixture (pH 10) yielded lower shear stresses. Replacing half of the volume of hematite particles with strongly mutually repelling quartz particles results in decrease of the amount of attractive interactions per unit volume in the suspension. This explains lower shear stresses and yield stresses obtained for the mix mineral suspension at pH 10 than those obtained for pure hematite suspension at pH 10.

At pH 4 the edges of the bentonite particles are attracted to the quartz particles (Table 3) and to the faces of bentonite particles (yielding house of cards arrangement). Addition of quartz particles to the bentonite suspensions causes charge-induced rearrangements in the matrix. The resulting arrangement is very well demonstrated in the Fig. 49c, where the bentonite particles oriented their edges towards the surface of the quartz particle. In general, the addition of quartz particles to the bentonite suspension at pH 4 yielded the matrix reinforcement, which goes in agreement with the suggestion of Bailey et al. (2014). The idea of matrix reinforcement through enhanced attractive

interactions at pH 4 is supported by the extent of yield stress increase upon quartz addition. At 10 vol% of quartz suspended in bentonite matrix, the yield stress is 7 times the one obtained for 10 vol% pure quartz suspension (pH 4) and more than 14 times the bentonite matrix itself (pH 4). The shear and yield stresses of quartz-containing bentonite suspensions at pH 4 were higher than those at pH 10. This is due to the negative charge taking place on all bentonite particle sites and the quartz surface at pH 10, meaning that overall interactions in the suspension are repulsive. In such conditions particles do not aggregate, but rather arrange in such way that all their negative sites are situated as far as possible from one another. Development of the yield stress in such conditions is due to the particle-particle physical contacts (e.g., friction) induced by the flow, repulsion-promoted arrangement and, possibly, some crowding-like effects (due to high polydispersity of solids).

Introducing hematite to the bentonite matrix at pH 4 causes charge-induced rearrangement of bentonite particles. However, in contrast with quartz-bentonite suspension at pH 4 (edge-quartz particle attraction), hematite particles will attract the faces of bentonite particles. In the Fig. 50a, c and d one can observe the hematite particles coated with the layer of bentonite particles. For comparison, the “uncoated” bentonite particles are depicted in the Fig. 50b. In the Fig. 50c and d the hematite particles are covered with the layer of bentonite particles and interrelated with the neighbor hematite particles through the bentonite matrix. Such arrangement yields higher area of contact with the matrix elementary units (bentonite particles), which explains sharp increase of the stress response with addition of relatively little quantity of hematite (0-1.5 vol% of hematite in the matrix, Fig. 47a). It is suggested that starting from 1.5-2 vol% of added hematite, the matrix is “saturated” with the hematite particles and further hematite addition does not yield matrix reinforcement. This finding supports the conclusion of Tombácz et al. (2001) concerning the existence of a concentration limit for reinforcement of iron oxide-montmorillonite heterocoagulated network. A well-defined concentration limit observed in the hematite-containing matrix at pH 4 was not found in the hematite-containing bentonite suspension at pH 10. In the Fig. 47b a gradual increase in the shear stress response with the increasing concentration of added hematite takes place. The hematite-containing bentonite suspension at pH 10 has changed its behavior from dilatant at low concentrations (1-3 vol%) of hematite to shear thinning at high (8-10 vol%) concentrations of hematite. At pH 10, hematite particles are slightly negatively charged, close to their IEP. The dilatancy at low volume fractions of hematite is due to the inter-particle contacts and

friction induced by the flow; minor heterocoagulation through van der Waals attraction can also occur. In the hematite-containing bentonite suspension at pH 10 increasing concentration of hematite particles leads their homocoagulation through van der Waals force. That explains characteristic for the aggregated suspensions shear thinning flow at 8 and 10 vol% of hematite in the bentonite suspension (pH 10).

In the quartz-hematite mixture suspended in bentonite matrix at pH 4 several types of attractive contacts are established, including: quartz-hematite, quartz-quartz, hematite-bentonite face, quartz-bentonite edge and bentonite edge-bentonite face. That explains high (in comparison to other suspensions tested in this work) shear stresses and yield stresses obtained for suspensions of this kind. However, considering the same volume percent solid, the shear stresses obtained for hematite suspended in bentonite matrix at pH 4 were higher than that obtained for quartz-hematite mixture in bentonite matrix at pH 4. That can be explained by the type of contacts formed between the matrix and the added particles. It is suggested that at the same volume percent of added mineral, hematite particles establish higher area of contact with the matrix constituents, than the quartz particles, due to their orientation. For this reason, the mixture of quartz and hematite suspended in the bentonite matrix is suggested to have lower area of contact with the matrix constituents than only hematite particles suspended in the matrix at the same volume concentration. The conclusion is supported by lower shear and yield stresses obtained for quartz-containing matrices at pH 4 than those obtained for quartz-hematite mixture in matrix at pH 4.

In the bentonite suspension containing quartz-hematite mixture at pH 10, the dominating interactions are repulsive. In fact, 1/1, 2.5/2.5 and 3/3 vol% quartz-hematite mixture (pH 10) without bentonite yields higher stresses than those found for quartz-hematite mixture in bentonite suspension (pH 10). The amount of repulsive interactions per unit volume of the mixture suspension containing bentonite is higher than that without bentonite at pH 10. It is suggested that the bentonite particles obstruct homocoagulation of hematite particles and possible minor heterocoagulation of quartz and hematite particles at pH 10. This explains lower stresses obtained for the mixture dispersed in bentonite suspension at pH 10. The difference between the flow behavior of 0.5/0.5 quartz-hematite mixture and 0.5/0.5 quartz-hematite mixture dispersed in bentonite (both at pH 10) is due to particle-particle contacts and friction induced by the flow in the bentonite-containing suspension.

Whereas difference in the flow curves obtained for quartz and hematite suspensions at the same pH is inevitably affected by the specific gravity difference of these minerals, the mixtures shall not display such problem. Specific gravity is an important parameter for the limiting quantity of the added mineral that the matrix can hold without yielding under its weight. This mechanism is opposed to the charge-induced reinforcement triggered by the addition of different mineral phase to the matrix. In multiple processes involving handling of mineral suspensions (e.g., pulp flows in mineral processing) specific gravity of minerals cannot be modified.

Basing on the above described principles of interaction, interpretation of the acquired flow curves and SEM images, the schematic organizations of particles occurring in mix-mineral suspensions at pH 4 and 10 were established, see Fig.51. The charge-based models of heterocoagulated networks were previously suggested by Ji et al. (2004) (montmorillonite with synthetic hematite particles), Tombácz at al. (2001) (montmorillonite clay with synthetic magnetite) and Bailey et al. (2014) and Hilhorst et al. (2014) (anionic or cationic silica and montmorillonite clay). The model of iron oxide-bentonite organization suggested in the present work agrees with the ones suggested by Tombácz et al. (2001) and Ji et al. (2004).

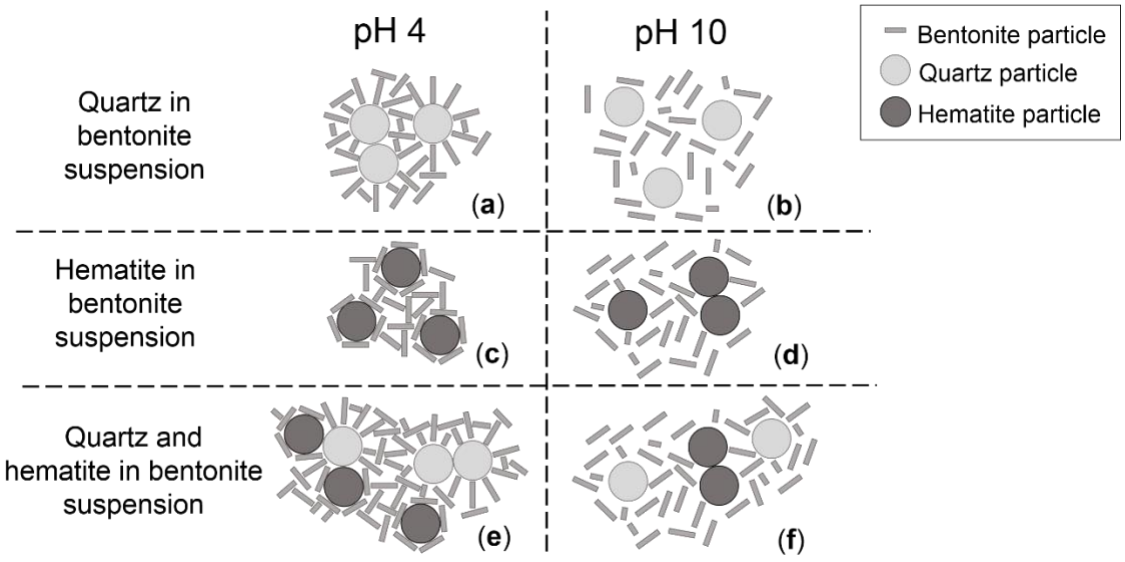


*Figure 49 - Schematic organizations occurring in bentonite suspensions of: quartz at pH 4 (a) and pH 10 (b), hematite at pH 4 (c) and 10 (d) and their mixture at pH 4 (e) and 10 (f).*

In the Fig. 51, both, the homo- and heterocoagulation of the mineral particles dispersed in bentonite suspension was taken into account. In case of pH 4, presence of discontinuities (particles of added mineral) in the bentonite matrix will inevitably disrupt the consistency of the particle organization (as suggested by ten Brinke et al. 2007). Reinforcement brought by the addition of quartz to bentonite matrix at pH 4 is due to the orientation of the bentonite particle edges towards the surface of the quartz particles (Fig. 51a). Quartz particles, as it follows from the flow curves of quartz suspensions (see Fig. 43a and b), will likely homocoagulate at pH 4, which is also depicted in the Fig. 51a. At pH 10 the bentonite particles shall not form the matrix, neither quartz-bentonite heterocoagulation shall occur (Fig. 51b). The addition of hematite in the place of quartz to the bentonite matrix at pH 4 allowed to establish higher area of contact with the added particles. This was achieved by orientation of the bentonite face towards surface of hematite particles (depicted in the Fig. 51c), which yielded the enhanced matrix reinforcement and, thus, high shear stress flow curves. The characteristic for aggregated suspensions shear thinning yield stress behavior that bentonite suspension at pH 10 gains with increasing hematite content is justified by hematite homocoagulation occurring at pH 10 (Fig. 51d). The contacts occurring in the quartz-hematite mixture suspended in bentonite matrix at pH 4 are depicted in the Fig. 51e. This complex system contains at least 5 contact types, including: quartz-hematite, hematite-bentonite face, quartz-bentonite edge, quartz-quartz, bentonite edge-bentonite face. Flow curves obtained for the quartz-hematite mixtures suspended in bentonite matrix at pH 4 were characterized with the intermediate shear stresses between those found for quartz-bentonite (pH 4) and hematite-bentonite (pH 4) suspensions with the same volume fractions. It is suggested that manipulation of the quartz/hematite ratio in such systems can allow to tune the rheological properties of suspensions through the quality and quantity of established inter-particle contacts. At pH 10 the quartz-hematite mixture dispersed in bentonite suspension possesses high amount of repulsive interactions per unit volume of the suspension (Fig. 51f), yielding even lower shear stresses than the quartz-hematite mixture without bentonite (pH 10). In such suspension (Fig. 51f) hematite homocoagulation and occasional heterocoagulation can take place.

## Conclusions

In this work the rheological properties of aqueous suspensions of bentonite, hematite, quartz and their mixtures were studied. The electrostatic and van der Waals interactions were used to explain the homo- and heterocoagulation occurring between the particles and the orientation of these particles relative to one another in the suspension. It was suggested that the orientation of the matrix constituents and their area of contact with the introduced mineral phase has a strong influence on the overall mechanical properties of the suspension. Introducing quartz or hematite to the bentonite matrix at pH 4 yields principally different rearrangements of bentonite particles around the introduced minerals. Analysis of theoretical interactions and SEM images revealed two major bentonite particle orientation types: bentonite edge-quartz particle and bentonite face-hematite particle (see Fig. 51a, c). Rheological tests yielded higher shear stresses and yield stresses attributed to the hematite-bentonite suspension at pH 4. This was explained through the higher area of contact established between the matrix constituents and the hematite particles than that between quartz and bentonite matrix constituents at pH 4.

Adhesive action of iron oxide species on the montmorillonite suspensions, previously reported by Tombácz et al. (2001), was found for the suspensions tested in this work; authors also report the existence of a concentration limit of hematite for the matrix reinforcement. However, the “weakening” of the structure found by Tombácz et al. (2001) expressed in lowering of the shear rate - shear stress flow curve was not found in the present study. Despite that, the hematite-containing matrices at pH 4 changed their behavior from dilatant ($n>1$) at low volume fractions of hematite to shear thinning ($n<1$) at high volume fractions of hematite. This indicates that with increasing hematite content the matrix became more sensitive to load applied above the yield stress.

Present work is in agreement with generalized conclusion derived by ten Brinke et al. (2007). It suggests that the addition of similarly charged particles of different shape to the gel can weaken it, whereas addition of oppositely charged particles - can strengthen the gel through attractive interactions. Here, we have demonstrated that the suspensions with dominating repulsive interactions yield lower shear and yield stresses than those with dominating attractive interactions in both, shape-homogeneous and shape-heterogeneous suspensions.

The experiments conducted on quartz-hematite mixtures suspended in bentonite matrix (pH 4) yielded behavior intermediate between the one of quartz and of hematite suspended in bentonite matrix at pH 4. Quartz-hematite mixtures in bentonite suspension at pH 10 allowed lower stresses than quartz-hematite mixtures without bentonite (pH 10). Minor addition (0.1 vol%) of bentonite clay in such suspension can intensify the flow through increasing the amount of repulsive interactions per unit volume of the suspension. This suggests that the mechanical properties of mix mineral suspensions can be tuned via: 1) changing the pH of the suspending media, 2) changing the mineralogical composition to increase or reduce the amount of attractive or repulsive interactions per unit volume of the suspension, when appropriate. Results of this work can be extended to the similar systems encountered in mineral processing, drilling or recycling industries or used in customization of non-Newtonian fluids.

## Funding

The financial support of Ministry of Higher Education, Research and Innovation of France is acknowledged.

## Acknowledgments

The authors thank the technical support from GeoRessources and LEMTA laboratories.

## Conflicts of Interest

The authors declare no conflict of interest.

## Bibliography


Abu-Jdayil B (2011) Rheology of sodium and calcium bentonite-water dispersions: Effect of electrolytes and aging time. Int J Miner Process 98:208–213 . doi: 10.1016/j.minpro.2011.01.001

Aguzzi C, Sánchez-Espejo R, Cerezo P, et al (2013) Networking and rheology of concentrated clay suspensions “matured” in mineral medicinal water. Int J Pharm 453:473–479 . doi: 10.1016/j.ijpharm.2013.06.002

Bailey L, Lekkerkerker HNWW, Maitland GC (2014) Rheology modification of montmorillonite dispersions by colloidal silica. Rheol Acta 53:373–384 . doi: 10.1007/s00397-014-0765-3

Baird JC, Walz JY (2006) The effects of added nanoparticles on aqueous kaolinite suspensions I. Structural effects. J Colloid Interface Sci 297:161–169 . doi: 10.1016/j.jcis.2005.10.022

Baird JC, Walz JY (2007) The effects of added nanoparticles on aqueous kaolinite suspensions II. Rheological effects. J Colloid Interface Sci 306:411–420 . doi: 10.1016/j.jcis.2006.10.066

Bakker CW, Meyer CJ, Deglon DA (2010) The development of a cavern model for mechanical flotation cells. In: Minerals Engineering. pp 968–972

Bakker CW, Meyer CJ, Deglon DA (2009) Numerical modelling of non-Newtonian slurry in a mechanical flotation cell. Miner Eng 22:944–950 . doi: 10.1016/j.mineng.2009.03.016

Barast G, Razakamanantsoa AR, Djeran-Maigre I, et al (2017) Swelling properties of natural and modified bentonites by rheological description. Appl Clay Sci 142:60–68 . doi: 10.1016/j.clay.2016.01.008

Barnes HA (1989) Shear-Thickening (“Dilatancy”) in Suspensions of Nonaggregating Solid Particles Dispersed in Newtonian Liquids. J Rheol (N Y N Y) 33:329–366 . doi: 10.1122/1.550017

Benna M, Kbir-Ariguib N, Magnin A, Bergaya F (1999) Effect of pH on Rheological Properties of Purified Sodium Bentonite Suspensions. J Colloid Interface Sci

Boger D V. (2009) Rheology and the resource industries. Chem Eng Sci 64:4525–4536 . doi: 10.1016/j.ces.2009.03.007

Chernoburova O, Jenny M, de Richter SK, Otsuki A (2018) Dynamic Behavior of Dilute Bentonite Suspensions under Different Chemical Conditions Studied via Magnetic Resonance Imaging Velocimetry. Colloids Interfaces 2018, Vol 2, Page 41 2:41 . doi: 10.3390/COLLOIDS2040041

Choo KY, Bai K (2015) Effects of bentonite concentration and solution pH on the rheological properties and long-term stabilities of bentonite suspensions. Appl Clay Sci 108:182–190 . doi: 10.1016/j.clay.2015.02.023

Cornell RM, Schwertmann U (2004) The Iron Oxides: Structure, Properties, Reactions, Occurences and Uses, Second Edition. In: The Iron Oxides. pp 201–221

Durán JDGDG, Ramos-Tejada MMM, Arroyo FJJ, González-Caballero F (2000) Rheological and Electrokinetic Properties of Sodium Montmorillonite Suspensions. J Colloid Interface Sci 229:107–117 . doi: 10.1006/jcis.2000.6956

Farrokhpay S (2012) The importance of rheology in mineral flotation: A review. Miner Eng 36–38:272–278 . doi: 10.1016/j.mineng.2012.05.009

Firth BA (1976) Flow Properties of Coagulated Colloidal Suspensions II. Experimental Properties of the Flow Curve Parameters

Firth BA, Hunter RJ (1976) Flow Properties of Coagulated Colloidal Suspensions I. Energy Dissipation in the Flow Units

Goh R, Leong YK, Lehane B (2011) Bentonite slurries-zeta potential, yield stress, adsorbed additive and time-dependent behaviour. Rheol Acta 50:29–38 . doi: 10.1007/s00397-010-0498-x

Hilhorst J, Meester V, Groeneveld E, et al (2014) Structure and rheology of mixed suspensions of montmorillonite and silica nanoparticles. J Phys Chem B 118:11816–11825 . doi: 10.1021/jp504217m

Huertas FJ, Carretero P, Delgado J, et al (2001) An Experimental Study on the Ion-Exchange Behavior of the Smectite of Cabo de Gata (Almería, Spain): FEBEX Bentonite. J Colloid Interface Sci 239:409–416 . doi: 10.1006/jcis.2001.7605

Ji Y-Q, Black L, Weidler PG, Janek MN (2004) Preparation of Nanostructured Materials by HeterocoagulationsInteraction of Montmorillonite with Synthetic Hematite Particles. Langmuir 20:9796–9806 . doi: 10.1021/la0495579

Kelessidis VC, Tsamantaki C, Dalamarinis P (2007) Effect of pH and electrolyte on the rheology of aqueous Wyoming bentonite dispersions. Appl Clay Sci 38:86–96 . doi: 10.1016/j.clay.2007.01.011

Kosmulski M (2016) Historical perspective Isoelectric points and points of zero charge of metal (hydr)oxides: 50 years after Parks' review. doi: 10.1016/j.cis.2016.10.005

Luckham PF, Rossi S (1999) The colloidal and rheological properties of bentonite suspensions. Adv Colloid Interface Sci 82:43–92

Mahto V, Sharma VP (2004) Rheological study of a water based oil well drilling fluid. J Pet Sci Eng 45:123–128 . doi: 10.1016/j.petrol.2004.03.008

Ndlovu B, Becker M, Forbes E, et al (2011) The influence of phyllosilicate mineralogy on the rheology of mineral slurries. Miner Eng 24:1314–1322 . doi: 10.1016/j.mineng.2011.05.008

Ndlovu B, Farrokhpay S, Bradshaw D (2013) The effect of phyllosilicate minerals on mineral processing industry. Int J Miner Process 125:149–156 . doi: 10.1016/j.minpro.2013.09.011

Norrish K (1954) The swelling of montmorillonite. Discuss Faraday Soc

Ohtsubo M (1989) Interaction of iron oxides with clays. Clay Sci 7:227–242

Ohtsubo M, Yoshimura A, Yong RN (1991) Particle interaction and rheology of illite-iron oxide complexes. Clays Clay Miner 39:347–354

Pecini EM, Avena MJ (2013) Measuring the isoelectric point of the edges of clay mineral particles: The case of montmorillonite. Langmuir 29:14926–14934 . doi: 10.1021/la403384g

Tadros TF (2010) Rheology of Dispersions: Principles and Applications

Tan X, Liu F, Hu L, et al (2017) Evaluation of the particle sizes of four clay minerals. doi: 10.1016/j.clay.2016.10.012

Ten Brinke AJW, Bailey L, Lekkerkerker HNW, Maitland GC (2007) Rheology modification in mixed shape colloidal dispersions. Part II: mixtures. doi: 10.1039/b713144e

Tombácz E, Csanaky C, Illés E (2001) Polydisperse fractal aggregate formation in clay mineral and iron oxide suspensions, pH and ionic strength dependence. Colloid Polym Sci 279:484–492 . doi: 10.1007/s003960100480

Tombácz E, Szekeres M (2004) Colloidal behavior of aqueous montmorillonite suspensions: the specific role of pH in the presence of indifferent electrolytes. Appl Clay Sci. doi: 10.1016/j.clay.2004.01.001

Tombácz E, Libor Z, Illes E, et al (2004) The role of reactive surface sites and

complexation by humic acids in the interaction of clay mineral and iron oxide particles. doi: 10.1016/j.orggeochem.2003.11.002

van Olphen H (1964) Internal mutual flocculation in clay suspensions. J Colloid Sci 19:313–322 . doi: 10.1016/0095-8522(64)90033-9

Vryzas Z, Kelessidis VC, Nalbantian L, et al (2017) Effect of temperature on the rheological properties of neat aqueous Wyoming sodium bentonite dispersions. Appl Clay Sci 136:26–36 . doi: 10.1016/j.clay.2016.11.007

# Conclusions

This work was dedicated to the rheology of fine particle mineral suspensions. In such suspensions, the ionic composition of the media defines particle charging, and thus, the degree of agglomeration or dispersion in the suspension. The inter-particle interaction was controlled through the physical chemistry of the mineral's surfaces via changing the pH of the suspending media and the type of electrolyte. Suspensions containing phyllosilicates have demonstrated the most dramatic change with chemistry. Changing the type of salt utilized in dilute suspensions of sodium bentonite allowed to influence the flow behavior of the bentonite suspension (e.g. reduce the yield stress and eliminate banding by replacing potassium nitrate with sodium chloride). The mechanism of influence involved increasing the inter-sheet distance in the clay particles and modifying the properties of the EDL through changing the salt cation. Complex polymieral systems have demonstrated significant dependency of the rheological properties on the individual charge of the mineral particles forming such systems. Attraction/repulsion and relative orientation of the particles to one another (and, thus, the area of contact between the mineral and the matrix) had a determining effect on the rheology of mix-mineral systems. Potential uses of discoveries made in this work include (but are not limited to) improvement of efficiency of slurry stirring and handling, flotation processes - in mineral beneficiation industry, customization of non-Newtonian fluids and improvement of fluids used for drilling.

First part of this work, presented in the form an article published in the peer reviewed journal *Colloids and Interfaces*, was dedicated to local rheology characterization of the dilute aqueous Na-bentonite suspensions using MRI velocimetry. The nature of this sheet phyllosilicate mineral leads its spatial chemical inhomogeneity, meaning, that the particle edge and face possess different chemical properties, and, thus, exhibit different physical properties. By manipulating the pH of the aqueous media of bentonite suspension, it is possible to create conditions for establishment of "card house" network. This network is characterized with significantly different mechanical properties than that of a system with mutually repelling particles. Coussot et al. (2002) reported that the structured fluids (e.g., suspensions of bentonite) at low and moderate shear rates cannot flow homogeneously, which complicates conduction of meaningful measurement via conventional viscometric methods. Present study investigates flow inhomogeneities in such fluids. In the first part of this work, the card house concept was used to explain the

differences among the local flow behaviors of dilute bentonite suspensions prepared under different solution chemistry. Using the MRI velocimetry, it was found that banding and localization were manifested in the clay suspensions with a low volumetric concentration of solids (0.1 vol.%), under chemical conditions favorable for the three-dimensional particle network formation (e.g., pH 4 in $1 \times 10^{-2}$ $KNO_3$ and NaCl salt solutions). Mechanical strength of E-F network was controlled through the particle swelling and the EDL of the particle surfaces, hence, the pH and type of salt used to make a suspension had a crucial influence. It was demonstrated that in dilute aqueous bentonite suspensions banding could be significantly hindered by: (a) increasing the suspension pH to close to or above the IEP of bentonite particle edge, (b) adding cations with smaller bare radius from monovalent salt to the suspension. In the latter case, formation of aggregates of different size with different monovalent salt was observed by means of SEM. The later findings suggest that in case of necessity to maintain a certain acidity in a stirred tank it is not essential to compromise the pH to eliminate the banding; but changing the type of electrolyte could help to diminish the banding effect. The absence of shear banding or localization in the suspensions at pH 8 and 10, both in $1 \times 10^{-2}$ M $KNO_3$ is due to very low or no yield stress present in these samples. Weak attractive particle interactions at pH 8 and repulsive interactions at pH 10 result in easy-flowing systems. A master curve with a single set of parameters can be established for the dilute suspensions without a continuous three-dimensional particle network (meaning, pH 8 and 10 in $1 \times 10^{-2}$ M $KNO_3$). It is possible due to their simple behavior under the load and low sensitivity to the history of shear. Suspension at pH 4 in $1 \times 10^{-2}$ M $KNO_3$ is characterized with a card house network and banded velocity profile; strong history-dependence of its flow properties justifies the existence of several flow curves, each correspondent to a particular state of the material. A concept of simple power-law master curve with a single set of parameters is inapplicable in this case, and a more complex model should be considered.

Coexistence of stagnant and agitated volumes in the stirred tanks (otherwise known as “caverns”) is an actual problem in mineral processing industry, that is often related to presence of phyllosilicates (Bakker et al. 2009, 2010). Flotation operations suffering from formation of caverns can potentially benefit from this discovery. The work also encourages further research in the area of mathematical modelling of rheological behavior of complex fluids.

Second part of this work presented as an article in process of preparation for publication is dedicated to the rheological properties of aqueous suspensions of bentonite, hematite, quartz and their mixtures. The electrostatic and van der Waals interactions were used to explain the homo- and heterocoagulation occurring between the particles and the orientation of these particles relative to one another in the suspension. It was suggested that the orientation of the matrix constituents and their area of contact with the introduced mineral phase has a strong influence on the overall mechanical properties of the suspension. Introducing quartz or hematite to the bentonite matrix at pH 4 yields principally different rearrangements of bentonite particles around the introduced minerals. Analysis of theoretical interactions and SEM images revealed two major bentonite particle orientation types: bentonite edge-quartz particle and bentonite face-hematite particle. Rheological tests yielded higher shear stresses and yield stresses attributed to the hematite-bentonite suspension at pH 4. This was explained through the higher area of contact established between the matrix constituents and the hematite particles than that between quartz and bentonite matrix constituents at pH 4.

Adhesive action of iron oxide species on the montmorillonite suspensions, previously reported by Tombácz et al. (2001), was found for the suspensions tested in this work; authors also report the existence of a concentration limit of hematite for the matrix reinforcement. However, the “weakening” of the structure found by Tombácz et al. (2001) expressed in lowering of the shear rate - shear stress flow curve was not found in the present study. Despite that, the hematite-containing matrices at pH 4 changed their behavior from dilatant ($n>1$) at low volume fractions of hematite to shear thinning ($n<1$) at high volume fractions of hematite. This indicates that with increasing hematite content the matrix became more sensitive to load applied above the yield stress.

Present work is in agreement with generalized conclusion derived by ten Brinke et al. (2007). It suggests that the addition of similarly charged particles of different shape to the gel can weaken it, whereas addition of oppositely charged particles - can strengthen the gel through attractive interactions. Here, it was demonstrated that the suspensions with dominating repulsive interactions yield lower shear and yield stresses than those with dominating attractive interactions in both, shape-homogeneous and shape-heterogeneous suspensions. The experiments conducted on quartz-hematite mixtures suspended in bentonite matrix (pH 4) yielded behavior intermediate between the one of quartz and of hematite suspended in bentonite matrix at pH 4. Quartz-hematite mixtures

in bentonite suspension at pH 10 allowed lower stresses than quartz-hematite mixtures without bentonite (pH 10). Minor addition (0.1 vol%) of bentonite clay in such suspension can intensify the flow through increasing the amount of repulsive interactions per unit volume of the suspension. This suggests that the mechanical properties of mix mineral suspensions can be tuned via: 1) changing the pH of the suspending media, 2) changing the mineralogical composition to increase or reduce the amount of attractive or repulsive interactions per unit volume of the suspension, when appropriate. Results of this work can be extended to the similar systems encountered in mineral processing, drilling or recycling industries or used in customization of non-Newtonian fluids.

## Bibliography


Bakker CW, Meyer CJ, Deglon DA (2010) The development of a cavern model for mechanical flotation cells. In: Minerals Engineering. pp 968–972

Bakker CW, Meyer CJ, Deglon DA (2009) Numerical modelling of non-Newtonian slurry in a mechanical flotation cell. Miner Eng 22:944–950 . doi: 10.1016/j.mineng.2009.03.016

Coleman BD, Markovitz H, Noll W (1966) Viscometric flows of Non-Newtonian Fluids. Springer-Verlag, Berlin

Coussot P (2005) Rheometry of Pastes, Suspensions, and Granular Materials: Applications in Industry and Environment

Coussot P, Nguyen QD, Huynh HT, Bonn D (2002) Viscosity bifurcation in thixotropic, yielding fluids. J Rheol (N Y N Y) 46:1213–847 . doi: 10.1122/1.1459447

Coussot P, Tocquer L, Lanos C, Ovarlez G (2009) Macroscopic vs. local rheology of yield stress fluids. J Non-Newtonian Fluid Mech 158:85–90 . doi: 10.1016/j.jnnfm.2008.08.003

Ovarlez G, Rodts S, Ragouilliaux A, et al (2008) Wide-gap Couette flows of dense emulsions: Local concentration measurements, and comparison between macroscopic and local constitutive law measurements through magnetic resonance imaging. Phys Rev E 78: . doi: 10.1103/PhysRevE.78.036307

Ten Brinke AJW, Bailey L, Lekkerkerker HNW, Maitland GC (2007) Rheology modification in mixed shape colloidal dispersions. Part II: mixtures. doi: 10.1039/b713144e

Tombácz E, Csanaky C, Illés E (2001) Polydisperse fractal aggregate formation in clay mineral and iron oxide suspensions, pH and ionic strength dependence. Colloid Polym Sci 279:484–492 . doi: 10.1007/s003960100480

# Résume élargi de la thèse en langue Français

Les suspensions minérales de particules fines sont connues pour leur comportement non-Newtonien pendant l'écoulement. Les interactions particule-particule dans de tels systèmes (c'est-à-dire, suspensions minérales) ne sont pas limitées au contact physique, e.g. collision et frottement. La capacité des minéraux de développer une charge dans l'environnement aqueux justifie des comportements différents des systèmes similaires de première vue. C'est à dire qu'étant caractérisées avec la même fraction volumétrique, composition chimique et granulométrie des solides et densité de dispersant, deux suspensions peuvent montrer un comportement rhéologique différent en raison de la chimie de la solution. Dans ce cas, la composition ionique du dispersant définira la charge des particules, et donc le degré d'agglomération/dispersion dans la suspension. Certains minéraux sont connus pour être particulièrement problématiques dans les processus d'enrichissement des minerais, comme, par exemple, les argiles phyllosilicates. En flottation par moussage – le processus principale dans l'enrichissement des minerais – les phyllosilicates posent beaucoup de problèmes, comme la réduction de la qualité du concentrât (à cause du transfert de particules des phillosilicates dans la mousse), la consommation augmentée de réactifs et la localisation du volume agité de la pulpe autour de l'élément agitatif.

L'origine de ces minéraux phyllosilicates implique leur inhomogénéité chimique spatiale. Pour faciliter la modélisation, les particules de phyllosilicates sont souvent représentées par des feuils ou des disques avec une charge différente sur le bord et la face. Le phyllosilicate utilisé dans ce travail est une bentonite à base de sodium (Kunipia-F bentonite par Kunimine Industries Co., Ltd). La charge sur la face de la particule de bentonite en solution aqueuse de sel de concentration modérée est négative et

indépendante du pH, alors que sur le bord de la particule le signe de la charge est dépendant du pH. Ce phénomène est la base du concept de « house of cards » introduit par van Olphen. Il a proposé qu'à cause des charges opposées développées sur les faces et les bords des particules de bentonite en solutions aqueuses acides, ces particules vont s'arranger en une structure rectangulaire ressemblant à un château de cartes. Il était proposé que les suspensions de particules caractérisées par cette structure (développée en milieu acide), possèdent plus de résistance à l'écoulement que les suspensions de particules en milieu neutre ou basique (et donc avec arrangement de particules différent). Ces hypothèses font la base théorique de ce travail.

En première partie pratique de ce travail, présentée sous la forme d'un article publié dans le journal international « Colloids and Interfaces », les suspensions aqueuses diluées de Na-bentonite ont été examinées par vélocimétrie par imagerie par résonance magnétique (IRM) pour étudier l'influence du pH et du type d'électrolyte monovalent sur leur comportement rhéologique local. Les résultats ont indiqué que les suspensions contenant 0,1% de solide en volume peuvent présenter une bande de cisaillement, une localisation de cisaillement ou aucun phénomène local en fonction de la chimie du milieu liquide de suspension (FIG. 1). Il était proposé que la bande de cisaillement (FIG. 1a, 6 rpm) dans la suspension diluée (0,1% de solide en volume, pH 4 dans $1 \times 10^{-2}$ M $KNO_3$) se produit en raison de la formation d'un réseau tridimensionnel de particules dans un environnement acide. En cas de pH 8 (FIG. 1b) les bords des particules de bentonite sont à la proximité de leur point isoélectrique. Dans ce cas les structures fragiles de type « rubans » sont formées dans la suspension. Ces structures ne présentent pas des bandes de cisaillement. En cas de pH 10 (FIG. 1c) aucune structure n'est formée à cause de la répulsion mutuelle de toutes les faces et bords des particules dans la suspension.

Cela explique le comportement proche de Newtonien de suspensions de bentonite diluée à pH 10.

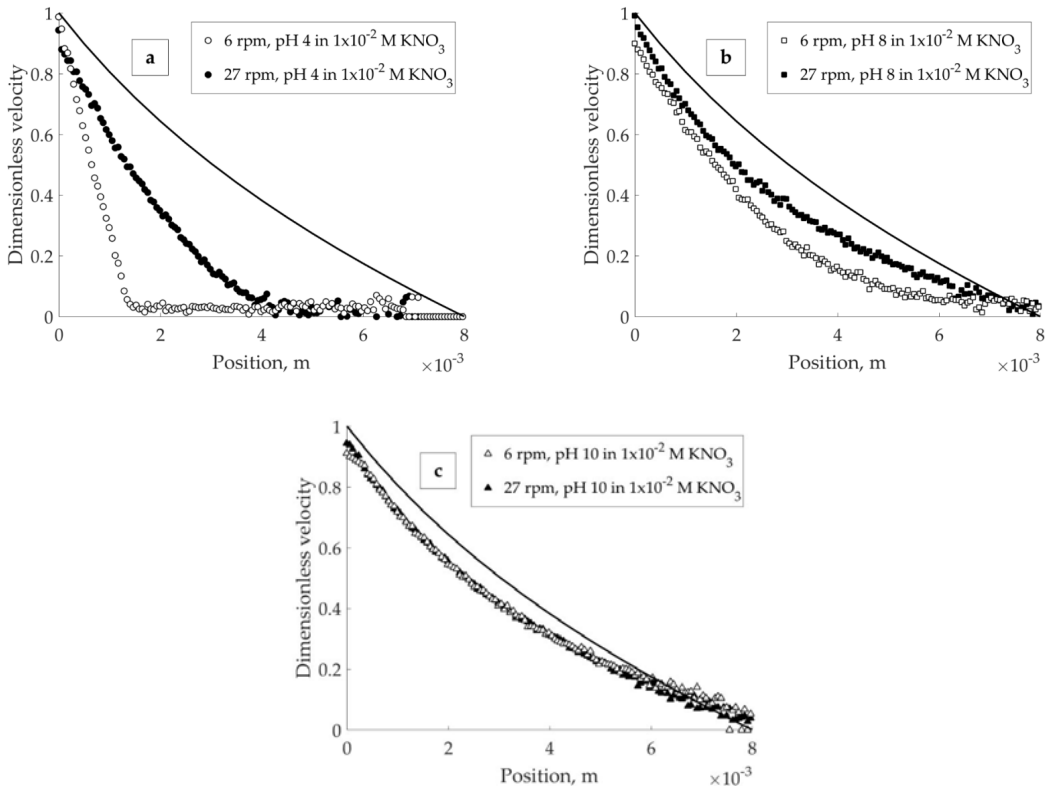


*FIG. 1 Profils de vitesse (sans dimension) pour les suspensions à: (a) pH 4; (b) pH 8; (c) pH10; dans 1 × 10-2 M KNO3, pour une vitesse de rotation de 6 et 27 tr / min*

Les changements structurels induits par la modification de la chimie des suspensions sont aussi examinés par microscopie électronique à balayage (MEB). Une méthode, déjà établie, basée sur le traitement des couples obtenus via une mesure rhéométrique conventionnelle, est également appliquée comme un moyen alternatif de récupérer des informations de flux locaux. Dans la plage du taux de cisaillement couverte par la vélocimétrie IRM, les résultats des deux méthodes concordent. Le résultat a été discuté du point de vue des théories DLVO (Derjaguin-Landau-Verwey-Overbeek) et « house of cards » (château de cartes). Il a été suggéré que l'existence d'une «master

curve» (ou courbe d'écoulement globale) pour les suspensions diluées dépendait de l'organisation des particules de bentonite dans la suspension, cette organisation est influencée par la chimie de solution et l'historique des contraintes précédentes.

Au cours de l'étape suivante (la deuxième partie pratique) de ce travail, présentée sous la forme d'un article en cours de rédaction, la complexité du système a été augmentée par l'ajout de la deuxième phase minérale, l'hématite ou le quartz, dans la matrice de bentonite. L'intérêt d'étudier ces systèmes est lié au comportement en écoulement d'une matrice formée avec différents types de contacts entre particules. Par exemple, à pH 4, l'interaction électrostatique résultante entre le bord de la bentonite chargé positivement et le quartz chargé négativement est attirante (FIG. 2a), alors qu'au même pH, elle est répulsive avec l'hématite car ce minéral est chargé positivement (FIG. 2c). D'autre part, la face de la particule de bentonite chargée négativement attirera la particule d'hématite à pH 4, mais repoussera le quartz (FIG. 2a, c, e). Ces interactions électrostatiques s'expriment par une organisation différente des particules de la matrice autour de l'autre phase minérale. Avec l'augmentation de la fraction volumique des particules d'hématite ou de silice ajoutées, la quantité de réarrangements dans la matrice augmente, ce que justifie une réponse rhéologique modifiée. Dans un système avec des interactions strictement répulsives entre tous les sites de toutes les phases minérales (par exemple quartz et bentonite, pH 10), la déviation du comportement Newtonien est justifiée par les réarrangements des particules, la collision et le frottement induits par le cisaillement (FIG. 2 b, d, f). La différence dans la position des agrégats de particules de bentonite autour des particules d'hématite ou de quartz a été observée avec le MEB.

Enfin, la complexité du système a été encore plus augmentée par l'ajout de la troisième phase minérale. Les types de contacts établis dans les suspensions avec une

chimie différente du milieu ont été discutés, ainsi que leur influence sur la formation de la matrice et sa manière d'écoulement.

La manipulation de la composante électrostatique de la balance de force inter-particules, en modifiant le pH du milieu de suspension, a permis de contrôler l'homo- et l'hétérocoagulation des particules dans la suspension. L'orientation des constituants de la matrice de bentonite et leur zone de contact avec la phase minérale introduite ont une forte influence sur les propriétés d'écoulement de la suspension. Plusieurs modèles d'association de particules ont été proposés pour expliquer le comportement des suspensions de minéraux mélangés sous la charge appliquée (FIG. 2).

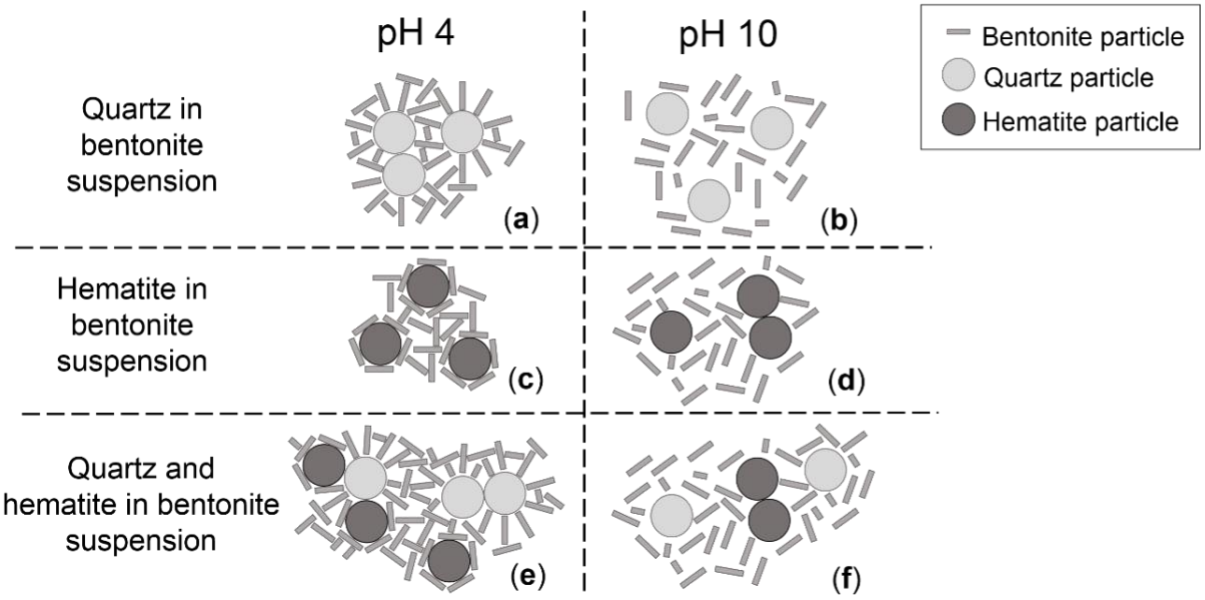


*FIG. 2 Organisations schématiques suggérées dans les suspensions de bentonite de: quartz à pH 4 (a) et pH 10 (b), hématite à pH 4 (c) et 10 (d) et leur mélange à pH 4 (e) et 10 (f).*

# Appendix

## Appendix I: Images of the froth captured for 0.05, 0.1 and 0.3 vol.% bentonite in flotation of -40 µm quartz-hematite mixture

F1, F2 and F3 correspond to the first, second and third flotation stage depicted in the figure 27.




**0.05 vol% of bentonite**

**0.1 vol% of bentonite**

**0.3 vol% of bentonite**

## Appendix II: Images of the froth captured for 0.05, 0.1 and 0.3 vol.% bentonite in flotation of 40-75 µm quartz-hematite mixture

F1, F2 and F3 correspond to the first, second and third flotation stage depicted in the figure 28.

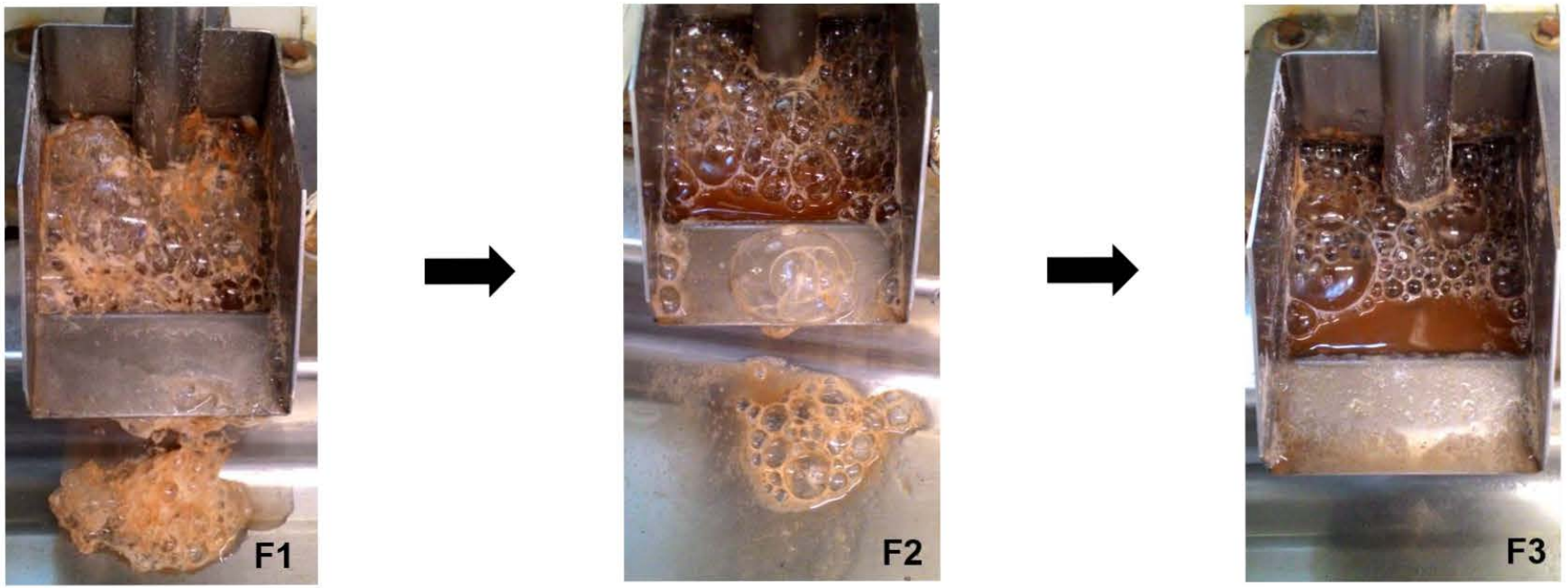


0.05 vol% of bentonite

0.1 vol% of bentonite

0.3 vol% of bentonite

## Appendix III: Full set of local rheological curves (6, 9, 12, 15, 18 and 21 rpm) for pH 8 in 1 × $10^{-2}$ M $KNO_3$

From the figure below one can conclude that the stratification in the Fig. 39d is apparent. The full set of profiles possesses rather a shape of a cloud, and does not suggest well-defined, separated curves.